Dissertation

miR-375 in Merkel cell carcinoma, more than a serum biomarker.

Submitted by

Kaiji Fan

for the Academic Degree of

Doctor of Philosophy

(PhD)

at the

Medical University of Graz

Department of Dermatology

under the Supervision of

Prof. Dr. Dr. Jürgen C. Becker

2020

Declaration

I hereby declare that this thesis is my own original work and that I have fully acknowledged by name all of those individuals and organizations that have contributed to the research for this thesis. Due acknowledgement has been made in the text to all other material used. Throughout this thesis and in all related publications I followed the "Standards of Good Scientific Practice and Ombuds Committee at the Medical University of Graz".

Date: 02.01.2020 Kaiji Fan

Disclosures

This thesis is written based on the following publications and manuscript, numbered in Roman and will be referred in the text:

I: ***Fan K***[1,2,3,4]***,*** *Ritter C*[2,3,4]*, Nghiem P*[5]*, Blom A*[5]*, Verhaegen ME*[6]*, Dlugosz A*[6]*, Ødum N*[7]*, Woetmann A*[7]*, Tothill RW*[8,9]*, Hicks RJ*[9,10]*, Sand M*[11]*, Schrama D*[12]*, Schadendorf D*[3,13]*, Ugurel S*[13]*, Becker JC*[2,3,4,13]*. Circulating cell-free miR-375 as surrogate marker of tumor burden in Merkel cell carcinoma Clin Cancer Res. 2018; 24(23):5873-5882*

II: ***Fan K***[1,2,3,4]*, Gravemeyer J*[2,3,4]*, Ritter C*[2,3,4]*, Rasheed K*[14]*, Gambichler T*[15]*, Moens U*[14]*, Shuda M*[16]*, Schrama D*[12]*, Becker JC*[2,3,4,13]*. MCPyV large T antigen-induced atonal homolog 1 is a lineage-dependency oncogene in Merkel cell carcinoma. J Invest Dermatol. 2019; pii: S0022-202Xs (19)31853-6.*

III: ***Fan K***[1,2,3,4]*, Zebisch A*[17,18]*, Horny K*[2,3,4]*, Schrama D*[12]*, Becker JC*[2,3,4,13]*. Highly expressed miR-375 is not an intracellular oncogene in Merkel cell polyomavirus-associated Merkel cell carcinoma. Preprint in BioRxiv. 2019.*

IV: ***Fan K***[1,2,3,4]*, Spassova I*[2,3,4]*, Gravemeyer J*[2,3,4]*, Ritter C*[2,3,4]*, Horny K*[2,3,4]*, Lange A*[19]*, Ødum N*[7]*, Schrama D*[12]*, Becker JC*[2,3,4,13]*. Merkel cell carcinoma derived exosomal miR-375 induces fibroblast polarization via inhibition of RBPJ and p53. Manuscript.*

Author affiliation:

1 Department of Dermatology, Medical University of Graz, Graz, Austria.

2 Department of Translational Skin Cancer Research, University Hospital Essen, Essen, Germany.

3 German Cancer Consortium (DKTK), Essen, Germany.

4 German Cancer Research Center (DKFZ), Heidelberg, Germany.

5 Department of Dermatology/Medicine, University of Washington, Seattle, Washington.

6 Department of Dermatology, University of Michigan, Ann Arbor, Michigan, USA.

7 Department of Immunology and Microbiology, University of Copenhagen, Copenhagen, Denmark.

8 Centre for Cancer Research, University of Melbourne, Melbourne, Australia.

9 Peter MacCallum Cancer Centre, Melbourne, Australia.

10 Sir Peter MacCallum Department of Oncology, University of Melbourne, Melbourne, Australia.

11 Department of Dermatology, Ruhr-University Bochum, Bochum, Germany.

12 Department of Dermatology, University Hospital Würzburg, Würzburg, Germany.

13 Department of Dermatology, University Hospital Essen, Essen, Germany.

14 Department of Medical Biology, University of Tromsø, Tromsø, Norway.

15 Department of Dermatology, Ruhr-Universität Bochum, Bochum, Germany.

16 Department of Microbiology and Molecular Genetics, University of Pittsburgh, Pittsburgh, USA.

17 Division of Hematology, Medical University of Graz, Graz, Austria

18 2Otto Loewi Research Center for Vascular Biology, Immunology and Inflammation, Division of Pharmacology, Medical University of Graz, Graz, Austria.

19 Research Group Bioinformatics, Faculty of Biology, University of Duisburg-Essen, Essen, Germany

Here I confirm that all co-authors have been acknowledged and agreed to use their data in my thesis. I have taken the permissions from American Association for Cancer Research (License: 4740670685410), Elsevier (No permission required as an author) and bioRxiv (No permission required as an author) for reproducing the publications into this thesis.

Acknowledgements

a. Doctoral College (DK): PhD student K. F. received funding from the Austrian Science Fund FWF (Grant ID: W 1241) and the Medical University of Graz through the PhD Program “DK-MOLIN”.

b. Doctoral School, funding by external grant: Doctoral student K. F. received funding from the “FP7 project IMMOMEC, Grant ID: 277775” and the Medical University of Graz through the Doctoral School.

The long, challenging PhD journey is coming to the end, I am so happy about meeting many great persons in the last years. First of all, I would like to thank DK-MOLIN program of Medical University of Graz as well as Prof. Heinemann and Prof. Becker for providing me the opportunity to study for a doctorate. I thank Austrian Science Fund (FWF) and FP7 project IMMOMEC for funding my project.

To my respectful supervisor Prof. Becker, my language is so limited that I have no idea how to express my gratitude. Thus, allow me to say thank you first. You enrolled me into your research group, always supported and encouraged me during my research. First two years in Graz and the rest years in Essen, you always trust me and help me in my research. When I was struck with unexpected experimental results, you are the one told me to look at the bright side in a different perspective.

The beginning of my PhD career in Graz was tough, because of my poor spoken English, my colleagues did not even understand what I was talking about in the first two months. In the lab of Graz, I would like specially thank Dr. David Schrama, who was supervising me directly in the lab. He was always patient about me and gave me suggestions about experiments. Cathrin and me have been working together for years, it is a great pleasure working with her and thanks for all the valuable inputs. Lab mama Gerlinde took care of me and helped a lot in the lab as well as in my daily life, thank you very much! Anna, Corrina and Richard, I am so glad that we worked together and thanks for always being there for me. Many thanks to personnel of Dermatology who helped me in my projects. Besides that, I would also like to thank my friends in Graz, Ge, Xue, Jianfeng, Cong, Qinghai, and so on, you guys added brilliance to my plain life. Most special thanks to the beautiful city Graz, where I met the love of life.

Later on, I followed prof. Becker's step and continued my PhD studying in Essen. I am grateful that we have such an energetic lab, and that was because of you, my lovely colleagues. I really was enjoying working together with them. Even most of time we were working independently in different projects, suggestions and discussions from them always benefit me in my project. Here I would like to say thanks to all of you, Ashwin, Lukas, Ivelina, Angela, Jan, Lina, Kai, Linda, Shakhlo, Corrina, Viola, Johnna and Lei. The same as in Graz, I would also thank personnel of Dermatology of Uniklinik Essen who helped me in my research. Thanks to my friends in the badminton club, I enjoyed a lot playing together with you, wonderful leisure activities actually promoted my research work on the other hand. Beside all that, many humble thanks to my other two thesis committee members Prof. Heinemann and Prof. Zebisch for their help and guidance.

Sure, this page would be incomplete if I stop here, I would like to thank my love Yuzhu, I have no idea if I could make it without your love and support. To my parents thousands of kilometers away, I would like to say that it's my honor to be your son and thanks for supporting me with everything I am doing. I love you. To all my friends and family members, thanks for your love and support. At last, love and peace to everyone who have supported me during my Ph.D. study.

Table of Contents

Abbreviations

AGO, Argonaute; **α-SMA**, alpha-smooth muscle actin; **ATOH1**, atonal BHLH transcription factor 1; **AUC**, calculated area under a ROC Curve; **anta-375**; antagomirs against miR-375; **anta-NC**, antagomirs negative control; **BCC**, basal cell carcinoma; **CAF**, cancer associated fibroblast; **ceRNA**, competing endogenous RNA; **CK20**, cytokeratin 20; **CM**, conditioned medium; **cMCC**, classical MCC; **CNVs**, copy number variations; **cSCC**, cutaneous squamous cell carcinoma; **CXCL2**, C-X-C motif chemokine ligand 2; **DC**, direct co-culture; **EMT**, Epithelial-mesenchymal transition; **EVs**, extracellular vesicles; **FAP**, fibroblast activation protein; **GSEA**, Gene Set Enrichment Analysis; **HLA**, leukocyte antigen; **HCV**, hepatitis C virus; **IF**, immunofluorescence; **IL-1β**, interleukin 1 beta; **LDHB**, lactate dehydrogenase b**; LT**, large T antigen; **MCC**, Merkel cell carcinoma; **MCPyV**, Merkel cell polyomavirus; **MHC**, major histocompatibility complex; **miRNA**, microRNA; **MRE**, miRNA response elements; **MVB**, multivesicular bodies**; NE**, neuroendocrine; **PD-1**, programmed cell death protein 1; **PD-L1,** programmed death ligand 1**; pre-miRNA**, precursor miRNA; **pri-miRNA**, primary miRNA transcripts; **RB1**, retinoblastoma protein; **RBPJ**, recombination signal binding protein for immunoglobulin kappa J region; **RISC**, RNA-induced silencing complex; **ROC**, receiver operating characteristic; **scRNAseq**, single cell RNA sequencing; **ST**, small T antigen; **TC**, transwell co-culture; **TP53**, tumor protein p53; **TME**, tumor microenvironment; **UV**, ultraviolet light; **vMCC**, variant MCC.

Abstract in German

Die Dysregulation von miRNAs ist bei allen bekannten Krebsarten zu finden und für die Karzinogenese, Metastasierung und das Behandlungsansprechen essentiell. Bestimmte Merkmale von miRNAs, wie die Zirkulation im Blut und die Stabilität, ermöglichen es ihnen, als Biomarker für die Diagnose, Prognose und Überwachung von Krebserkrankungen zu fungieren. Beim Merkelzellkarzinom (MCC), einem seltenen und aggressiven Hautkrebs, sind die Studien zu miRNAs eher begrenzt. Deshalb haben wir miRNA-Profiling in MCCs durchgeführt. miR-375 wurde als häufig vorkommende miRNA in klassischen MCC (cMCC) Zelllinien und Tumorgeweben identifiziert. Als nächstes zeigte das Vorhandensein von miR-375 in MCC-konditionierten Medien und Seren von zwei präklinischen MCC-Modellen, dass es wahrscheinlich als zirkulierende miRNA bei MCC-Patienten vorhanden ist. Tatsächlich unterscheiden sich miR-375-Serumspiegel zwischen MCC-Patienten mit und ohne Tumorlast, korrelieren mit dem MCC-Tumorstadium und dienen als wertvoller Marker für die MCC-Überwachung.

Als nächstes untersuchten wir die Funktionsweise der transkriptionellen Regulation von hochexprimierter miR-375 in MCCs. Der atonale BHLH-Transkriptionsfaktor 1 (ATOH1) gilt als abgeleiteter miR-375-Regulator. Die hohe Expression von ATOH1 wird in cMCC-Zelllinien und MCC-Geweben bestätigt und weist ein ähnliches Expressionsmuster wie miR-375 auf. Wir zeigen mittels Knockdown und Überexpression, dass ATOH1 der Induktor von miR-375 in MCC-Zellen und Fibroblasten ist. Interessanterweise induzieren die ektopische Expression von MCPyV LTs und ATOH1 ähnliche zellmorphologische Veränderungen, und die Expression von ATOH1 und miR-375 wird durch MCPyV LTs induziert.

Darüber hinaus untersuchten wir durch Knockdown mittels Antagomirs via Nukleofektion, die Rolle von miR-375 in MCC-Zellen. Der fast vollständige miR-375 Knockdown in cMCC-Zelllinien hat weder die Zellvitalität, noch die Zellmorphologie verändert. Zwei onkogene Signalwege, nämlich Hippo und EMT, die in MCC-Zellen durch miR-375 reguliert werden, wurden nur geringfügig verändert. Diese Beobachtungen machen miR-375 als intrazelluläres Onkogen in MCC-Zellen unwahrscheinlich.

Schließlich haben wir die Funktion von miR-375 in der interzellulären Signalübertragung untersucht, wobei wir uns auf die krebsassoziierte Fibroblasten-(CAF)-Polarisation konzentrierten. Exosomale MCC-abgeleitete miR-375 wurde auf Fibroblasten übertragen,

die ihre Polarisation in Richtung CAF-Phänotyp, einschließlich einer erhöhten Expression von α-SMA, CXCL2 und IL-1β, verursacht. Die in der Kokultur induzierte Fibroblastenpolarisation wird durch miR-375 Antagomire gehemmt oder durch ektopische miR-375 Expression, die RBPJ und p53 beeinflusst, imitiert. Eine Reihe von in situ Beobachtungen aus MCC-Tumorproben stimmen mit unserer Hypothese überein. So liefern wir mehrere Beweislinien, dass die miR-375-Expression in MCC eine protumorigene Mikroumgebung erzeugt, indem sie eine Fibroblastenpolarisation induziert. Zusammengefasst, zeigen wir in dieser Arbeit nicht nur, dass miR-375 als zirkulierender Serummarker für MCC dient, sondern erläutern auch die transkriptionelle Funktionsweise und Rolle in MCC-Zellen. Noch wichtiger ist, dass wir exosomale miR-375 aus MCC-Zellen zeigen, die Fibroblasten Richtung CAF-Phänotyp polarisieren.

Abstract in English

Dysregulation of miRNAs is found in all known cancer types and essential for carcinogenesis, metastasis and treatment responses. Certain features of miRNAs, such as circulating in the blood and stability, allow them to act as biomarker for cancer diagnosis, prognosis and monitoring. In Merkel cell carcinoma (MCC), rare and aggressive skin cancer, studies regarding miRNAs are rather limited. Thus, we performed miRNAs profiling in MCCs. miR-375 is identified and confirmed as highly abundant miRNAs in classical MCC cell lines and tumor tissues. Next, presence of miR-375 in MCC conditioned mediums and sera of two preclinical MCC models indicates it is likely present as a circulating miRNA in MCC patients. Indeed, miR-375 serum levels distinguish MCC patients with tumor burden or without, correlate with MCC tumor stage, and serve as valuable marker for MCC monitoring.

Next, we explored underline mechanism of transcriptional regulation of highly expressed miR-375 in MCCs. atonal BHLH transcription factor 1 (ATOH1) is considered as deduced miR-375 regulator. High expression of ATOH1 is confirmed in cMCC cell lines and MCC tissues and exhibits similar expression pattern as miR-375. We demonstrate that ATOH1 is the inducer of miR-375 in MCC cells and fibroblasts via knockdown and overexpression experiments. Interestingly, ectopic expression of Merkel cell polyomavirus large T antigens (MCPyV LTs) and ATOH1 induce similar cell morphologic changes, and ATOH1 and miR-375 expression are both induced by MCPyV LTs.

Furthermore, we examined the role of miR-375 in MCC cells via knockdown experiments using antagomirs via nucleofection. Nearly complete miR-375 knockdown in cMCC cell lines did neither change cell viability nor cell morphology. Hippo and epithelial–mesenchymal transition (EMT) related oncogenic signaling pathways, which are predicted as regulated by miR-375 in MCC cells, was only slightly altered. These observations render miR-375 unlikely as an intracellular oncogene in MCC cells.

At last, we scrutinized the function of miR-375 in intercellular signaling, focusing on cancer associated fibroblasts (CAF) polarization. Exosomal MCC-derived miR-375 is transferred to fibroblasts causing their polarization towards CAF phenotype including increased expression of alpha-smooth muscle actin (α-SMA), C-X-C motif chemokine ligand 2 (CXCL2) and interleukin 1 beta (IL-1β). Coculture induced fibroblast polarization

is inhibited by miR-375 antagomirs or mimicked by ectopic miR-375 expression via targeting recombination signal binding protein for immunoglobulin kappa J region (RBPJ) and p53. A series of *in situ* observations from MCC tumor samples are consistent with our hypothesis. Thus, we provide several lines of evidence that miR-375 expression in MCC generates a protumorigenic microenvironment by inducing fibroblast polarization.

Taken together, in this thesis, we not only demonstrate that miR-375 serves as a circulating serum marker for MCC, but also explore its transcriptional mechanism and functional role in MCC cells. More importantly, we demonstrate exosomal miR-375 derived from MCC cells polarizes fibroblasts into CAF phenotype.

1. Introduction

1.1 Merkel cell carcinoma

Merkel cell carcinoma (MCC), also called neuroendocrine tumor of the skin, is a rare and aggressive skin cancer. It was first described as "trabecular carcinoma of the skin" in 1972 by Cyril Toker (Toker, 1972). The following studies demonstrated that these tumor cells were bearing a phenotypic resemblance to Merkel cells, which were present in the basal layer of the epidermis and served as mechanoreceptors essential for light touch sensation (Maricich et al., 2009). Thus, the name was changed to Merkel cell carcinoma. Both Merkel cells and MCC cells are sharing similar neuroendocrine phenotypes, such as expressing markers cytokeratin 20 (CK 20), chromogranin-A and synaptophysin. Comparing to malignant melanoma, it is less common, but the case fatality rate (33%) is much higher than malignant melanoma (15%) (Stang et al., 2018, Kaae et al., 2010), largely due to the high probability of metastatic progression. As reported to date, relevant risk factors of MCC are including advanced age, ultraviolet light (UV) exposure, immune suppression and bearing chronic inflammatory disorders (Becker et al., 2017). Merkel cell polyomavirus (MCPyV) integration in the cell genome or exposure to UV radiation is considered associated with MCC pathogenesis. However, the distinct molecular pathogenesis of MCC and its link to MCPyV or UV exposure mostly remains elusive. Thus, the development of effective targeted therapies for MCC is impeded. For advanced MCCs, which are not amenable to surgery and/or radiotherapy, chemotherapy does not provide a concomitant survival advantage due to relatively high treatment-related morbidity and mortality (Duprat et al., 2011). But since 2016, using immune-checkpoint inhibitors therapies for MCC patients resulted in a strong survival benefit for metastatic MCC (Kaufman et al., 2016, Nghiem et al., 2016, Terheyden and Becker, 2017).

1.1.1 Epidemiology

MCC incidence rate was observed increasing in in Sweden, the Netherlands and the United States during 2005-2008, whereas the incidence date has been stable since 1995 in Denmark, Finland, Iceland and Norway (Agelli and Clegg, 2003, Girschik et al., 2011, Hodgson, 2005, Kukko et al., 2012). Improvements in cancer diagnosis, including the use of CK 20 immunostaining and identification of MCPyV integration in most MCCs, might contribute to the increase of the incidence of MCC. As a rare disease, the epidemiology of

MCC is not well studied. A comparison of MCC incidence between different countries is difficult because different measurements were applied in different studies. However, the incidence of MCC differs among geographic areas and ethnic groups (Agelli et al., 2010). Most representative MCC patient is a white male at his 70s or 80s with a history of extensive solar UV exposure. In the United States, around 1600 MCC patients were diagnosed every year, the median age of MCC patients at diagnosis is 75 to 80 years (Soltani et al., 2014, Youlden et al., 2014, Zaar et al., 2016). 5 years relative survival of patients in United States was around 60% (1973 -1999) and only 40% in Queensland, Australia (2006-2010) (Youlden et al., 2014).

1.1.2 Pathophysiology

Clonal integration of MCPyV in the genome or solar UV radiation-related DNA damage and mutations are considered as the original drive for MCC carcinogenesis (Becker et al., 2017). Notably, exposure to UV radiation not only can cause DNA damage but also result in local immunosuppression, which might be also essential for viral carcinogenesis (Prasad and Katiyar, 2017, Popp et al., 2002). UV radiation induces the generation of inflammatory mediators and alters the function of antigen-presenting dendritic cells, which causes a cascade of events and further decreases the local immune sensitivity (Prasad and Katiyar, 2017).

The MCC cells share morphological, immunohistological as well as ultrastructural features with Merkel cells, together with gene expression profiling and molecular analysis evidence, Merkel cells or Merkel precursor cells were hypothesized as the cellular origin of MCC. However, the direct histogenetic link between MCC and Merkel cells is missing, and Merkel cells are specialized as terminally differentiated cells, which are unable to divide (Becker et al., 2017). Thus, they are might not the origin of MCC cells. Researchers also provided evidence that MCC cells might also originate from pre-B/ pro-B cells (Zur Hausen et al., 2013), or dermal fibroblasts (Tilling et al., 2014).

1.1.2.1. Merkel cell polyomavirus

The fact that MCC tumors occur more frequently among the patients suffering long-term immune suppression indicates the involvement of infectious pathogens. Chang-Moore group performed unbiased metagenomic next-generation sequencing and identified a new human polyomavirus in MCC (Feng et al., 2008). They also demonstrated viral DNA was clonally integrated in the host DNA in eight of ten tumor samples (Feng et al., 2008).

Ensuring studies on more MCC patient cohorts confirmed the presence of MCPyV in most of tested samples (Shuda et al., 2008, Becker et al., 2009). Further evidence indicates that virus integration is an early event in the MCC tumorigenic process and likely playing an essential etiologic role (Houben et al., 2010, Schrama et al., 2019). However, the association between MCPyV status in the tumor and patient survival rate is controversial (Laude et al., 2010, Bhatia et al., 2010, Schrama et al., 2011).

MCPyV is a small-sized, circular and double-stranded DNA virus, which belongs to the Polyomaviridae family (Gheit et al., 2017). MCPyV infection is common on the skin, high seroprevalence is detected in the healthy adult population (Pastrana et al., 2009), no sign or symptom is observed in the primary MCPyV infection (Tolstov et al., 2011). These evidences indicate that MCPyV is a general component of normal microbial skin flora (Loyo et al., 2010). Similar to other members of Polyomaviridae family, MCPyV genome contains an early region encoding proteins for viral replication (large T antigen (LT), small T antigen (ST) and 57k T antigen) and late region encoding proteins for viral capsid (viral protein 1 and viral protein 2) (Feng et al., 2008, Schowalter and Buck, 2013). Moreover, a viral miRNA named as MCV-miR-M1 is also encoded by in the virus genome (Lee et al., 2011), its function is not yet explored.

1.1.2.2. Oncogenic role of MCPyV

After MCPyV was reported as an MCC-associated virus, the gap between common MCPyV infection and low incidence of MCC leads to the question: Why? Based on the observed pieces of evidence, at least two events are required for MCPyV to act as an oncogenic role in MCC tumor development. The first is MCPyV genome integration into the host genome and the second is that LT is truncated due to different mutations impeding viral replication (Feng et al., 2008, Shuda et al., 2008). The virus genome might occasionally integrate into the host genome during replication, it remains unclear whether MCPyV possesses preferred integration sites in human genome, it seems that MCPyV is randomly integrated into host genome (Martel-Jantin et al., 2012, Duncavage et al., 2011). Another event is LT truncation, the helicase domain, DNA binding domain, and cell growth inhibitory domain are disrupted, but retinoblastoma-associated protein (RB1) binding motif remains intact, which allows LT to bind to RB1 protein and supports growth of tumor cells (Shuda et al., 2008, Kwun et al., 2009, Li et al., 2013). MCPyV virions are no longer produced in the MCC cells carrying integrated and mutated MCPyV genome. Despite the fact that the mechanism of MCPyV integration is largely unknown, those two

events are reported essential for the MCC development (Becker et al., 2017, Harms et al., 2018). Regarding which event occurs first, David et al. indicated that LT mutations happened before MCPyV integration based on their observation of discrete stop-codon mutations in MCC cells with concatemeric virus integration (Schrama et al., 2019). Moreover, the extremely low probability of both events may give an explanation about the gap mentioned in the question above.

Early genes of MCPyV, LT and ST are considered as viral oncoproteins contributing to oncogenesis of MCC (Houben et al., 2010, Houben et al., 2012, Shuda et al., 2014). Knockdown expression of LT and ST results in cell death of MCPyV positive MCC cells, indicating they are required for proliferation and/ or cell survival. As mentioned above, truncated MCPyV LT binds to RB1 protein and promote cell growth via upregulation of the survivin expression (Houben et al., 2012). Growing evidences indicate that MCPyV ST is an oncogenic protein in MCPyV positive MCC oncogenesis, especially in cell transformation step. ST expression alone could transform rat-1 fibroblasts (Shuda et al., 2011), and human fibroblasts when co-expressing truncated LT *in vitro* (Cheng et al., 2013). ST transgenic mice experiments indicate that ST expression can lead to tumor formation in different organ systems (Verhaegen et al., 2015, Spurgeon et al., 2015). More important, co-expressing atonal BHLH transcription factor 1 (ATOH1) and MCPyV ST in mice result in MCC-like tumor formation (Verhaegen et al., 2017). Besides that, MCPyV ST harbors a domain known as LT-stabilizing domain inhibiting different E3 ubiquitin ligases via binding to F-Box And WD Repeat Domain Containing 7 (FBXW7) (Kwun et al., 2013, Shuda et al., 2015). Co-expression LT and ST shows that LT is stabilized by ST expression, other oncogenes like C-myc might be also benefited from ST expression in MCC cells (Kwun et al., 2013). MCPyV LT could also regulate host gene expression, it promotes cap-dependent mRNA translation of proglycolytic genes via phosphorylation of eukaryotic translation initiation factor 4E (eIF4E)-binding protein 1 (4E-BP1) (Shuda et al., 2015).

1.1.2.3. Mutation patterns in MCC subtypes

MCC tumors were classified into two MCC subtypes according to the MCPyV status: MCPyV+ MCCs and MCPyV- MCCs. Besides MCPyV integration is associated with MCC oncogenesis, mutation load in MCC tumors, including chromosomal copy number variations (CNVs) and other mutations, are scrutinized by different research groups. Almost all the MCC tumors are carrying chromosomal CNVs, MCPyV- MCCs typically

harbor more CNVs than MCPyV+ MCCs (Paulson et al., 2009). Comparing to MCPyV+ MCCs, MCPyV- MCCs possess much a higher somatic mutation load associated with UV radiation, which is the feature of other skin cancer types, e.g. melanoma, and cutaneous squamous cell carcinoma (SCC) and basal cell carcinoma (BCC) (Harms et al., 2015, Goh et al., 2016, Wong et al., 2015).

In MCPyV- MCCs, mutations associated with inactivation of tumor suppressor genes is another feature, such as TP53, RB1, the members of Notch signaling pathway (Wong et al., 2015, Cimino et al., 2014). On the contrary, TP53 and RB1 are intact in most of MCPyV+ MCCs (Cimino et al., 2014). Some the hotspot activating mutations in other human cancers, i.e. KRAS, HRAS, and PIK3CA, are detected in both MCPyV+ MCCs and MCPyV- MCCs, while other hotspot activating mutations, like AKT1, RAC1, EZH2, and CTNNB1, are only observed in MCPyV- MCCs (Hafner et al., 2012, Nardi et al., 2012, Cimino et al., 2014, Wong et al., 2015, Goh et al., 2016, Harms et al., 2015). Those mutations are conducive to intracellular signaling changes involved in MCC tumorigenesis.

1.1.2.4. Immunogenicity of MCC tumors

Integrated MCPyV in MCPyV+ MCCs and high mutational load in MCPyV- MCCs composed the immunogenicity of MCC. In most patients with MCPyV+ MCC tumors, epitopes of $CD8^+$ T cells against LT and ST are frequently observed (Lyngaa et al., 2014), and $CD8^+$ T cells infiltration in MCC tumors indicates better prognosis (Paulson et al., 2011). However, intratumoral $CD8^+$ T cells infiltration only occurs in less than 20% MCC tumors, and those infiltrated $CD8^+$ T cells in MCC tumors are frequently categorized as exhausted T cells (Paulson et al., 2011, Walsh et al., 2016, Dowlatshahi et al., 2013). Moreover, human leukocyte antigen (HLA) class I expression was found deregulated in MCC cells, which might contribute to lack of CD8+ T cells infiltration in MCC tumors (Ritter et al., 2017).

1.1.3 Immunotherapy treatment on MCC and urgent necessity for biomarker

Immune checkpoint inhibitors treatment results in a strong therapeutic effect on MCC patients base on the immunogenicity of MCC tumors. Programmed cell death protein 1/ligand 1(PD-1/PD-L1) checkpoint inhibitors have been demonstrated to create durable tumor response (Terheyden and Becker, 2017, Kaufman et al., 2016, Nghiem et al., 2016). To be noted here, highest tumor responses exists in first-line therapy of patients bearing

limited tumor burden, stressing the demand for reliable approaches for early detection of tumor recurrence in MCC patients who has no tumor burden after surgery or chemotherapy (Kaufman et al., 2016, Nghiem et al., 2016, Terheyden and Becker, 2017). Furthermore, around 40-60% of patients do not respond to checkpoint inhibitor treatment (Terheyden and Becker, 2017). Thus, a blood-based surrogate biomarker of tumor burden, which can be serially assessed, could be a useful tool for both early detection of tumor relapse and monitoring of different treatment.

1.2 microRNAs

1.2.1 Biogenesis pathway of miRNAs

miRNAs located at different regions in the human genome: introns of protein-encoding genes, intergenic regions or even within the exons of the genes (Lagos-Quintana et al., 2001, Lagos-Quintana et al., 2003). According to the different locations, the transcription regulation mechanisms are also different. miRNAs in the introns are typically transcribed together with the host genes (Rodriguez et al., 2004, Aravin et al., 2003, Lim et al., 2003), while intergenic miRNAs are transcribed independently utilizing their own promoters (Lagos-Quintana et al., 2003, Rodriguez et al., 2004).

Generally, two cleavage events occurred in the miRNA's biogenesis process: Drosha complex in the nuclear and following Dicer complex in the cytoplasm, both of them are ribonuclease III endonucleases (Denli et al., 2004, Gregory et al., 2004, Hutvagner et al., 2001, Lee et al., 2003). Primary miRNA (pri-miRNA) is transcribed by RNA Pol II or Pol III with a stem-loop secondary structure, cleaved by protein complex composed of Drosha and RNA-binding protein DiGeorge syndrome chromosomal region 8 (DGCR8) in the nuclear (Borchert et al., 2006, Han et al., 2006). Subsequently, cleaved pri-miRNA, so called miRNA precursor (pre-miRNA), is exported into the cytoplasm through transporter Exportin-5 complex (Bohnsack et al., 2004, Okada et al., 2009, Zeng and Cullen, 2004). Pre-miRNA is cleaved by the Dicer complex into miRNA duplex in the cytoplasm (Chendrimada et al., 2005). At last, mature miRNA incorporates with Argonaute (AGO) protein of RNA-induced silencing complex (RISC). To be noted, besides the conical biogenesis pathway described above, a few miRNAs maturation process doesn't require Drosha or Dicer cleavage, such as mirtrons can bypass Drosha processing (Babiarz et al., 2008, Okamura et al., 2007, Ruby et al., 2007).

1.2.2 Function of miRNAs

In general, miRNAs bind to the 3' UTR of target mRNAs and downregulate their expression. One miRNA can target to hundreds of mRNAs while the same mRNA can be regulated by handful of individual miRNAs (Bartel, 2004). miRNA largely recognize target mRNAs through "seed pairing", positions 2-8 from the miRNA 5´-end, which is the principle for target sites prediction (Bartel, 2009).

miRNAs mostly mediate gene silencing at post-transcriptional level, mRNA degradation and/ or translational repression. In plants, mRNA degradation is mediated by perfect base-pairing between miRNA and target mRNA, cleaved by Argonaute (Yekta et al., 2004). In animals, miRNA-mediated mRNA poly(A) tail removal lead to trigger mRNA degradation, a glycine-tryptophan protein of 182 kDa (GW182) is recruited by AGO in this process (Behm-Ansmant et al., 2006). Imperfect base-pairing between miRNA and target mRNA generally result in translational repression. Regarding the silencing mechanism, most experimental evidences indicate that the miRISC induces eIF4A-I and eIF4A-II dissociation from target mRNAs, thus eIF4F translation initiation complex assembly is inhibited (Petersen et al., 2006, Meijer et al., 2013, Fukao et al., 2014). However, to data, the miRNA mediated translation repression is still not fully understood (Gebert and MacRae, 2019).

On the contrary, miRNAs can also induce target genes expression, such as miR-122 binds to hepatitis C virus (HCV) RNA 5'UTR and protect HCV RNA from degradation (Jopling et al., 2005), miR-369-3p binds to tumor necrosis factor (TNF) mRNA 3'UTR and increase its translation (Vasudevan and Steitz, 2007, Vasudevan et al., 2007). Further studies demonstrated that miRNAs could influence other miRNAs expression, for example, mouse miR-709 can inhibit primary miR-15a/16-1 cleavage by binding to its target sequence (Tang et al., 2012).

1.2.3 miRNAs in human cancer disease

Deregulation of miRNAs expression is confirmed in all known human cancer types after decade research. Underline mechanisms include genomic alterations, transcriptional factors dysregulation, defects in miRNA biogenesis and epigenetic modifications (Gebert and MacRae, 2019). Genomic alterations, including amplification, deletion or translocation of miRNA gene copy number or location, often provoke irregular miRNA expression in human cancer cells. Frequent deletion of miR-143/145 harboring region (5q33) leads to down-regulation of their expression in human colorectal and breast cancer (Iorio et al.,

2005, Michael et al., 2003). Same as protein encoding genes, miRNA expression is also tightly controlled by transcriptional factors network. Therefore, dysregulation of different key transcriptional factors, e.g. C-myc and p53, results in abnormal miRNAs expression (Gebert and MacRae, 2019, Peng and Croce, 2016). Ectopic C-myc expression in malignant cells impedes the expression of miR-15/26/29/30 and let-7 family, which are classified as tumor suppressive miRNAs (Chang et al., 2008). p53 binds to miR-34a promoter to induce its expression and trigger apoptosis. miRNA biogenesis is controlled by different key enzymes and proteins as described above (Raver-Shapira et al., 2007). Thus, atypical expression or mutations of those genes often cause disruption of miRNA expression. For example, in a rare kidney cancer, single nucleotide mutations on DGCR8 and Drosha significantly diminish the expression of miR-200 and let-7 family (Walz et al., 2015). Another hallmark of cancer is epigenetic alterations, including ectopic DNA hypomethylation or hypermethylation and abnormal histone acetylation and deacetylation patterns. For example, due to DNA hypermethylation of respective promoter regions, miR-124a, miR-145 and miR-9-1 expression is inhibited in lung, colon and breast cancer cells respectively (Lehmann et al., 2008, Lujambio and Esteller, 2007, Donzelli et al., 2015). In addition to those factors, miRNA response elements (MRE)-containing non-coding RNA transcripts, also called competing endogenous RNAs (ceRNAs), are reported as miRNA sponge regulating miRNA function and expression level, such as phosphatase and tensin homolog pseudogene 1 (PTENP1) can impound miR-19b/ 20a targeting phosphatase and tensin homolog (PTEN) (Poliseno et al., 2010).

Function of miRNAs in cancer cells reflects in all features of human cancers, which was surmised as six hallmarks (Hanahan and Weinberg, 2011). Upregulation of oncogenic miRNAs or downregulation of tumor suppressive miRNAs sustain proliferative signaling, e.g. oncogenic miR-17-92 cluster targets E2F Transcription Factor 1 (E2F1) to promote cell proliferation (Coller et al., 2007), decreased miR-486 expression in non-small-cell lung cancer influence cell proliferation as well as cell migration by regulating insulin-like growth factor (IGF) and PI3K-AKT signaling (Peng et al., 2013). Similar to miRNAs regulate cell proliferation signaling, differentially expressed miRNAs are deeply involved in regulating signaling pathways controlling evading growth suppressors (miR-221/222 target to cell-cycle inhibitor p27 in glioblastoma cells) (Gillies and Lorimer, 2007), resisting cell death (Decreased expression of miR-15a/16-1 upregulate Bcl-2 expression to inhibit cell apoptosis in chronic lymphocytic leukemia) (Cimmino et al., 2005), enabling

replicative immortality (Fas ligand is targeted by miR-590 to promote cell survival in acute myeloid leukemia) (Shaffiey et al., 2013), activating invasion and metastasis (miR-200/205 family targets ZEB1 and SIP1 to promote Epithelial-mesenchymal transition (EMT) and tumor metastasis) (Gregory et al., 2008, Bracken et al., 2008) and inducing angiogenesis (hypoxia induced miR-210 targets EFNA3 ephrin A3 to boost VEGF expression) (Camps et al., 2008, Liu et al., 2012).

1.2.4 Human cancer virus related miRNAs

Around 20% human cancers are associated with virus infection, including Epstein-Barr Virus (EBV) in Burkitt lymphoma, Hepatitis C virus (HCV) and Hepatitis B virus (HBV) in liver cancer, human papillomavirus (HPV) in cervical cancer, Human T-cell leukemia virus (HTLV-1) in leukemia as well as Merkel cell polyomavirus (MCPyV) in Merkel cell carcinoma (Vojtechova and Tachezy, 2018). To be noted, most of the cancer associated virus can not cause carcinogenesis themselves, they might live together with the host for decades without tumor development (Vojtechova and Tachezy, 2018). Therefore, other factors like immune suppression, oncogenic mutations in host cells and chronic inflammation are essential to trigger carcinogenesis of virus associated cancers.

Viruses gain the ability to manipulate host miRNAs for their replication during evolution. As described before, 5'UTR of HCV RNA is protected by miR-122 binding to against RNA degradation induced by the cellular antiviral response (Jopling, 2008). On the other hand, HBV significantly decreased miR-122 expression in liver cells, because miR-122 impede its infection (Wang et al., 2012b).

Utilizing miRNA processing machinery of host cells, viruses encode their own miRNAs. Plenty of virus-encoded miRNAs were discovered by deep sequencing and identified in the last 20 years, such as miR-BHRF1-3 encoded by Epstein–Barr virus (EBV) (Feederle et al., 2011), miR-S1 encoded by simian virus 40 (SV40) (You et al., 2012, Sullivan et al., 2005), miR-UL112 encoded by Cytomegalovirus (CMV) (Nachmani et al., 2010), and so on… Virus-encoded miRNAs are proved not only targets to their own viral genes but also regulate the expression of host cellular genes associated with cell proliferation or apoptosis. For example, SV40 miR-S1 can regulate SV40 large T antigen expression in the late stage of infection (Sullivan et al., 2005), while EBV miR-BART5 targets to proapoptotic gene PUMA to sustain host cell survival (Choy et al., 2008).

1.2.5 miRNAs in Merkel cell carcinoma

miRNAs profiling using next generation sequencing (NGS) or miRNA microarray has been performed in MCC by different research groups (Renwick et al., 2013, Xie et al., 2014, Veija et al., 2015, Ning et al., 2014, Abraham et al., 2016a), however, the results are not consistent. We performed miRNA microarray as well as Nanostring miRNA panel with MCC cell lines and confirmed miR-375 as the highly expressed miRNA in MCPyV+ cell lines comparing to MCPyV- cell lines (Fan et al., 2018). Renwick et al and Xie et al also identified miR-375 as highly expressed miRNAs in the MCPyV+ cell lines (Renwick et al., 2013, Xie et al., 2014), however, in the study of Veija et al and Ning et al (Ning et al., 2014, Veija et al., 2015), miR-375 was not identified as highly expressed miRNA. Regarding the biological function of miR-375 in MCCs, different studies also draw different conclusions. Abraham et al stated that miR-375 was a positive regulator of NE differentiation vie targeting Notch pathway molecules (Abraham et al., 2016a), while Xie et al revealed that miR-375 and its target lactate dehydrogenase b (LDHB) were playing dual roles in MCPyV+ and MCPyV- MCC cell lines, overexpression of miR-375 in MCPyV- MCC cells resulted in cell growth arrest and increased apoptosis while miR-375 inhibition in MCPyV+ MCC cells had a similar effect (Xie et al., 2014). Besides miR-375, the functional role of miRNA downregulated in MCCs, such as miR-209, was also explored. miR-203 overexpression decreased cell growth ability via regulating expression of the survivin in MCPyV- MCC cells, but not MCPyV+ cells (Xie et al., 2014).

1.3 miRNAs, exosomes and cancer

Functions of miRNAs in the cytoplasm are simply described as above, miRNA targeting gene regulation is restricted in the same cell, however, the discovery of intact miRNAs in exosomes provided solid evidence that they might be essential in various intercellular signaling.

1.3.1 Biogenesis and composition of exosomes

Exosomes are secreted extracellular vesicles originated from endosomal, size between 40 to 100nm (Johnstone et al., 1987). In the last decade, exosomes were proved to be released by plenty of different cell types and now researchers assume that all the cell types secret exosomes (Zitvogel et al., 1998). Exosomes also display the similar phenotypic state of the cells in which they were produced (Samanta et al., 2018). They are formed through endocytic invagination in the cells, multivesicular bodies (MVBs) are generated in the intracellular endosomes, then MVBs fuse with the plasma membrane and release to

extracellular space as exosomes (Akers et al., 2013). Exosomes are released from the plasma membrane, thus have the ability to fuse with the plasma membrane of recipient cells (Svensson et al., 2013). They contain various proteins (tetraspannins CD63 and CD81, heat shock proteins Hsp70 and Hsp 90, membrane transport and fusion proteins- Annexins, GTPases, major histocompatibility complex (MHC) class I or II, integrins and others diverse proteins), significant amounts of miRNAs named as exosomal miRNAs, long non-coding RNAs, functional mRNAs and even fragments of single-stranded DNA (Samanta et al., 2018, Mathieu et al., 2019).

1.3.2 miRNAs packaging in exosomes

After miRNAs were identified in exosomes, question is raised as followed: are those miRNAs actively and selectively packed into exosomes? To answer this question, the first evidence is that miRNAs are enriched in the exosomes comparing in the cells (Goldie et al., 2014). Following investigations not only answered that question, but also provided evidence of different miRNAs sorting mechanisms into exosomes. Proteins in RNA-induced silencing complex (RISC), such as GW182 and Ago2 (Lee et al., 2009, Gibbings et al., 2009), waxy lipid molecules called ceramide are reported regulating miRNA sorting (Kosaka et al., 2010) into exosomes. GGAG motif of miRNAs as well as their guide protein (e.g. miR-17 and Heterogeneous nuclear ribonucleoprotein (hnRNP) A2B1) are also important for miRNA sorting into exosomes (Villarroya-Beltri et al., 2013, Santangelo et al., 2016). Furthermore, expression level of both miRNAs and relative miRNA targets influence exosome miRNA sorting, which was proved by overexpression of miR-511-3p and its target gene Rock2 in Dicer *fl/fl* murine bone marrow derived macrophages (Squadrito et al., 2014).

1.3.3 Exosomes (ExomiRs) functions in cancer

As exosomes can be secreted by any type of cells, the functions of exosomes are extensive. Exosomes are reported regulating specific immune responses of T cells via expression of MHC class I/II on their surface (Zitvogel et al., 1998). In this thesis, we mainly introduce the function of exosomes in cancer. It's well known that communications between tumor cells and stromal cells are essential for cancer progression, which will be introduced in the next section.

More and more investigations indicate that tumor cells transfer proteins and RNAs, especially miRNAs, via exosomes, thus modulate stromal cells and immune cells activity

to create a tumor supportive microenvironment (Mathieu et al., 2019). Endothelial cells can be activated by exosomes derived from tumor cells to favor angiogenesis and further tumor metastasis. Exosomal miR-25-3p transferred from colorectal cancer cells target KLF2 and KLF4 in endothelial cells, thus promote angiogenesis (Zeng et al., 2018). Growing evidences have demonstrated that exosomes from cancer cells are playing a critical role in building immunosuppressive microenvironments by modulating infiltrated immune cells, including CD8+ effector T cells, regulator T cells, natural killer cells as well as dendritic cells and myeloid-derived suppressor cells (Samanta et al., 2018, Zhang et al., 2015b). Another function of exosomes derived from tumors is that they can reprogram stromal cells into cancer associated fibroblasts (CAFs) to promote tumor progression or metastasis (Paggetti et al., 2015).

In turn, stromal cells and immune cells derived exosomes also have an impact on cancer cells. Exosomes derived from CAFs, miRNAs as miR-21 and miR143, were transferred into cancer cells and enhanced EMT related genes expression in breast cancer (Donnarumma et al., 2017). Besides CAFs, exosomes from marrow-derived mesenchymal stem cells (BM-MSCs) could inhibit cancer cells proliferation but enhanced resistance to chemotherapy in breast cancer cell line MDA231 (Ono et al., 2014). Other stromal cells like endothelial cells, macrophages and T cells can promote tumor progression via exosomes transferring (Zhang et al., 2015b). However, exosomes released by natural killer (NK) cells have different functions, exosomes containing granzymes A/B and cytotoxicity factors perforin 1 could kill tumor cells (Zhu et al., 2017), and exosomal miR-186 from NK cells reduces cell proliferation as well as immune escape in neuroblastoma (Neviani et al., 2019). Besides NK cells, exosomes derived from dendritic cells were showed to be able to activate immune response against cancer cells (Pitt et al., 2016).

In addition to the communications between tumor cells and stromal cells in the tumor microenvironments, tumor cells themselves also exchange materials through exosomes (Samanta et al., 2018). Exosomes derived from tumor cells can transfer oncogenic traits between cancer cells, for example, miR-200 transferred between cancer cells via exosomes drives EMT in breast cancer cells (Le et al., 2014). Moreover, tumor cells could develop drug resistance by receiving exosomes containing drug-resistant proteins or miRNAs from other tumor cells (Maacha et al., 2019).

1.4 Circulating miRNAs

Circulating miRNAs presence is first discovered in human blood by Chim et al in 2008 (Chim et al., 2008), following researches demonstrate that miRNAs exist in almost all the body fluids, such as urine, saliva, tears, milk, cerebrospinal fluid, colostrum, bronchial lavage, peritoneal fluid, ovarian follicular fluid and seminal fluid (Weber et al., 2010). Here we focus on the researches about circulating miRNAs in serum/ plasma. Questions are asked about circulating miRNAs are as follows: What's the features of those circulating miRNAs comparing to the cellular miRNAs? Due to the low amount and tiny size of circulating miRNAs, how to solve the challenge to quantify them? Are those circulating miRNAs specific for different disease and what's the function of them?

1.4.1 Features of circulating miRNAs

One important feature of circulating miRNAs is that they are very stable comparing to the cellular miRNAs, resistant to endogenous RNase activity (Hamam et al., 2017). Circulating miRNAs are stable at room temperature up to four days, even after boiling, freeze-thaw cycles, and extreme pH change (Mitchell et al., 2008, Dong et al., 2017). Underline mechanisms are also explored, part of the circulating miRNAs is protected in the exosomes or other extracellular vesicles like microvesicles (Gibbings et al., 2009), and apoptotic bodies, part of the circulating miRNAs is binding with proteins like AGO2 and/or high-density lipoprotein (HDL) (Arroyo et al., 2011, Vickers et al., 2015). However, it remains unsettled about the percentage of miRNAs travelling in exosomes, some groups reported only a few circulating miRNAs existing in exosomes in human serum (around 10%) (Arroyo et al., 2011, Turchinovich et al., 2011), while other groups reported that most of the circulating miRNAs in the serum are exosome-associated (83% to 99%) (Gallo et al., 2012). The difference might due to different methods were used for exosome isolation or limited miRNAs in a few plasma samples were measured (Gallo et al., 2012). As part of the circulating miRNAs is associated with exosomes, exosome associated miRNAs are sorted as introduced above, secretion of circulating miRNAs is also under selection, not randomly released (Hamam et al., 2017). Nevertheless, the uptake mechanisms of circulating miRNAs are not well known, recipient cells might receive exosome associated circulating miRNAs by exosome endocytosis, while exosome-free miRNAs might enter recipient cells through specific cell surface receptors, such as

miRNAs associated with HDL can enter the cells by HDL receptor (Turchinovich et al., 2013, Turchinovich et al., 2011).

1.4.2 Quantification of circulating miRNA

It is a challenge to quantify circulating miRNA accurately in body fluids. Several methods have been established to solve this problem, however, each of them has its own advantages and drawbacks. miRNA qRT-PCR is widely used for the measurement, it possesses high sensitivity, but it is mostly used to quantify a small set of miRNAs (Hardikar et al., 2014). Thus, instead of high-throughput profiling, this method is suitable for validation of result from profiling. While miRNA microarray allows researchers to detect large numbers of circulating miRNAs at the same time, but the dynamic range is low, novel miRNAs (unannotated) could be missed (Garcia-Elias et al., 2017). Another method is next-generation sequencing, then all the miRNAs could be detected using this method, however, large amounts of material is required, therefore some patient serums are not feasible to use this method (Coenen-Stass et al., 2018). Moreover, data generated from next-generation sequencing is complex, bioinformatics tools are required for analysis. miRNA NanoString nCounter panel can measure the exact copy number of miRNAs in samples, but now only 800 miRNAs can be detected in human samples (Shukla et al., 2018).

1.4.3 Circulating miRNAs as cancer biomarkers

Several features of circulating miRNAs make them to become outstanding biomarkers (Wang et al., 2018). Firstly, materials for circulating miRNAs, such as patient serum/ plasma, are easy to access. The second is the stability of circulating miRNAs, they are protected in the exosomes or binding proteins. The last one is that, as introduced before, exosomes miRNAs could reflect the miRNA expression profile of parental tumor cells. Circulating miRNAs together with already established protein and circulating tumor DNA markers are promising to provide better solution for different human cancers diagnosis and/ or prognosis. Circulating miRNAs have been identified as biomarker in many cancer types: miR-141 for advanced prostate cancer (de Souza et al., 2017), miR-1246 for breast cancer (Hamam et al., 2017), an exosomal miRNA panel (let-7a, miR-21, miR-23, miR-150, miR-223, miR-1229, and miR-1246) for colorectal cancer (Ogata-Kawata et al., 2014), miR-92a for acute leukemia (Elhamamsy et al., 2017), miR-192 and miR-29a-3p for HBV positive hepatocellular carcinoma (Zhu et al., 2016) and so on… To be noted, we also have

identified miR-375 as MCC serum marker for MCC tumor burden recently in Paper I (Fan et al., 2018) .

1.4.4 Possible functions of circulating miRNAs

Besides being used as cancer biomarkers, we are also interested in whether those miRNAs in biological fluid still have certain function in the human body. Growing evidences strongly demonstrate that miRNAs transferred via exosomes result in downregulation of their target genes and subsequently phenotypic and genetic alteration in the recipient cells, however, for circulating miRNAs, it remains unsettled that whether they could decrease target genes expression in recipient cells due to the low concentration in the blood (Sohel, 2016). Several studies indicate that circulating miRNAs might promote tumor cells metastasis via contributing to building a premetastatic niche, such as miR-122 could reprogram glucose metabolism of the recipient cells in premetastatic niche in breast cancer (Fong et al., 2015), circulating miRNAs targeting PTEN also contribute to tumor metastasis to the brain (Zhang et al., 2015a). However, circulating miRNAs are associated with exosomes as introduced above, it is not clear that those changes in recipient cells are induced by miRNAs or other exosomal components. Thus, more investigations are required to better understand the functions of circulating miRNAs.

1.5 Cancer associated fibroblasts in the tumor microenvironment

Tumor microenvironment is defined as a common term of diverse cell types including resident and infiltrated immune cells (lymphocytes, macrophages, myeloid-derived suppressor cells), fibroblasts, endothelial cells and other cell types, extracellular matrix and a variety of secreted factors in the tumor (Binnewies et al., 2018). In primary tumors, the fate of tumor, eliminated by immune cells, initiate dormant micro-metastasis or long-distance metastasis, is highly influenced by the tumor microenvironment, and finally determined by the interaction of stromal cells and cancer cells. Immune escape/ evasion, hypoxia, angiogenesis and invasion caused by these interactions are essential for tumor progression and therapeutic response or resistance. Targeting stromal cells instead of tumor cells achieved great success, the best example is the application of immune checkpoint inhibitors for treatment (Havel et al., 2019, Nghiem et al., 2016).

Among different cell types in the tumor microenvironment, cancer associated fibroblasts are the most abundant component of the stroma (Kalluri, 2016). All the fibroblasts existing in the tumor mass are defined as CAF, growing evidence demonstrate that they

are deeply involved in affecting tumor progression (Kalluri, 2016, Chen and Song, 2019). CAFs are heterogeneous, composed of various subtypes, the origin of CAF is not well known now, researches demonstrate that some CAFs subtypes are polarized from local fibroblasts and others might differentiated from mesenchymal stem cells (Kalluri, 2016, Chen and Song, 2019).

1.5.1 CAF heterogeneity

Plenty of surface, intracellular and secreted protein markers are applied to identify and define CAF subtypes. To date, α-SMA (Tomasek et al., 2002, Ayala et al., 2003), fibroblast-specific protein 1 (FSP1/ S100A4) (Iwano et al., 2002, Orimo et al., 2005), serine protease fibroblast activation protein (FAP) (Tchou et al., 2013, Arnold et al., 2014), platelet-derived growth factor receptor-β (PDGFRβ) (Pietras et al., 2008, Pena et al., 2013), CXC-chemokine ligands (CXCL2, CXCL12) (Erez et al., 2010, Ahirwar et al., 2018), component of collagen type I (COL1A1) (Wei et al., 2018), interleukins (IL-1β, IL-6) (Erez et al., 2010, Qiao et al., 2018), matrix metalloproteinases (MMPs) (Hassona et al., 2014) and other related proteins are reported as CAF markers in different investigations. However, none of those reported CAF markers are exclusive for activated fibroblasts identification, take α-SMA as example, it is most used and well-established CAF marker (Kalluri, 2016), but it cannot be used to identify all CAF subtypes in the tumor microenvironment (Ohlund et al., 2017, Ayala et al., 2003) and also serves as common marker for smooth muscle cells (Ohlund et al., 2014). FAP can be detected in CD45 positive immune cells and FSP1 is also present in macrophages (Österreicher et al., 2011, Arnold et al., 2014). It's also important to point out that functional activated fibroblasts generally only express part of the listed CAF markers, not all of them. According to those expression pattern of CAF markers, CAFs are classify into different subsets (Kalluri, 2016). Beside the markers, different CAF origin precursor fibroblasts also contribute to fibroblasts heterogeneity (Kalluri, 2016, Quail and Joyce, 2013).

1.5.2 CAF activation/ polarization

CAFs are generally considered tumor supportive, however, fibroblasts derived from normal tissues demonstrate anti-tumor effects in vitro experiments (Alkasalias et al., 2014). Thus, CAF activation is the process that normal fibroblasts or other CAF precursor cells being reprogrammed into tumor supportive CAFs by cancer cells, also

known as “educated by cancer cells”. A pile of factors derived from cancer cells and particular tumor microenvironment (TME) factors, such as oxidative stress (Toullec et al., 2010) and hypoxia, are governing this process (Chen and Song, 2019). Regarding cancer derived factors, TGF-β (Quante et al., 2011), IL-6 (Giannoni et al., 2010) and PDGF (Pietras et al., 2008) are mostly studied factors activating fibroblasts (Kalluri, 2016). Those factors bind to their corresponding receptors and trigger cell signaling associated with CAF phenotypes and enhanced proliferative and invasive properties. Besides that, RBPJ and p53 were also reported involved in CAF activation (Procopio et al., 2015, Kim et al., 2017, Goruppi et al., 2017, Arandkar et al., 2018).

Alternately, stromal fibroblasts can be activated/ polarized by receiving exosomes derived from cancer cells or other stromal cells (Webber et al., 2010, Goulet et al., 2018). As introduced above, exosomes are carrying various growth factors and/ or cytokines, functional DNA/RNA fragments, especially miRNAs as introduced above. Take exosomal miR-1247 for example, it is derived from Hepatocellular carcinoma cells with a highly metastatic feature, promoting lung metastasis by inducing CAF activation in the pre-metastatic niche (Fang et al., 2018).

1.5.3 CAF function

In the tumor microenvironment, CAFs are growing along with cancer cells and have an essential impact on multiple tumor malignant features via paracrine signaling. To be noted, cytokines and chemokines secreted by CAFs are heterogeneous in various cancer types at different stages. More and more investigations demonstrate that CAFs are deeply involved in tumor tumorigenesis, angiogenesis, metastasis as well as drug resistance (Chen and Song, 2019). The first experimental evidence of the tumorigenic role of CAFs in tumor tumorigenesis was uncovered in mice model bearing human prostate cancer mass (Olumi et al., 1999). In the model, CAFs could promote tumorigenesis of immortalized prostatic epithelial cells, but not normal fibroblasts. Following studies were performed in multiple cancer types, take breast cancer for example, CAFs promote cancer stem-like cell proliferation via CAFs released Stromal cell-derived factor 1 (SDF1) and cancer cells expressed CXC-chemokine receptor 4, (CXCR4) interaction (Huang et al., 2010, Orimo et al., 2005). Other factors secreted by CAFs, such as heat-shock factor 1 (HSF1), matrix metallopeptidase 2 (MMP2) and fibroblast growth factor 1 (FGF1), were proved to foster proliferation of cancer cells (Martens et al., 2003, Scherz-Shouval et al., 2014).

Regrading tumor angiogenesis, CAFs could generate plentiful fibroblast growth factor 2 (FGF2), platelet derived growth factor C (PDGFC), vascular endothelial growth factor A (VEGFA), secreted frizzled related protein 2 (SFRP2) and osteopontin to trigger or intensify the angiogenic programming of the tumor tissue (de Palma et al., 2017).

CAFs have been reported involved in multistage of tumor metastasis, start from tumor cells migration, invasion, intravasation, and eventually establish long distance metastasis. CAFs could release different chemokines into the TME to facilitate metastasis, like in breast tumors, insulin-like growth factor 1 (IGF1) and SDF1 produced by CAFs could help breast cancer cells to colonize in bone marrow microenvironment (Zhang et al., 2013). CAF related chemokine, galectin-1 in oral SCC, stanniocalcin-1 in colorectal cancer, bone morphogenetic protein (BMP) in prostate cancer, are proved to support tumor metastasis (Chen and Song, 2019). Besides secreted factors, CAFs re also reported to create gaps for tumor cell invasion in the matrix (Gaggioli et al., 2007, Glentis et al., 2017). Moreover, exosome derived from CAFs also contribute to tumor metastasis (Wortzel et al., 2019). In the breast cancer models, CAF associated exosomes promote cancer cell migration and invasion via the WNT signaling pathway (Chen et al., 2017a).

High risk tumors often develop resistance to various therapeutic treatments, including chemotherapy, targeted therapy and immunotherapy, stromal CAFs are protective to cancer cell in different aspects. In the chemotherapy, CAFs could secret IL-6 to boost EMT and resistance to cisplatin treatment in non-small cell lung carcinoma (Shintani et al., 2016). Cancer stem cells, as a group chemotherapy resistant cells in tumors (Lytle et al., 2018), are also protected by CAFs. In lung and breast cancers, a subtype CAFs expressing G protein-coupled receptor 77 (GPR77) and CD10 could generate a niche to keep cancer stem cells away from chemotherapeutic treatment (Su et al., 2018). In the targeted therapy, for example, hepatocyte growth factor (HGF) released from CAFs could activates MAPK and PI3K-AKT signaling in BRAF mutated cancer cells against RAF inhibitor treatment in melanoma (Straussman et al., 2012). Despite the success of immune checkpoint inhibitors treatment in recent years, around 60% of tumors are not responsive to any of those therapies (Yan et al., 2018b). CAFs was reported contributing to the immunotherapy resistance, they could eliminate CD8+ T cells in TME via FAS ligand and PD-L2 to protect cancer cells (Lakins et al., 2018).

Besides all the tumor protective CAFs subtypes, tumor suppressive CAFs subtypes are also discovered and identified in TME. In breast cancer, CD146+ CAFs could sustain estrogen

receptor expression in cancer cells and maintain sensitivity to tamoxifen treatment, while CD146- CAFs have opposite function (Brechbuhl et al., 2017).

1.5.3 CAF in Merkel cell carcinoma

Not like common skin cancer types, such as melanoma, basal cell carcinoma (BCC), and squamous cell carcinoma (SCC), as a rare skin tumor type, CAFs in Merkle cell carcinoma is largely unknown. Dermal fibroblasts are considered as one of the cell origins of MCC, since they can be infected by MCPyV (Sunshine et al., 2018), however, fibroblasts in MCC tumor mass were not yet explored. In this thesis, we identified α-SMA positive cancer associated fibroblasts utilizing immunostaining on MCC tumor tissue sections. Analysis of data from single cell RNA sequencing using fresh MCC tissue revealed that fibroblasts in the MCC tumor were heterogeneous with CAF features. Next, we scrutinized the role of exosome miR-375 and came up with a possible explanation of CAF polarization in MCCs.

2. Material and methods

2.1 Cell lines and primary cell culture

24 MCC cell lines including 21 cMCC cell lines and three vMCC cell lines, 16 non-MCC tumor cell lines, one fibroblast cell line, one embryonic kidney cell lines as well as four primary skin fibroblasts were utilized in this thesis, details were listed in Table 1 and Table 2 in the Appendix. All cell lines are authenticated by STR analysis on a regular basis (last performed in June 2019).

2.1.1 Generation of primary skin fibroblasts

A series of primary skin fibroblasts were generated from biopsies of healthy skin in our lab and used in **Paper I, II** and **IV**. Biopsies were cut into small pieces and incubated with 130 µM Dispase II (Sigma-Aldrich, Darmstadt, Germany) in hanks balanced salt solution (HBSS, Sigma-Aldrich) at 4°C overnight to separate the dermis from the epidermis. The dermis was then transferred into fresh medium (1:1 DMEM+DMEM/F-12 (PAN-Biotech) supplemented with 1% penicillin and streptomycin (P/S, PAN-Biotech) and 15% fetal bovine serum (FBS, PAN-Biotech, Aidenbach, Germany), 10µM amphotericin B (AMP-B, Sigma-Aldrich) and 75µM ciprofloxacin (CIPRO, Sigma-Aldrich) and incubated overnight in a humidified incubator at 37°C. The medium was replaced after 24h and 48h, gradually reducing the AMP-B and CIPRO concentrations to 5µM and 35µM respectively. After that, the medium was changed once a week, until fibroblasts began to form confluent patches. At this point, the excess tissues were discarded and the remaining adherent fibroblasts were cultured in total culture medium (1:1 DMEM+ DMEM/F-12 supplemented with 1% P/S and 15 % FBS).

2.1.2 Coculture conditions between MCC cells and fibroblasts

Coculture experiments between MCC cells and fibroblasts were performed in **Paper IV**, conditions are described as follows:

Cell conditioned medium (CM) was generated by culturing cells ($2x10_6$) in fresh RPMI 1640 supplemented with 10% FBS and 1% P/S for 72 hours. Culture supernatants were centrifuged to remove floating cells and cell debris. CM was added to 70% confluent fibroblasts and incubated for 72 hours.

For transwell co-culture (TC), $5x10^5$ MRC-5 cells or $2x10^5$ primary skin fibroblasts were seeded in lower part of the 6-well-plate with 0.4µm pore polyester membrane inserts (Corning, Hagen, Germany). After 24 hours $1x10^6$ MCC cells were seeded into the inserts. Fibroblasts were harvested after 72 hours of co-culture.

For direct co-culture (DC): MCC cells were added to 70% confluent adherent growing fibroblasts. After 72 hours co-culture, the supernatants and floating cells were carefully removed, and the remaining adherent cells were washed at least 3 times with PBS to remove all floating cells. Adherent fibroblasts were harvested.

2.2 MCC tissue and serum samples

In this thesis, in total 67 formalin-fixed and paraffin-embedded (FFPE) MCC tissue samples, 48 melanomas tissue samples, and 10 basal cell carcinomas (BCC) tissue samples were used. 44 MCC and 10 BCC samples were obtained from Dermatology of Medical University of Graz; the other 23 MCC and 48 melanoma samples were from Dermatology of University Hospital Essen. RNAs were isolated from these tissue samples and used for respective assays in **Paper I, II,** and **IV**, besides that, MCC samples were also used for Immunohistochemistry (IHC) staining (**Paper IV**), Immunofluorescence (IF) staining (**Paper IV**) and miRNA in situ hybridization (ISH) (**Paper I, IV**). To be noted, one primary MCC tissue from Dermatology of University Hospital Essen was used for single cell RNA sequencing (scRNAseq).

In total 438 serum samples were used in **Paper I**, including serum samples from 30 healthy control subjects and 109 MCC patients including four different cohorts. Control serum samples were obtained from Dermatology of Medical University of Graz, MCC serum samples were from Dermatology of Medical University of Graz, University of Washington/Seattle, University Hospital Essen, and University of Melbourne. Clinical information of these patients is described in supplementary tables of **Paper I**.

The investigational protocols using human biopsies were approved by the Institutional Review Board/Ethic Committee (17-7539-BO; Ethics Committee of the University Duisburg-Essen and sharing of de-identified samples was approved by the ethics committees in Graz, Melbourne, and Seattle.

2.3 Plasmids and Oligos

2.3.1 Luciferase reporter related plasmids

pTA_luc plasmids were kindly provided by Tsuchiya's lab (Tokyo Medical and Dental University, Tokyo, Japan), pTA_3E_luc (3x E-boxes) and pTA_3EM_luc (3x mutated E-boxes) plasmids were generated based on pTA_luc plasmids in our lab. pcDNA3.1_ mCherry_ATOH1 plasmids were also provided by Tsuchiya's lab, control plasmids pcDNA3.1 and pCMV-betaGAL were kindly provided by Jianfeng Huang (Medical University of Graz, Graz, Austria). These plasmids were used for luciferase activity assay in **paper II**.

2.3.2 Lentivirus related plasmids

Lentiviral plasmids pLJM1_EGFP were provided by David Sabatini (Addgene plasmid # 19319), and plasmids expressing different truncated MCPyV LTAs (MS1_LT, MKL1_LT, MKL2_LT) were generated based on pLJM1_EGFP plasmids in our lab. Besides that, Lentivirus helper plasmids (pHCMV-G, pRSV rev and pMDLg/pRRE) and pcDH_EGFP _P2A_MCS_puro plasmids were kindly provided from David Schrama (University Hospital Würzburg, Würzburg, Germany). These plasmids were used for lentivirus production in **Paper II** and **IV**.

2.3.3 miRNA mimics and antagomirs

miR-375 mimics (Mission microRNA Mimic, HMI0537, Sigma-Aldrich) or negative control (Mission miRNA negative control 1, HMC0002, Sigma-Aldrich) were used in this thesis to overexpress miR-375 in fibroblasts in **Paper IV**; miR-375 antagomirs (Assay ID: MH10327, Catalog: 4464084, Thermo Fisher Scientific, Frankfurt, Germany) or respective controls (Catalog: 4464076, Thermo Fisher Scientific) were used for miR-375 knockdown in MCC cells and fibroblasts in **Paper III** and **IV**.

2.4 Transfection and lentiviral transduction

2.4.1 Lipofectamine-based transfection and nucleofection

Lipofectamine 3000 reagent (Thermo Fisher Scientific) was used for transfection of different expression plasmids, reporter plasmids, miRNA mimics and miRNA antagomirs in MCC cell lines and fibroblasts according to the instructions of manufacturer **(Paper II - IV)**.

Nucleofection transfection was applied to achieve higher transfection efficiency for miRNA knockdown on Nucleofector™ 2b Device (Lonza, Basel, Switzerland) in **Paper III**. Transfection buffer Cell Line Nucleofector® Kit V (Lonza) and transfection program

D23 were determined as the optimized conditions for nuclear transfection of cMCC cell lines.

2.4.2 Lentivirus production and transduction

Lentivirus production was performed using respective lentiviral expression plasmids and helper plasmids (pHCMV-G, pRSV rev and pMDLg/pRRE) in HEK293T cells. Supernatants containing virus were harvested 48- 72 hours after transfection, cell debris was then removed by 0.45 μm filters. In **Paper II**, pLJM1-EGFP plasmids and different truncated MCPyV LTs expressing plasmids were used, while in **Paper IV**, pcDH_EGFP _P2A_MCS_puro plasmids were used. For the lentivirus transduction in fibroblasts, 4μg/ml polybrene and proper amount of virus supernatants were added into fibroblasts for 12 hours, then cells were cultured in total culture medium. Two days later, 1μg/ml puromycin was applied for 5 days for positive selection.

2.5 RNA isolation, qRT-PCR, multiplexed scRNAseq and miRNA hybridization.

2.5.1 RNA isolation

Total RNA was isolated using the PeqGOLD total RNA Kit (VWR/ Peqlab, Erlangen, Germany) for cultured cell lines, miRNeasy FFPE Kit (Qiagen, Hilden, Germany) for FFPE tumor tissues and miRNeasy Serum/Plasma Kit (Qiagen) for serum samples. Isolated RNA concentrations were determined with FLUOstar Omega (BMG LABTECH, Ortenberg, Germany) (**Paper I- IV**).

2.5.2 Real-Time Quantitative Reverse Transcription PCR (qRT-PCR)

For mRNA transcripts, cDNAs were generated using SuperScript IV reverse transcriptase (Thermo Fisher Scientific) according to the given protocols from manufacturer. All the qRT-PCR experiments were performed on the CFX Real-Time PCR system (Bio-Rad, Düsseldorf, Germany), SYBR green assay and Taqman assay were used for different targets genes. In this thesis, SYBR green assay was used for ATOH1, ASCL1, MCPyV-LTA, pri-miR-375, α-SMA, IL-1β, CXCL2, p53, RBPJ and HPRT, Taqman assay was used for RPLP0. HPRT or RPLP0 were used as endogenous control, relative quantification was calculated by the $2^{-\Delta\Delta Cq}$ method using the respective control as indicated (**Paper I-IV**). The sequences of used primers are listed in Table 3 in the Appendix.

For miRNAs, miR-cDNAs and following qRT-PCR were performed using pre-designed Applied Biosystems TaqMan MicroRNA assays (Thermo Fisher Scientific): miR-182 (ID002334), miR-106b (ID000442), miR-19b (ID000396), miR-200c (ID002300), miR-375 (ID000564), cel-miR-39 (ID000200) and small nucleolar RNA RNU6B (ID001093). RNU6B was used as endogenous control or cel-miR-39 for serum miRNAs, relative quantification was calculated by the $2^{-\Delta\Delta Cq}$ method using the respective control as indicated (**Paper I- IV**).

2.5.3 Multiplexed scRNAseq and data analysis

Multiplexed scRNAseq is perform using fresh primary MCC tumor tissue in **Paper IV**. Tumor cells were dissociated into single cell suspension and barcoded using the 10x Genomics Chromium v2.0 platform (Zheng et al., 2017) (10x Genomics, Leiden, Netherland). Library preparation was performed according to the given protocol and the library was sequenced on an Illumina HiSeq 4000 platform (Illumina, Eindhoven, Netherland). The Cell Ranger Single Cell Software Suite version 2.1.1 (http://10xgenomics.com/) was used to align cDNA reads to the hg19 human reference genome. Cell types were annotated using the following marker genes (Proliferation marker: MKI67, TOP2A, fibroblasts: VIM, FN1, S100A4, T-cells: CD3E, CD8A; MCC: CHGA, ENO2, KRT20, CD44, endothelial cells: VIM, VWF, CAV1). A CAF signature score was computed using the Seurat AddModuleScore function based on the following CAF marker genes: FAP, TAGLN, THY1, DCN, COL1A1, COL1A2, COL6A1, COL6A2, COL6A3, ACAT2, CAV1, S100A4. For normalization, dimension reduction and visualization we used the Seurat R package v2 (Butler et al., 2018). Differentially expressed genes were called using Seurat's FindMarkers function with default settings. RNA velocity estimates were calculated using the corresponding velocyto R package with a gene-relative model based on Principal component analysis (PCA) cell-cell distances calculated by Seurat(La Manno et al., 2018). Extrapolated cell states were projected onto a tSNE embedding that summarizes transcriptional variability in the data on a lower-dimensional space. Inferred trajectories are depicted as arrows, where the base of the arrow indicates the current and the tip of the error the extrapolated cell state.

2.5.4 miRNA hybridization

Locked nucleic acid (LNA)-based miRNA *in situ* hybridization was performed on FFPE fixed MCC tissue sections by Bioneer ISH services (Hørsholm, Denmark). MCC sections

were incubated with 20nM of a specific probe against miR-375 (DIG-TCACGCGAG CCGAACGAAA-DIG) or a scrambled control probe (DIG-TGTAACACGTCTATACG CCCA-DIG) at a 58°C following a previously described protocol (Lindahl et al., 2016). This method is used in **Paper I** and **IV** to determine miR-375 expression on MCC tumor tissues.

2.6 Protein expression determination

2.6.1 Immunoblot

Immunoblot, also called western blot, is using specific antibodies to determine the expression level of target proteins according to their molecular weight. The first step is the protein isolation from cells or tissues using lysis buffer, then protein lysate was separated on the electrophoresis gel, transferred onto nitrocellulose membrane. The membrane was blocked in milk and incubated with specific first antibody overnight, then secondary antibody with species-specific horseradish peroxidase (HRP) was added after the washing step. At last, the result is visualized using the ECL Western Blotting Substrate (Pierce, Rockford, IL, USA) in a chemiluminescence imager (Amersham imager 600, GE Healthcare, New York, United States). Quantifications of immunoblots were performed with ImageJ and Graphpad software (GraphPad Software Inc., San Diego, CA, USA). First antibodies used in this thesis are listed here: anti-mCherry antibody (1:200; 1C51, Novus Biologicals, Littleton, Colorado, United States) for ATOH1-mCherry, anti-ATOH1 antibody (1:1000; B6529, LSBio, Eching, Germany), α-SMA (clone 1A4, 1:1000, Dako, Düsseldorf, Germany), p53 (clone DO7, 1:1000, Dako), RBPJ (clone D10A4, 1:500, Cell Signaling Technology, Leiden, Netherlands) and for β-tubulin (clone TUB2.1, 1:2000, Sigma-Aldrich) in **Paper II** and **IV**.

2.6.2 Immunohistochemistry (IHC) staining and staining score determination

IHC staining was usually used to visualize protein expression on the tissue *in situ* using a specific antibody. In this thesis, IHC staining was performed on FFPE MCC tissue sections after deparaffinization to visualize α-SMA expression using an α-SMA specific antibody (clone 1A4, Dako) in **Paper IV**. Antigens were retrieved and incubated with peroxidase blocking solution (3% H_2O_2 in methanol). Sections were then incubated for the first antibody and following HPR-polymer anti-mouse antibody (POL2DS-006, Zytomed, Eching, Germany), the detection was obtained using permanent HRP green stain (Zytomed). After nuclei were counterstained with hematoxylin, sections were dehydrated

and mounted in mounting media. The stained sections were then scored for α-SMA positive fibroblasts using the Mantra quantitative pathology workstation with inForm analysis software (Perkin Elmer). In detail, the instrument was trained by manually categorizing the tissue sections into tumor and stromal segments followed by automated cell segmentation via their hematoxylin-stained nuclei. The system was then trained to automatically distinguish between cell phenotypes by manually identifying 100 tumor and stromal cells. The final α-SMA staining score was determined as the percentage of α-SMA positive stromal cells. The cutoff for α-SMA positive cells was set at an optical density of intensity above 0.26. For each section four areas at the border of the tumor and four areas in the middle of the tumor were gripped and analyzed as explained above. The mean of the values for tumor border and tumor middle was taken for the final scoring.

2.6.3 Immunofluorescence (IF) staining

IF staining was used in **Paper IV** to determine α-SMA protein expression in fibroblasts. Fibroblasts grow on cover slides (Thermo Fisher Scientific) in 12-well plates. Before staining, cells were fixed in 4% paraformaldehyde (PFA) for 10 minutes, permeabilized in PBS with 0.2% Tween 20 for 15 minutes and blocked with 1% BSA in PBS for 1 hour. Then a primary antibody specific against α-SMA (clone1A4, Dako), diluted 1:200 in 1% BSA in PBS was added and incubated overnight at 4°C. After two washes, an Alexa Fluor 546 labeled goat-anti-mouse secondary antibody (1:200, Thermo Fisher Scientific) was added for one hour. Following two washes with 5 µg/ml wheat germ agglutinin (WGA, conjugated with Alexa Fluor 647, Thermo Fisher Scientific) for 30 minutes and DAPI (1:2000, Thermo Fisher Scientific) was added to visualize nuclei. After three washes cells were embedded with Prolong Diamond Antifade Mountant (Thermo Fisher Scientific) and then Axio Observer.Z1 microscope (Zeiss, Oberkochen, Germany).

2.6.4 Multiple IF staining

Multiplex IF staining was performed using the Opal 7-color IHC kit (Perkin Elmer, Velbert, Germany) according to manufacturer's instructions in **Paper IV**. In short, FFPE fixed tissue sections were incubated at 60°C for 1h, deparaffinized in xylene and rehydrated with 100%, 96% and 70% ethanol for 2 minutes each. Sections were then cross-linked to the slide by incubation in 10% Formalin (Sigma-Aldrich) for 10 minutes, followed by two five-minute washes in distilled water. Before incubated with each antibody, antigens were retrieved by microwaving in a suitable Opal antigen retrieval Buffer pH9 (AR9) or pH 6

(AR6) for 15 minutes. After cooling down, sections were blocked with antibody blocking solution for 10 minutes before incubation for 30 minutes at room temperature with the respective primary antibodies. After three washes in TBS with 0,05% Tween 20 (TBST), sections were incubated with Opal polymer HRP mouse and rabbit for 10 minutes at room temperature. After washing trice in TBST the respective Opal fluorophore was added in a dilution of 1:50 and incubated for 10 minutes at room temperature. After three washes in TBST the process was started over with the respective retrieval of the next antibody. The order in which the antibodies were added to the sections is summarized in Table 4 in the Appendix. After the last antibody incubation nuclei were stained with DAPI for five minutes, sections were embedded with ProLong Diamond Antifade Mountant (Thermo Fisher Scientific) and incubated at room temperature in the dark for 24 h before imaging with the Mantra quantitative pathology workstation (Perkin Elmer).

2.7 Exosome isolation and characterization

Exosomes related experiments were performed in **Paper IV**: exosomes were isolated from 2mL conditioned medium using the ExoQuick-TC kit (System Biosciences, Palo Alto, CA, USA) following the manufacturer's instruction. Isolated exosome fractions were analyzed using violet side scatter in the Cytoflex (Beckmann Coulter, Brea, California, United States). Standardized nanoparticles of 50nm, 100nm and 200nm were served to determine the size of isolated exosomes. Isolated exosomes were stained with Exo-Red RNA fluorescent label (System Biosciences), according to manufacturer's instruction.

2.8 Cell viability or proliferation assays

2.8.1 Live/ dead cell determination

In this thesis, two methods were applied to distinguish live or dead cells, one is Trypan blue exclusion, which was used in Paper **III**. Dead cells can be stained by Trypan blue dye (Sigma-Aldrich) due to their intact cell membranes, thus, live and dead cells can be determined under bright field microscopy, cell counting was used to determine percentage of live cells or dead cells. Another method is using NucView 488 and MitoView 633 apoptosis assay kit (Biotium, Fremont, United States) in **Paper II**. Cells stained with MitoView 633 exhibit far-red fluorescent signal, which is positively correlated with their mitochondrial membrane potential, while cells stained NucView 488 exhibit green fluorescent signal, which is positively correlated with caspase-3 activity in the cells. Basically, live cells are stained with red and apoptotic cells are showing green. The kit

(1:1000) was used to manifest the cell status of MCC cells and fibroblasts after transfection or lentiviral transduction.

2.8.2 Dead cells/ cell debris removal

Dead cells /cell debris removal step was performed in **Paper III** after nucleofection. Ficoll solution (Biochrom, Berlin, Germany) was used to remove dead cells and cell debris. Cells suspension were mixed with 1x PBS (1: 1), slowly added on the top of an equal volume of Ficoll solution. Following the centrifugation step (1200g, 20min, no break) separated the cells, the layer containing living cells was harvested and washed with PBS. At last, these cells were cultured in a culture medium.

2.8.3 Cell proliferation assay

Cell counting from time to time was used to determine cell proliferation/ viability of MCC cells after transfection in **Paper II** and **IV**. The cell suspension was mixed with Trypan blue dye (1:1) to exclude dead cells, cells were counted every second day and the relative value was relative to seeded cell number.

2.9 Luciferase assay

Luciferase assay was applied in **Paper II** to determine if ATOH1 or MCPyV LT induced transcription factors could bind to E-boxes on the promoter of miR-375 in vMCC cell lines and fibroblasts. ATOH1 or truncated MCPyV LT expressing and control plasmids were co-transfected with different reporter plasmids (pTA-luc, pTA-3E-luc or pTA-3EM-luc, Beta-Gal) into MCC cells or fibroblasts. 48 hours post-transfection, cells were harvested and ONE-Glo and Beta-Glo assay system (Promega, Wisconsin, United States) were used to detect luciferase signals in FLUOstar Omega (BMG LABTECH) according to instructions of the manufacturer, Beta-Gal signal was used as endogenous control.

2.10 Preclinical in vivo models

In this thesis, two preclinical models were used in **Paper I**, chicken chorioallantoic membrane (CAM) and mice xenotransplantation. For CAM assays, MCC cells in culture medium were mixed with Matrigel (1:1) (BD Bioscience) and planted on the CAM (nine days after incubation). For the mice xenotransplantation assays, MCC cells in culture medium were mixed with Matrigel (1:1) and subcutaneously injected into the lateral flank of NOD.CB17-Prkdcscid/J mice (six weeks, female) (Charles River Laboratories). Those mice were housed under specific pathogen-free conditions. Blood form chicken or mouse

grafted with MCC cells were collected at the certain time point (CAM, four days; mice, 28 days) to prepare serum for subsequent experiments. Animal studies were approved by the Austrian Ministry of Education and Science (BMWF-66.010/0151-II/3b/ 2012).

2.11 Pathway finder gene expression arrays

Pathway finder gene expression arrays were performed using the RT2 Profiler PCR arrays (SABioscience via Qiagen) in **Paper III**. Expression of genes involved in epithelial to mesenchymal transition (EMT) (PAHS-090Z) and Hippo signaling (PAHS-172Z) was determined in MCC cells transfected with miR-375 antagomirs or negative control. cDNAs were generated from isolated total RNAs using RT2 first strand kit (Qiagen) and used in the expression array. Realtime qRT-PCR was performed as described above, the relative expression of genes was analyzed in RT² Profiler PCR Array software from Qiagen (https://dataanalysis.qiagen.com/pcr/arrayanalysis.php).

2.12 Gene set enrichment analysis (GSEA)

For gene set enrichment analysis (GSEA), GSEA version 3.0 was used in **Paper III** and **IV** (Subramanian et al., 2005). Pre-ranked analyses were performed by sorting differentially expressed genes according to their fold changes without prior filtering on significance or effect size. In paper III, GSEA was performed to check whether any prior defined gene set shows significant differences between miR-375_high or miR-375_low MCC cell lines; while in Paper IV, it was used to check if any prior defined gene set are significantly regulated in CAF_high and CAF_low fibroblasts. Enrichment was then tested for the KEGG gene set and the hallmark of cancer gene set (Liberzon et al., 2015).

2.13 DNA methylation microarray analysis

DNA methylation level in MCC cell lines (8), SCC cell lines (4) and fibroblasts (3) were determined using Infinium MethylationEPIC BeadChips (Illumina, Ense-Höingen, Germany) in **Paper II**. All related data analyses were performed in R (version 3.4.4), Bioconductor packages minfi and limma were used in the data processing workflow. The methylation level of each CpG island was converted to beta-values to visualize the methylation percentage. Human genome (hg19) reference coordinates provided by Illumina were applied for annotation information.

2.14 Statistical analysis

Statistical analyses were performed in GraphPad Prism (Version 6.0 to 8.0) (GraphPad Software Inc., San Diego, CA, USA) in **Paper I- IV**. Mann-Whitney U test was used for analysis in two groups experiments, while the Kruskal-Wallis test was applied for experiments containing more than two groups. Multiple statistical analyses were performed in R studio using different R packages: ggpubr R package for correlation analysis in **Paper I, II** and **IV**, or dot plot in **Paper III**; heatmap.2 for miRNAs expression pattern in **Paper I**; pROC for ROC curve analysis in **Paper I**, minfi and limma in **Paper II** for DNA methylation analysis; Seurat v2 and velocyto for scRNAseq analysis in **paper IV**. p-values smaller than 0.05 are considered significant; respective p-values are indicated in the figures as follows: *$p < 0.05$, **$p < 0.01$, ***$p < 0.001$.

3. Results

Part of the results may resemble the results sections from my published papers (Fan et al., 2019a, Fan et al., 2018, Fan et al., 2019b).

3.1 "Circulating cell-free miR-375 as a surrogate marker of tumor burden in Merkel cell carcinoma" (Paper I)

miRNAs have been investigated in human cancers in the last decades, however, studies about miRNAs in MCC are limited when we initiated our project. Here, we scrutinized miRNAs expression in MCC cell line and discovered miR-375 as one of the most abundant miRNAs in cMCC cell lines and later confirmed in MCC tissues. In this paper, we manifested how we discovered and validated miR-375 as a circulating miRNA marker for MCC tumor burden.

3.1.1 miR-375 is strongly expressed in cMCC cell lines and tumor tissues

We performed Nanostring miRNA assay using nCounter Human v2 miRNA Expression Assay kit on six cMCC cell lines, which revealed that miR-375 was one of the most expressed miRNAs in those cell lines (**Fig. 1A**). Following qRT-PCR experiments using large cell lines panel, including 21 cMCC cell lines, 3 vMCC cell lines and 23 non-MCC cell lines, further confirmed the previous discovery (**Fig. 1B**). To be noted, miR-375 was also highly expressed in MCC tissues comparing to non-MCC skin tumor tissues, which was not MCPyV status dependent (**Fig. 1C**). Furthermore, miRNA hybridization assay provided the *in situ* evidence that miR-375 was strongly expressed on MCC tissues (**Fig. 1A**).

3.1.2 miR-375 is detected in MCC-conditioned medium and serum of preclinical models bearing MCC xenografts

Since circulating miRNAs have been detected in cancer patient serums and they might serve as communication factors between different cells (Xu et al., 2013, Mahn et al., 2011). In our experiments, we tested if miR-375 was present in the cell culture medium of cMCC cell lines. Indeed, among all five previously reported highly expressed miRNAs (miR-106b, miR-375, miR-19b, miR-182, miR-200c) in MCC cells, only miR-375 was readily detected in the conditioned medium (CM) by qRT-PCR (**Fig. 1E**). Following experiments

using multiple MCC cell lines further demonstrated the presence of miR-375 in CM of miR-375 expressing cMCC cell lines, but not vMCC cell lines (**Fig. 1F**).

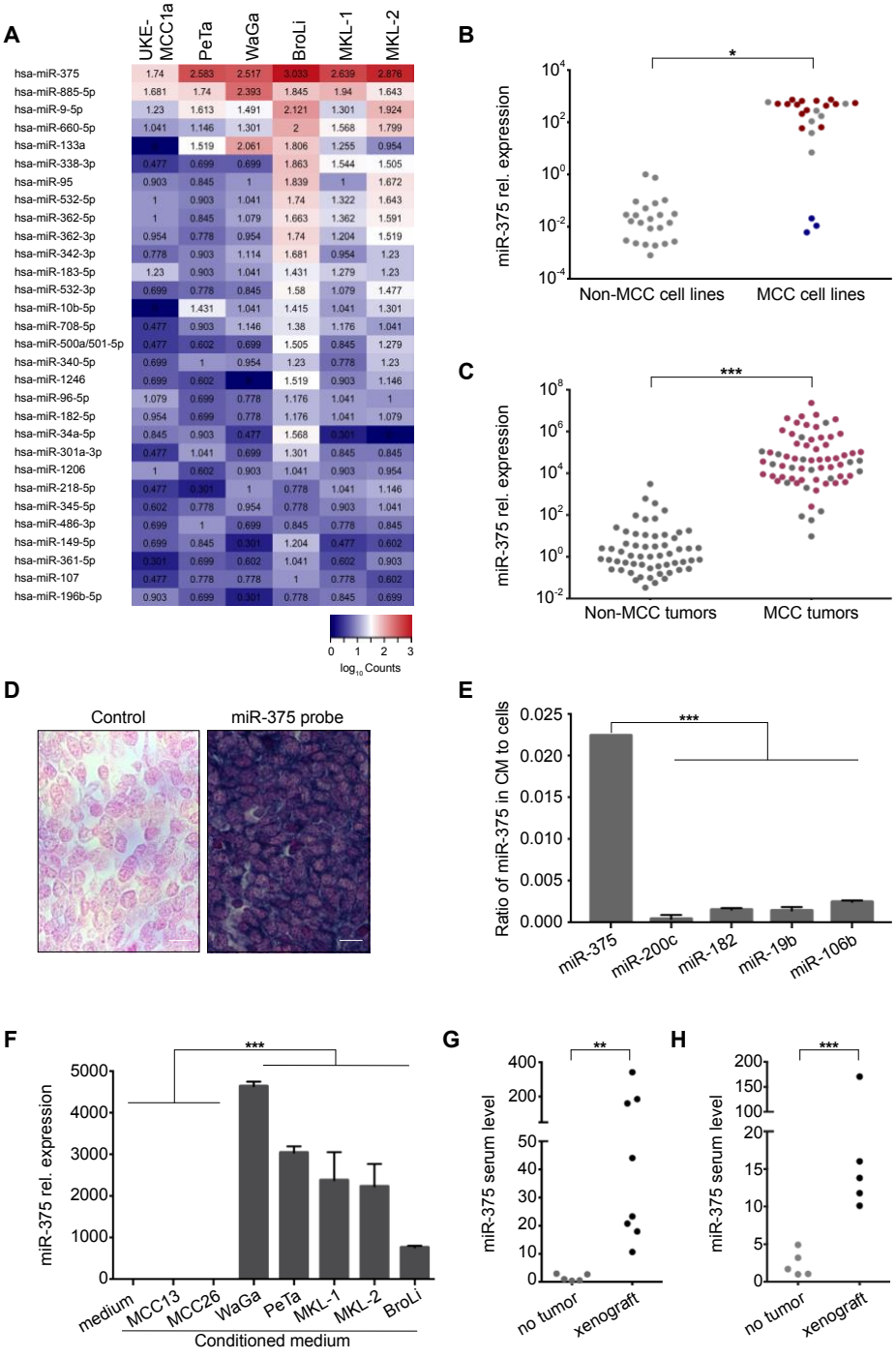

"Fig. 1: **The highly expressed miR-375 in MCC cell lines and tissues is also present as cell-free miRNA in MCC-conditioned media as well as in sera of MCC-bearing preclinical models.**

A: Heat map depicting the relative expression of the 30 most abundant miRNAs in six MCC cell lines. Data obtained by nCounter® Human v2 miRNA Expression Assay (NanoString Technology). **B**: miR-375 expression in 24 MCC cell lines (21 classical MCPyV positive [n=14, red] or negative [n=7, gray], and three

variant MCC cell lines [blue]; details in S. Tab. 1) as well as 23 non-MCC skin cancer (melanoma, squamous cell carcinoma), lung cancer, kidney, and fibroblast cell lines (details in S. Tab. 2) was quantified by RT-qPCR in triplicates. The relative expression of miR-375 was normalized to U6 and is depicted relative to 293T cells as calculated by the $2^{-\Delta\Delta Cq}$ method. **C**: miR-375 expression in 58 non-MCC skin cancer tissue samples (48 melanomas and ten basal cell carcinomas) as well as 67 MCC tissue samples (49 MCPyV positive [red] and 18 MCPyV negative [gray]) was determined by RT-qPCR in triplicate. The expression level of miR-375 was normalized to U6 and is depicted relative to one randomly selected melanoma sample as calculated by the $2^{-\Delta\Delta Cq}$ method. **D**: *In situ* hybridization (ISH) for miR-375 in a representative MCC tissue. Intense miR-375 ISH signal (right), and background staining for the scrambled control (left). Scale bar, 10 µm. **E**: The presence of miR-375, miR-200c, miR-182, miR-19b and miR-106b in 200µl of conditioned medium from the MCC cell line WaGa (48 hours culture of 106 cells per ml) and in the cells themselves was determined by RT-qPCR in triplicate. The ratio of respective miRNA calculated by the $2^{-\Delta\Delta Cq}$ method in conditioned medium to the cells is depicted. **F**: miR-375 presence in conditioned medium from seven different MCC cell lines was determined in triplicate. The expression level of miR-375 was normalized to spiked-in cel-mir-39 and is depicted relative to MCC13-conditioned medium as calculated by the $2^{-\Delta\Delta Cq}$ method. **G**: Circulating cell-free (cf) miR-375 in sera of chicken embryos bearing 4-day-old xenotransplants of WaGa MCC cells on the chorioallantoic membrane was determined by RT-qPCR in triplicate. The expression level of miR-375 was normalized to spiked-in cel-mir-39 and is depicted relative to the serum of an untreated chicken embryo as calculated by the 2-ΔΔCq method. **H**: cf miR-375 in sera of NOD.CB17-Prkdcscid/J mice with or without subcutaneous WaGa MCC xenografts was determined by RT-qPCR in triplicate. The expression level of miR-375 was normalized to spiked-in cel-mir-39 and is depicted relative to the sera of tumor-free NOD.CB17-Prkdcscid/J control mice as calculated by the $2^{-\Delta\Delta Cq}$ method. Mann-Whitney U test were performed as described in Statistical analysis; p*<0.05, p**<0.005, p***<0.001." The data shown above are from my published article (Fan et al., 2018, Paper I) and reproduced here with permission from American Association for Cancer Research.

Next, two established MCC xenograft bearing preclinical models were applied to check if miR-375 was present in the serum of animals bearing MCC tumor xenografts. WaGa cells were either placed on the chicken chorioallantoic membrane (CAM) or injected into the flank of nude mice in the MCC xenograft experiments. Serums were prepared from these two models and the amount of miR-375 is higher in animals bearing MCC tumors comparing to the controls in both models (**Fig. 1G, H**). These data indicate that miR-375 is secreted from MCC cells, thus, miR-375 might be also present in the serum of MCC patients with tumor burden.

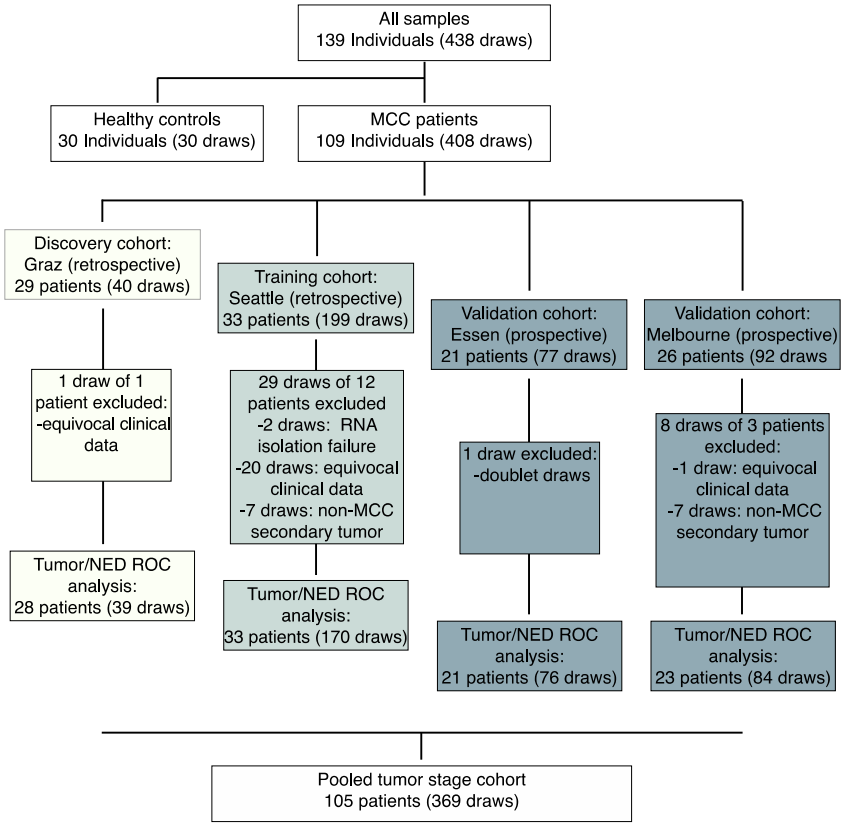

"Fig. 2: Study flow diagram of serum analysis for circulating cell-free miR-375, including two retrospective and two prospective MCC patient cohorts." The data shown above are from my published article (Fan et al., 2018), Paper I and reproduced here with permission from American Association for Cancer Research.

3.1.3 miR-375 serum levels differentiate patients with MCC tumor burden or without evidence of disease

As encouraged by the results showed above, we measured the amount of circulating miR-375 in the serum of MCC patients with tumor burden or no evidence of disease (NED) using established Realtime qRT-PCR for miRNAs. In total, we analyzed miR-375 in four different patient cohorts, which was regarded as discovery cohort (Graz, 40 serum samples from 29 patients), training cohort (Seattle, 199 serum samples from 33 patients) and validation cohorts (Essen, 77 serum samples from 21 patients and Melbourne, 92 serum samples from 26 patients) (**Fig. 2**). In the discovery cohort, circulating miR-375 serum levels were significantly higher in patients with measurable tumor comparing to NED patients (**Fig. 3A**). Receiver Operating Characteristic (ROC) curve analysis revealed that miR-375 serum level of 2.299 as the best cutoff to distinguish patients with tumor or NED with a sensitivity of 0.826 and specificity of 1.000, calculated area under a ROC Curve (AUC) was 0.954 (**Fig. 3C**). Next, we checked miR-375 serum level of patients in the

training cohort, which again revealed that miR-375 serum levels were significantly higher in the patients with tumor burden (**Fig. 3B**). miR-375 serum level of 2.595 as optimal cutoff value was determined by ROC curve analysis with sensitivity of 0.703 and specificity of 0.810, calculated AUC was 0.800 (**Fig. 3D**).

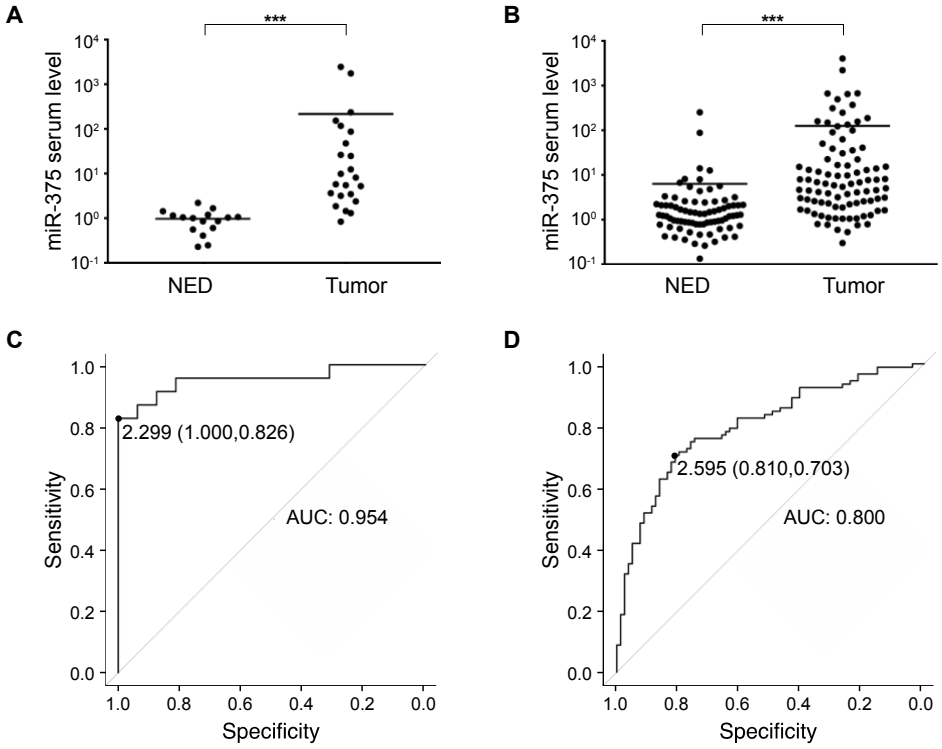

"Fig. 3: Circulating cell-free miR-375 in serum discriminates MCC patients with and without presence of disease: The retrospective discovery and training cohorts.

A, B: cf miR-375 in sera of MCC patients was determined by RT-qPCR in duplicate and normalized to spiked-in cel-mir-39. Values were calculated relative to the serum of an MCC patient with no evidence of disease (Graz cohort) by the $2^{-\Delta\Delta Cq}$ method. Results are depicted in Cleveland dot plots categorized in patients with no (NED) or with evidence of disease. **C, D**: Receiver operating characteristic (ROC) curves showing the sensitivity and specificity of miR-375 serum levels to discriminate tumor-bearing versus NED patients. The areas under the curve (AUC), optimal cut-off values and their sensitivity and specificity are given. **A**, **C**: Graz cohort; **B**, **D**: Seattle cohort. Patients' characteristics are given in S. Tab. 3 and 4. The horizontal line indicates the median, Mann-Whitney U test and pROC R were performed as described in Statistical analysis; p***<0.001." The data shown above are from my published article (Fan et al., 2018), Paper I and reproduced here with permission from American Association for Cancer Research.

To validate our hypothesis, another two independent cohorts were used to check their serum levels of miR-375. In both tested cohorts, serum miR-375 levels were much higher in patients with MCC tumor burden comparing to patients with NED (**Fig. 4A, B**). In the Essen cohort, the optimal cutoff of miR-375 serum level was 3.693 with a sensitivity of 0.893 and specificity of 0.812, calculated AUC was 0.929 (**Fig. 4C**). In another cohort, the optimal cutoff was 2.953 with a sensitivity of 0.938 and specificity of 0.917, calculated

AUC was 0.959 (**Fig. 4D**). Optimal cutoff of miR-375 serum level from retrospective cohorts (Graz and Seattle) was calculated as 2.42 as the mean of these two cohorts. When applying this value to distinguish the tumor-bearing or NED patients in the validation cohorts, the rate of tumor-bearing patients with miR-375 serum levels lower versus higher than the cutoff was 3.1% vs. 61.4 in Essen cohort (**Fig. 4E**) and in Melbourne cohort the rate is 9.1% vs. 88.2% (**Fig. 4F**). Moreover, combining the miR-375 serum levels in 30 healthy controls, we are safe to conclude that miR-375 is a valuable biomarker to distinguish patients with or without MCC tumor burden.

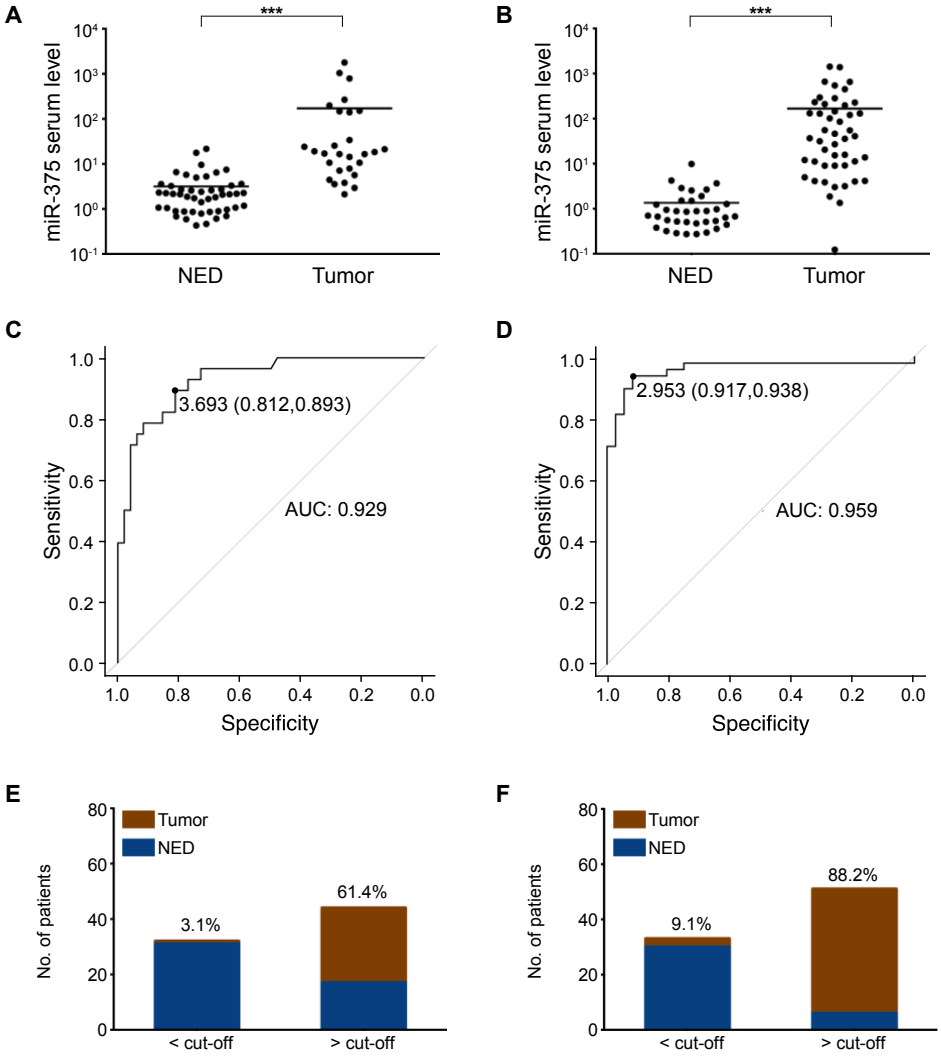

"Fig. 4: Circulating cell-free miR-375 in serum discriminates MCC patients with and without presence of disease: The prospective validation cohorts.

A, B: cf miR-375 in sera of MCC patients was determined by RT-qPCR in duplicate and normalized to spiked-in cel-mir-39. Values were calculated relative to the serum of an MCC patient with no evidence of disease (Graz cohort) by the 2-ΔΔCq method. Results are depicted in Cleveland dot plots categorized in patients with no (NED) or with evidence of disease. **C, D**: Receiver operating characteristic (ROC) curves showing the sensitivity and specificity of miR-375 serum levels to discriminate tumor-bearing versus NED patients. The areas under the curve (AUC), optimal cut-off values and their sensitivity and specificity are

given. **E, F**: The mean optimal miR-375 serum level cut-off was calculated from the optimal cut-off values of the retrospective discovery and validation cohorts as 2.42. Proportions of MCC patients of the prospective cohorts with (red) or without (blue) tumor burden below or above this mean optimal cut-off are depicted. Percentages of MCC patients with tumor burden within each group are given. **A**, **C** and **E**: Essen cohort, **B**, **D** and **F**: Melbourne cohort. Patients' characteristics are given in S. Tab. 3-4. The horizontal line indicates the median, Mann-Whitney U test and pROC R were performed as described in Statistical analysis; p*<0.05, p**<0.005, p***<0.001." The data shown above are from my published article (Fan et al., 2018), Paper I and reproduced here with permission from American Association for Cancer Research.

3.1.4 miR-375 serum levels correlate with tumor stages in patients bearing MCC tumors

When inspecting the miR-375 serum level values and respective clinical information, we discovered a pattern that miR-375 serum levels are higher in the patients with tumor burden at tumor stage III or IV. Indeed, combined with all these four cohorts, miR-375 serum levels are significantly correlated with their AJCC stages in the tumor-bearing patients, but not in the patients with NED (**Fig. 5A, B**). More practically, miR-375 serum levels correlated with exact metabolic tumor volumes (MTV) measured by Positron emission tomography–computed tomography (PET/CT) scans in the Melbourne patient cohort (**Fig. 5C**).

3.1.5 Serum miR-375 levels can be used for monitoring MCC tumor progression

Series serum samples from the same patients with progressed disease or effective treatment allowed us to check if miR-375 serum level could be used as a monitor for MCC treatment or disease progression. Indeed, miR-375 serum levels changed according to MCC tumor regression or tumor shrinkage after treatment in multiple tested MCC patients (**Fig. 6**). Three patients from Melbourne cohort with their metabolic tumor volume measured by PET/CT showed the best examples of miR-375 as monitor of MCC tumor progression (**Fig. 5D-F**). Take one as an example (**Fig. 5D**), one patient with a large tumor (405.8 mL) held a high miR-375 serum level (54.9), when the tumor volume shrunk into 69.4mL, the respective serum level was 15.8. However, when MCC tumor progressed again, miR-375 serum level increased to 46.2 accordingly. Following immunotherapy nearly eliminated the tumor (volume 2.4mL), the serum level also dropped to a very low level as 0.52. These experimental evidence clearly indicate that miR-375 is a promising monitor for MCC tumor progression and different treatment management.

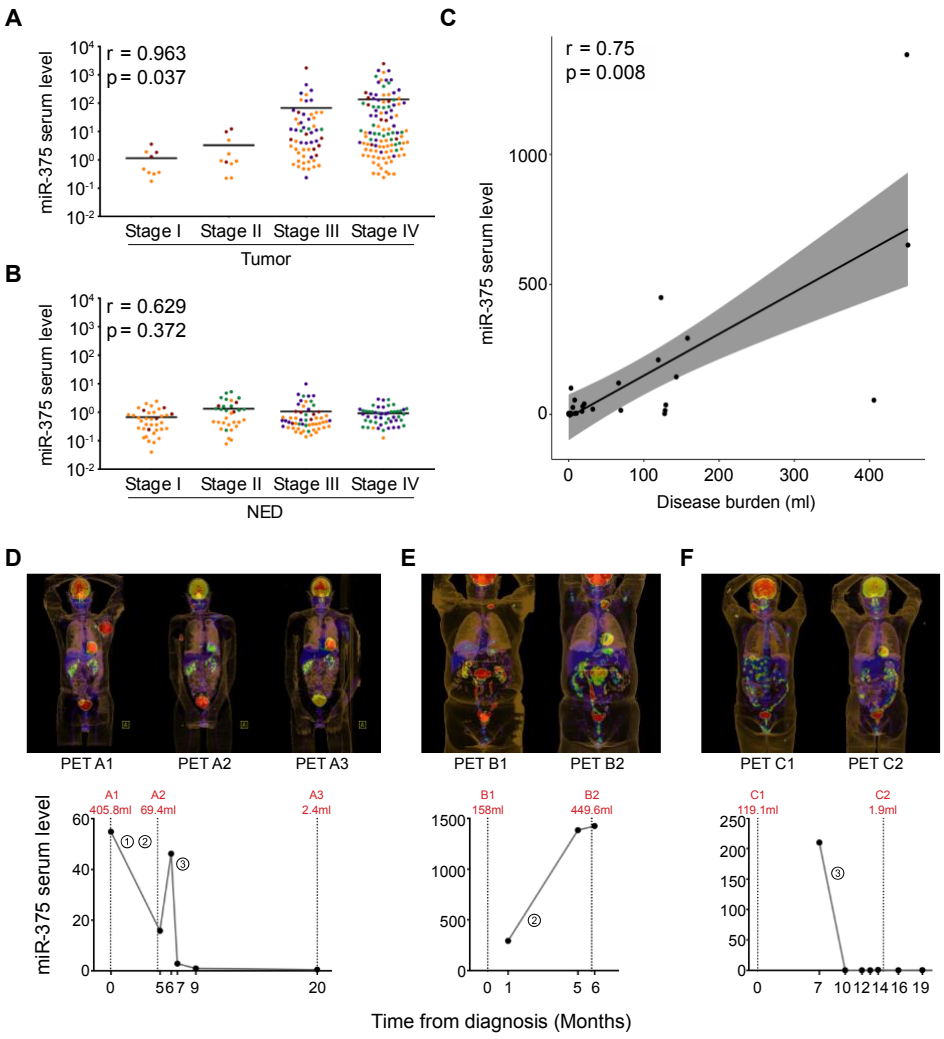

"Fig. 5: Circulating cell-free miR-375 serum levels correlate with disease stage and tumor burden of MCC patients

cf miR-375 in sera of MCC patients was determined by RT-qPCR in duplicate and normalized to spiked-in cel-mir-39. Values were calculated relative to the serum of an MCC patient with no evidence of disease (Graz cohort) by the 2-ΔΔCq method. **A**, **B**: Results are depicted in Cleveland dot plots combined for all four cohorts categorized by AJCC stage at the time of blood draw for patients with (**A**) or without (**B**) evidence of disease; to discern from which cohorts the samples were derived, the data points were color-coded: Graz - green, Seattle - yellow, Essen - dark red, Melbourne - purple. Correlation analysis between cf miR-375 serum levels and MCC tumor stages was performed in R using the "ggpubr" package, the horizontal line indicates the median. **C**: Correlation analysis for cf miR-375 serum level and MCC tumor burden as quantified by PET/CT scan for the Melbourne cohort was performed in R using the "ggpubr" package. **D**, **E** and **F**: cf miR-375 serum levels are plotted over the course of disease together with the tumor volume which was calculated from PET/CT scans depicted above the respective graphs for three exemplary patients from the Melbourne cohort (**D**: p_#16, **E**: p_#6 and **F**: p_#10). The numbers circled indicate the different therapies: ①Radiation therapy, ②Chemotherapy and ③Immunotherapy. The clinical course of patient **D** is described in Results; patient **E** showed disease progression during chemotherapy; patient **F** showed a complete response to checkpoint inhibition." The data shown above are from my published article (Fan et al., 2018), Paper I and reproduced here with permission from American Association for Cancer Research.

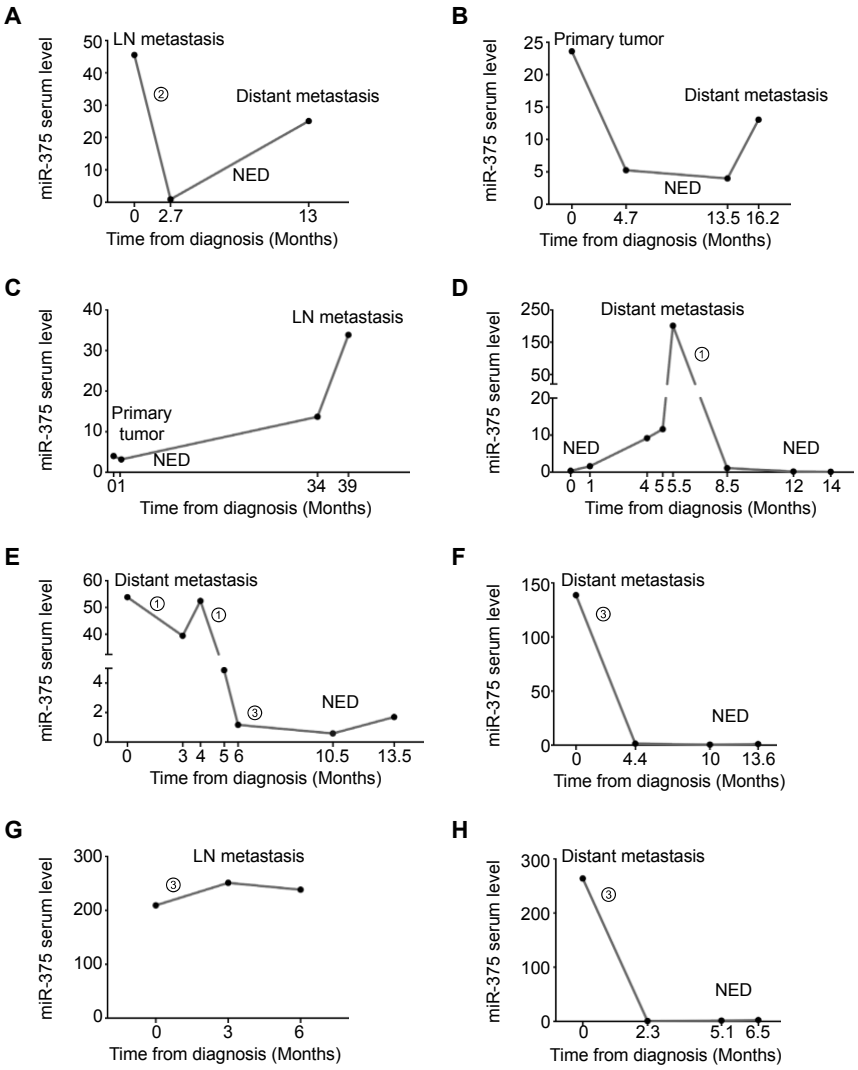

"Fig. 6: Tracking the course of disease in MCC patients using circulating cell-free miR-375

cf miR-375 in sera of MCC patients was determined by RT-qPCR in duplicate, normalized to spiked-in cel-mir-39, and values were calculated relative to the serum of an MCC patient with no evidence of disease (Graz cohort) by the 2-ΔΔCq method. Results are plotted over time together with the narrative description of the course of disease. (**A**: t_#3 and **B**: t_#6 from Graz cohort; **C**: c_#08, **D**: c_#30 and **E**: c_#31 from Seattle Cohort; **F**: e_#4, **G**: e_#2 and **H**: e_#8 from Essen cohort). The numbers circled indicate the different therapies: ①Radiation therapy, ②Chemotherapy and ③Immunotherapy." The data shown above are from my published article (Fan et al., 2018), Paper I and reproduced here with permission from American Association for Cancer Research.

3.2 "MCPyV Large T antigen induced atonal homolog 1 (ATOH1) is a lineage-dependency oncogene in Merkel cell carcinoma" (Paper II)

MCC is also named as NE tumor of the skin, however, the NE differentiation in MCC carcinogenesis is still largely unknown. Merkel cells share similar NE phenotype with MCC cells, thus, it's likely that research on NE differentiation in Merkel cells might help us to better understand the question. Atonal BHLH transcription factor 1 (ATOH1) was reported as a master regulator in Merkel cell NE differentiation, but its function in MCC

was controversial. In this paper, ATOH1 is demonstrated as lineage dependent oncogene by multiple lines of experimental evidence.

3.2.1 Expression levels of ATOH1 and miR-375 are correlated in MCC cell lines

ATOH1 mRNA was highly expressed in 19 cMCC cell lines comparing three vMCC cell lines and 13 non-MCC cell lines via qRT-PCR (**Fig. 7a**). To be noted, vMCC cell lines and cMCC cells are grouped by their growth patterns: vMCC as adherent growing cells and cMCC as suspensions or spheroids growing cells. Subsequent immunoblot experiment confirmed that ATOH1 protein level was consistent as its mRNA level in tested cell lines (**Fig. 7b**). Moreover, ATOH1 mRNA in MCC tissues were also significantly higher compared to other non-MCC skin tumor tissues (**Fig. 7c**). DNA methylation analysis of the ATOH1 promoter region revealed that CpG islands in this region were hypermethylated in vMCCs and hypomethylated in cMCCs, which likely mediated the differential ATOH1 expression in MCCs (**Fig. 7d**). As expected, ATOH1 mRNA expression levels negatively correlated with its promoter methylation levels in all tested MCC cell lines ($r= -0.86$, $p= 0.03$) (**Fig. 7e**).

As introduced in Paper I, miR-375 was identified as high abundant miRNA in MCCs, however, its molecular regulation mechanism was largely unknown. In NE lung cancer, ASCL1 was reported as a miR-375 inducer (Nishikawa et al., 2011), but it was lowly expressed in MCC cells and not correlated with miR-375 expression. Another fact that ASCL1 was mostly absent in MCC tumor tissue also proved that ASCL1 was not responsible for high miR-375 expression (Chteinberg et al., 2018). ATOH1 and ASCL1 belong to BHLH transcription factor family, both of them could bind to the E-boxes on the promoter of miR-375. Expression of ATOH1 and miR-375 showed comparable expression patterns in MCC cell lines, high in cMCC and low vMCC. Thus, ATOH1 might be the transcription factor for miR-375 in MCC cells. The first evidence was that ATOH1 mRNA expression was significantly correlated miR-375 expression (**Fig. 7f**). Moreover, miR-375 promoter region was hypomethylated in both cMCC and vMCC cell lines (**Fig. 7g**). Notably, an E47 binding site was also present in the promoter region miR-375, which was important for ATOH1 mediated transcriptional activity as reported (Aguado-Llera et al., 2010).

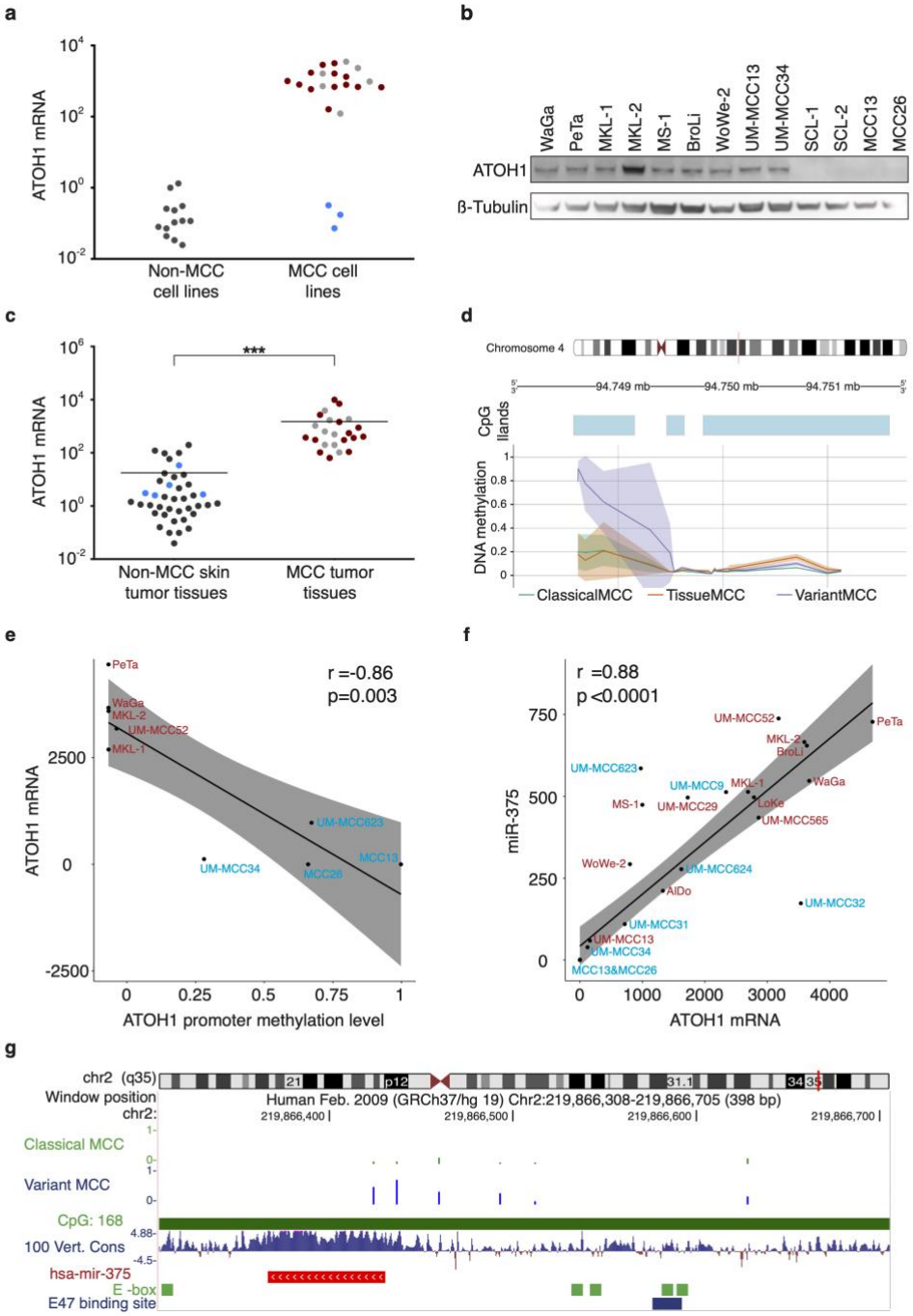

"Fig. 7: The highly expressed ATOH1 in MCC cell lines and tissues correlates with miR-375 expression

a: ATOH1 expression in 22 MCC cell lines (19 classical MCPyV positive [n=13, red] or negative [n=6, gray], and three variant MCC cell lines [blue] (details are described in Fan et al., 2018 (Table S1)) as well as 13 non-MCC skin cancer (melanoma, squamous cell carcinoma), lung cancer, kidney, and fibroblast cell lines (details are described in Fan et al., 2018 (Table S2)) was quantified by RT-qPCR in triplicates. The expression of ATOH1 was normalized to HPRT and is depicted relative to 293T cells as calculated by the $2^{-\Delta\Delta Cq}$ method. **b**: Immunoblot of ATOH1 in MCC and SCC cell lines, β-Tubulin served as endogenous control. **c**: ATOH1 expression in 40 non-MCC skin cancer tissue samples (35 melanoma [black] and 5 BCC [blue]) as well as 23 MCC tissue samples (14 MCPyV+ [red] and 9 MCPyV- [gray]) was determined by RT-qPCR in triplicate. The expression level of ATOH1 was normalized to HPRT and is depicted relative to one randomly selected melanoma sample as calculated by the $2^{-\Delta\Delta Cq}$ method. **d**: DNA methylation status of the

CpG islands in ATOH1 promoter region (<1500bp before ATG) from classical MCC (green, n=9), variant MCC (purple, n=3) cell lines and MCC tissues (orange, n=3) was analyzed by Methylation EPIC Array. DNA methylation levels (β-values) were indicated as the line and shaded areas are defined by 95% confidence interval. **e**: Correlation analysis for ATOH1 promoter methylation level and ATOH1 mRNA expression level in MCC cell lines (5 MCPyV+ [red] and 4 MCPyV- [blue]) was performed in R using the "ggpubr" package. **f**: Correlation analysis for miR-375 expression level and ATOH1 mRNA expression level in MCC cell lines (13 MCPyV+ [red] and 8 MCPyV- [blue]) was performed in R using the "ggpubr" package. The expression of ATOH1 mRNA/ miR-375 was normalized to HPRT/ U6 and is depicted relative to 293T cells as calculated by the $2^{-\Delta\Delta Cq}$ method. **g**: Methylation patterns of the miR-375 gene are depicted. The red bottom track refers to the miR-375 single exon gene structure annotation, whereby the arrows indicate the genomic orientation. The classical (green, n=9) and variant (blue, n=3) MCC tracks refer to the degree of methylation in percent over the classical and variant MCC cell lines. Each bar represents one single CpG site. The horizontal green block represents the location of a known CpG-islands (CpG rich regions). The 100 Vertebrates Conservation (Vert. Cons) track displays the DNA sequence conservation within vertebrates. A high degree of conservation outside of an exon in combination with a CpG-island suggests the possible presence of a promoter region." The data shown above are from my published article (Fan et al., 2019a), Paper II and reproduced here with permission from Elsevier.

3.2.2 Knockdown of ATOH1 downregulated miR-375 expression of MCC cells

To verify if ATOH1 mediates miR-375 expression in cMCC cell lines, we performed ATOH1 knockdown experiments using two pre-designed siRNAs (dicer-substrate siRNAs) against ATOH1 in WaGa and MKL1 cells. Nucleofection was applied for siRNAs transfection to increase transfection efficiency, ATOH1 mRNA decreased about 50% in both cell lines after siRNA transfection (**Fig. 8a**). Immunoblot experiments demonstrated that siRNA induced ATOH1 knockdown was stronger in ATOH1 protein level (**Fig. 8b**).

Accordingly, as expected, miR-375 expression was significantly reduced after ATOH1 knockdown (**Fig. 8c**). However, knockdown of ATOH1 did not change cell proliferation ability of MCC cells transfected with siRNAs against ATOH1(**Fig. 8D**). Here we suggest that ATOH1 might be not a lineage survive related oncogene, but a lineage dependency related oncogene (Garraway and Sellers, 2006). However, migration or invasion ability and other cell features were not investigated in this study.

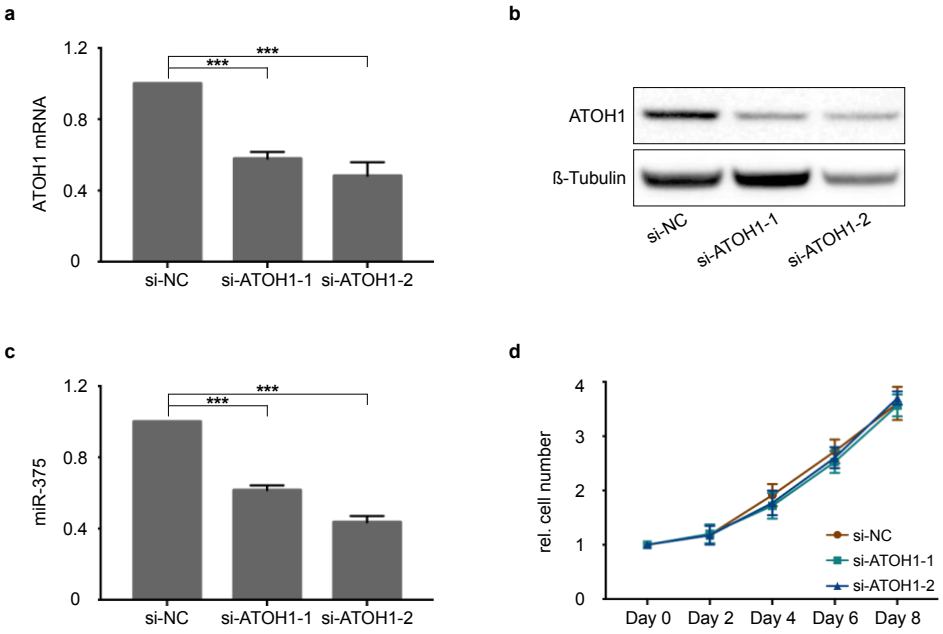

"Fig. 8: ATOH1 knockdown in WaGa cells downregulates miR-375 expression

a: ATOH1 expression in WaGa cells transfected with siRNAs against ATOH1 or control siRNA was quantified by RT-qPCR in triplicates. The expression of ATOH1 was normalized to HPRT and is depicted relative to control siRNA transfected cells as calculated by the $2^{-\Delta\Delta Cq}$ method (mean + SD). **b**: Immunoblot of ATOH1 in WaGa cells transfected with siRNAs against ATOH1 or control siRNA, β-Tubulin was used as endogenous control. **c**: miR-375 expression in WaGa cells transfected with siRNAs against ATOH1 or control siRNA was quantified by RT-qPCR in triplicates. The expression of miR-375 was normalized to U6 and is depicted relative to control siRNA transfected cells as calculated by the $2^{-\Delta\Delta Cq}$ method (mean + SD). **d**: 24 hours after nuclear transfection cells were seeded (1x 10_5 cells per well) and counted every two days. Values represent relative cell number to seeded transfected cells at day 0." The data shown above are from my published article (Fan et al., 2019a), Paper II and reproduced here with permission from Elsevier.

3.2.3 miR-375 expression was induced by ectopic ATOH1 expression in vMCC cells and fibroblasts

vMCC cells are both negative for ATOH1 and miR-375, thus, we overexpressed ATOH1 in MCC13 and MCC26 cells to check the function of ATOH1 and if miR-375 expression was induced (**Fig. 9a, b**). Interestingly, after 48 hours ATOH1 transfection, more than 70% of cells transformed into suspension growing cells, bearing a resemblance to NE growth pattern (**Fig. 9c**). In suspension growing cells, more ATOH1 mRNA was overexpressed comparing to adherent growing cells (**Fig. 9a**). To dispel such doubts that suspension cells derived from adherent cells were only dying cells, we performed live or dead cell staining.

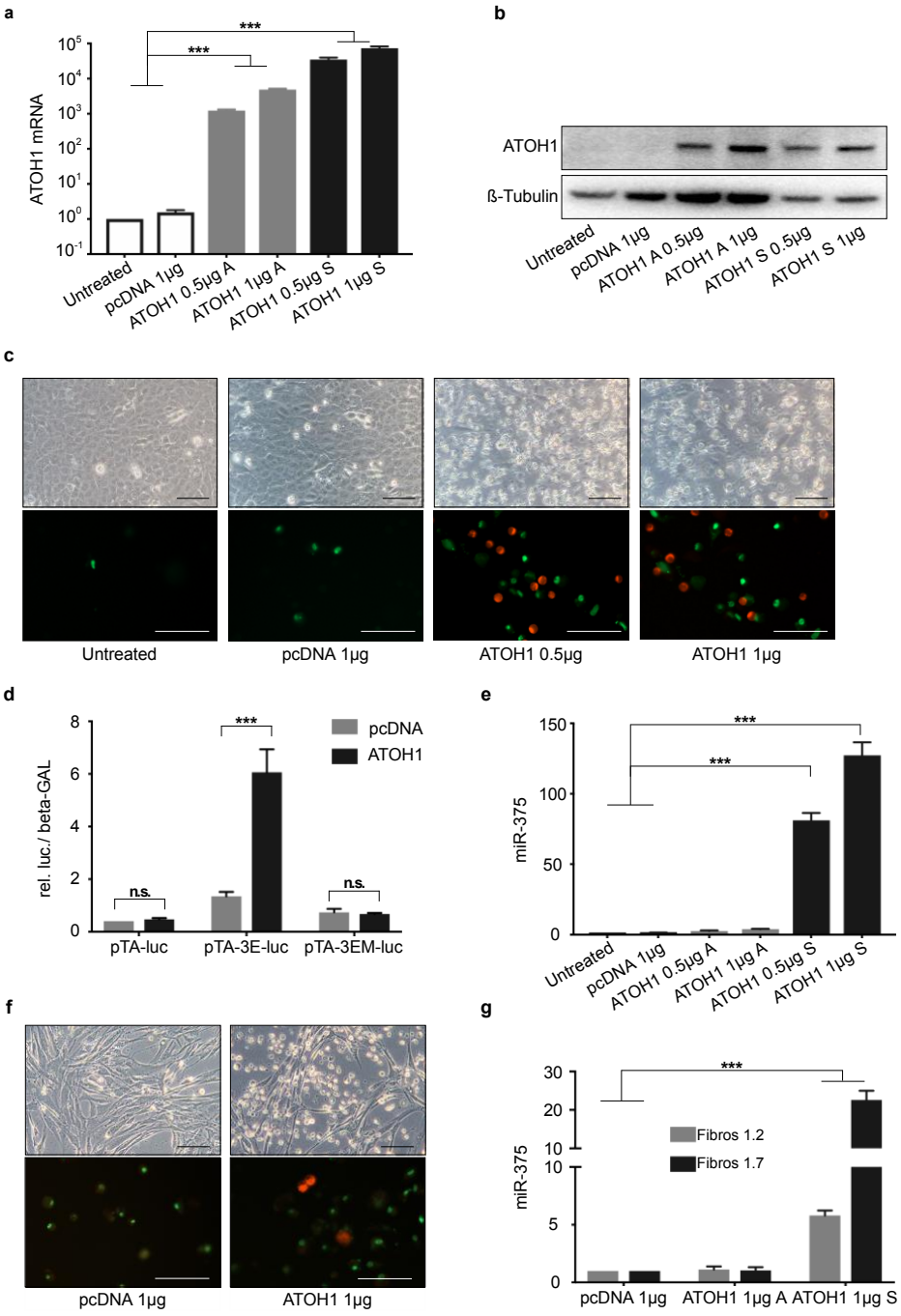

"Fig. 9: Overexpressing ATOH1 in MCC13 cells induces miR-375 expression

a: ATOH1 expression in MCC13 cells transfected with ATOH1 expression plasmid or control plasmid and stratified by their growth pattern (A= adherent; S= suspension) was quantified by RT-qPCR in triplicates. The expression of ATOH1 was normalized to HPRT and is depicted relative to untreated cells as calculated by the $2^{-\Delta\Delta Cq}$ method (mean + SD). **b**: Immunoblot of ATOH1 in MCC13 cells overexpressing ATOH1 (cells growing adherent or in suspension were separated before analysis); beta-Tubulin served as endogenous control. **c**: upper row- morphology change of MCC13 cells overexpressing ATOH1; lower row- floating cells were stained with NucView® 488 and MitoView™ 633 apoptosis assay kit. Living cells were stained with red while dead/apoptotic cells were stained with green. Scale bar = 50 µM. **d**: Luciferase reporter assay to determine E-box activity. MCC13 were co-transfected with pTA-luc, pTA-3E-luc or pTA-3EM-luc, pCMV-betaGAL as exogenous control, and either control vector or ATOH1 vector. Values represent luciferase activity relative to cells transfected with control plasmid. **e**: miR-375 expression in MCC13 cells transfected

with ATOH1 expression plasmid or control plasmid was quantified by RT-qPCR in triplicates. The expression of miR-375 was normalized to U6 and is depicted relative to untreated cells as calculated by the $2^{-\Delta\Delta Cq}$ method (mean + SD). **f**: Upper row- morphology change of primary skin fibroblasts (Fibro 1.7) overexpressing ATOH1; lower row- floating cells stained with NucView® 488 and MitoView™ 633 apoptosis assay kit. Living cells were stained with red and dead/apoptotic cells were stained with green. Scale bar = 50 μM. **g**: miR-375 expression in primary skin fibroblasts (Fibro 1.2 and Fibro 1.7) transfected with ATOH1 expression plasmid or control plasmid was quantified by RT-qPCR in triplicates. The expression of miR-375 was normalized to U6 and is depicted relative to control cells as calculated by the $2^{-\Delta\Delta Cq}$ method (mean + SD)." The data shown above are from my published article (Fan et al., 2019a), Paper II and reproduced here with permission from Elsevier.

Indeed, there were dead cells among the suspension cells, however, living cells were also present at a certain ratio (**Fig. 9c**). On the other hand, to verify if ATOH1 could bind to the E-boxes of the miR-375 promoter, luciferase reporters carrying 3 E-boxes, mutated E-boxes or without E-box were used. Indeed, only reporters containing 3 E-boxes demonstrated a strong induction of luciferase activity when co-transfected with ATOH1 (**Fig. 9d**). Thus, we could infer that in MCC cells ATOH1 induces miR-375 via binding E-boxes in its promoter. More importantly, the ectopic expression of ATOH1 significantly increased miR-375 expression, particularly in suspension growing cells (**Fig. 9e**). We also the tested function of ATOH1 overexpression in primary skin fibroblasts, ATOH1 overexpression induced similar cell morphology changes as well as miR-375 expression (**Fig. 9f, g**).

3.2.4 MCPyV LTs induces ATOH1 and miR-375 expression as well as a NE-like growth pattern

MCPyV LTs are deeply involved in MCC carcinogenesis in MCPyV positive tumors. Here we overexpressed different truncated MCPyV LTs derived from different MCC cell lines in MRC-5 cells to test if ATOH1 and miR-375 expression were also triggered. Similar in the skin fibroblasts with ATOH1 overexpressing, part of MRC-5 cells transduced with MCPyV LTs turned into suspension growing cells (**Fig. 10a**). Importantly, expression of ATOH1 and miR-375 was induced by MCPyV LTs transduction, especially in the suspension growing MRC-5 cells (**Fig. 10b, c**). To be noted, ASCL1 expression was not induced by MCPyV LTs expression (data not shown). Moreover, consistent with the fact that ATOH1 expression is induced by MCPyV LTs, in our scRNAseq experiment using WaGa cells we noticed that high expression of LT and ATOH1 are located in the same cells, and their expression levels were correlated in all tested WaGa cells (**Fig. 10d-f**).

Taken together, we reveal that ATOH1 is likely a lineage-dependency oncogene in MCC by several lines of experimental evidence: forced ATOH1 expression induces morphology changed to NE-like growth pattern and miR-375 expression, and both of them are induced by truncated MCPyV LT. Therefore, MCPyV might trigger NE differentiation via induction of ATOH1 during MCC carcinogenesis.

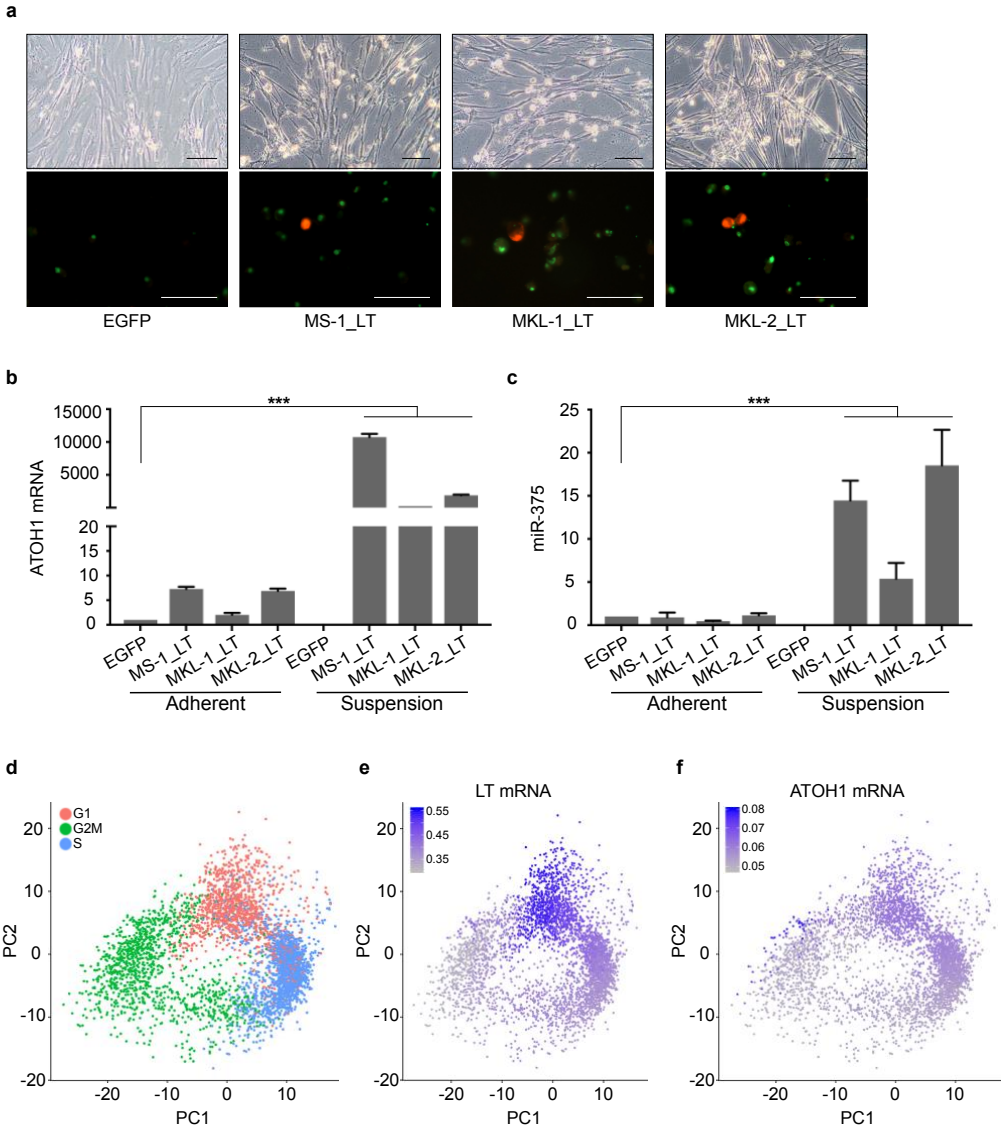

"Fig. 10: Overexpressed truncated MCPyV LTAs induces ATOH1 expression as well as miR-375 expression in MRC-5 cells

a: Upper row- morphology changes of MRC-5 cells transduced with different truncated MCPyV LTAs derived from MCC cell lines; lower row- floating growing cells stained with NucView® 488 and MitoView™ 633 apoptosis assay kit. Living cells were stained with red and dead/apoptotic cells were stained with green. Scale bar = 50 µM. **b**: ATOH1 expression in MRC-5 cells (adherent and suspension cells were analyzed separately) transduced with different truncated MCPyV LTAs expression constructs quantified by RT-qPCR in triplicates. The expression of ATOH1 was normalized to RPLP0 and is depicted relative to EGFP cells as calculated by the $2^{-\Delta\Delta Cq}$ method (mean + SD). **c**: miR-375 expression in MRC-5 cells expressing different truncated MCPyV LTAs was quantified by RT-qPCR in triplicates. The expression of miR-375 was normalized to U6 and is depicted relative to EGFP cells as calculated by the $2^{-\Delta\Delta Cq}$ method

(mean + SD). **d-f**: Principle component analysis (PCA) of single cell sequenced WaGa cells. **d**: PCA based exclusively on cell cycle marker genes, cells are colored with respect to their cell cycle. **e** and **f**: Expression level of MCPyV LTA mRNA (**e**) and ATOH1 mRNA (**f**) in WaGa cells in principle component reduced space. Expression values were imputed using the software MAGIC to compensate for dropouts typical for 10x Genomics scRNA-seq." The data shown above are from my published article (Fan et al., 2019a), Paper II and reproduced here with permission from Elsevier.

3.3 "Highly expressed miR-375 is not an intracellular oncogene in Merkel cell polyomavirus-associated Merkel cell carcinoma"（Paper III）

As we learned from previous studies, miR-375 was one of the most abundant miRNAs in MCCs. Regarding the function of miR-375, it acts as oncogene or tumor suppressor in different human cancers, while in MCCs, the role of miR-375 in cMCCs in different investigations are inconsistent. In this paper, we applied a more effective way to knockdown miR-375 in cMCCs to better understand its function in MCCs.

3.3.1 Knockdown of miR-375 in cMCC cells

For abundant miRNAs in cells, miRNA knockdown was essential to explore their functions, moreover, high knockdown efficacy is required. To achieve compete miR-375 knockdown in cMCC cell lines, we performed transfection in two different methods, i.e., lipofectamine-based and nucleofection, using antagomirs against miR-375 or NC in WaGa and PeTa cells. Expression of miR-375 decreased via lipofectamine-based transfection using miR-375 antagomirs in a dose-dependent manner in WaGa and PeTa

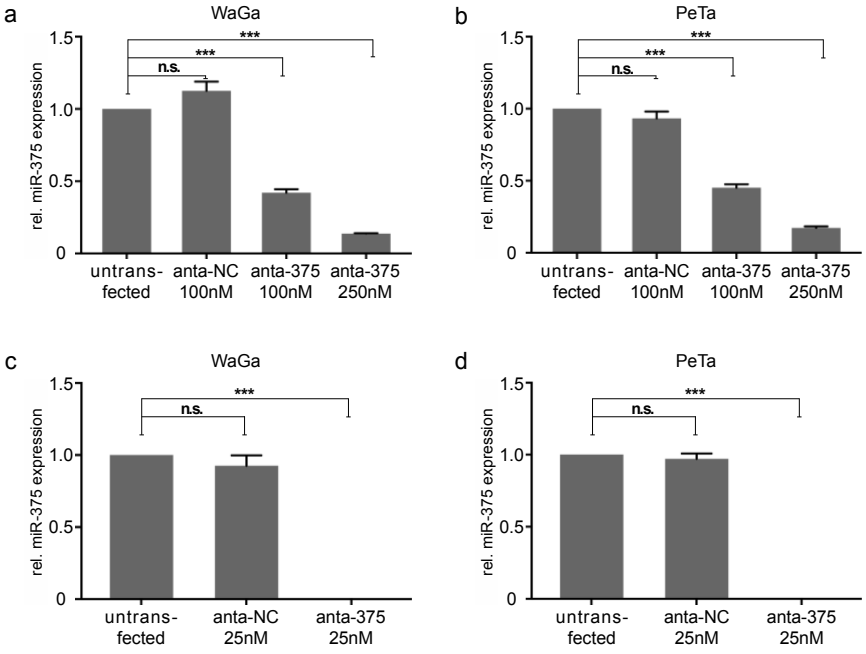

"Figure 11: miR-375 is knockdown in classical MCC cell lines

Relative miR-375 expression was determined in triplicates by RT-qPCR in WaGa (**a, c**) and PeTa (**b, d**) cells transfected with miR-375 antagomirs or negative control using lipofectamine (**a, b**) or nucleofection (**c, d**). Ct values were normalized to U6 and calibrated to the untreated WaGa cells. All experiments were independently repeated three times. Error bars represent SD, *** indicates p<0.001." The data shown above are from my preprint paper (Fan et al., 2019b), Paper III and reproduced here with the permission of bioRxiv.

cells (**Fig. 11a, b**), however, knockdown efficiency was not enough for this high expressed miR-375. Then we optimized nucleofection conditions for WaGa and PeTa cells and determined transfection program D23 and 25nM of miR-375 antagomirs as the best condition. Nearly compete miR-375 knockdown was achieved using this condition, almost no measurable miR-375 was detected in WaGa and PeTa cells after nucleofection (**Fig. 11c, d**).

3.3.2 miR-375 knockdown did not alter morphology or proliferation of MCC cells

Nucleofection resulted in nearly compete miR-375 knockdown, on the other hand, harsh transfection condition was associated with about 50% cell death in both cell lines. For subsequent experiments to determine phenotypic changes after miR-375 knockdown, dead cells and cell debris were removed using Ficoll centrifugation. However, cell morphology was not affected by nearly compete knockdown of miR-375, and cell proliferation ability was also not altered after miR-375 was knockdown (**Fig. 12**).

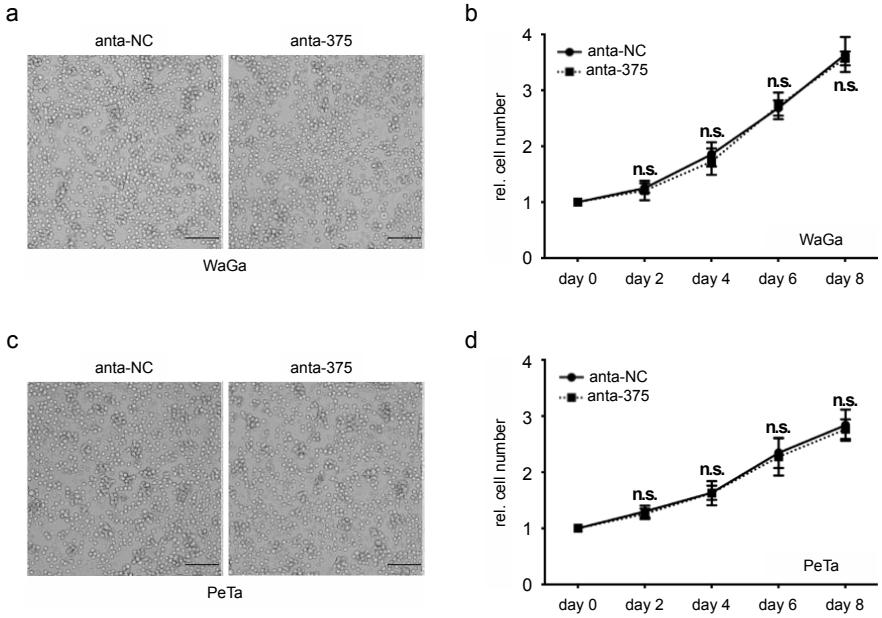

"Figure 12: miR-375 knockdown does not alter cell morphology and viability of MCC cells

Morphology of WaGa (**a**) and PeTa (**b**) cells 72 hours after nucleofection. Relative cell numbers of WaGa (**b**) and PeTa (**d**) cells seeded at 10_5 cells per well 48 hours after nucleofection with miR-375 antagomirs or negative control. Scale bar represents 50µm. All experiments were independently repeated three times, error

bars represent SD." The data shown above are from my preprint paper (Fan et al., 2019b), Paper III and reproduced here with the permission of bioRxiv.

3.3.3 EMT and Hippo signaling pathways related genes might be regulated by miR-375

Despite the fact that nearly compete knockdown of miR-375 didn't change cell morphology and proliferation ability in cMCC cells, in order to better understand the role if miR-375 in MCC, we predicted its target genes in ENCORI, an online tool for miRNA targets prediction. Top ranking genes (500) were selected among more than 3000 target genes for next step analysis, these genes related signaling pathways were determined by Gene ontology (GO) analysis. Several pathways were identified, such as cell junction assembly,

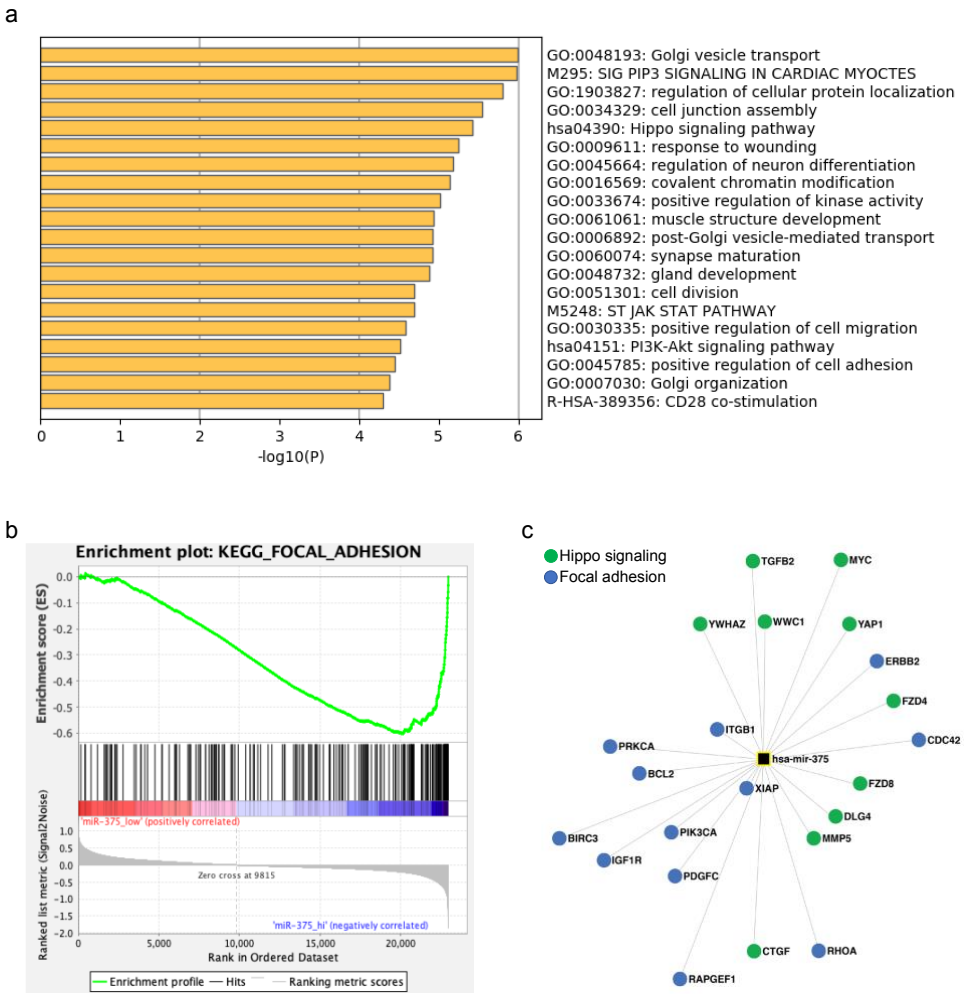

"Figure 13: miR-375 target genes are involved in Hippo and EMT signaling pathways

a: Gene ontology analysis was performed in Metascape using the top 500 predicted miR-375 target genes. **b**: Gene set enrichment analysis was performed using previously published transcriptome microarray data of MCC cell lines with high (WaGa, MKL1) and low (MCC13, MCC26) miR-375 expression. Enrichment plot

of kegg_focal_adhesion signaling pathway is depicted. **c**: miR-375 target genes involved in Hippo and focal adhesion signaling pathway." The data shown above are from my preprint paper (Fan et al., 2019b), Paper III and reproduced here with the permission of bioRxiv.

Golgi transport, neuron differentiation and Hippo signaling (**Fig. 13a**). To find out which predicted signaling pathways are more relevant in MCC cells, we performed gene set enrichment analysis (GSEA) using published transcriptome data of MCC cell lines. Four cell lines were used, WaGa and MKL-1 as miR-375_high as well as MCC13 and MCC26 as miR-375_low. GSEA revealed that genes in focal adhesion related signaling pathway were differentially expressed, lower in miR-375_high cells (**Fig. 13b**). Moreover, most of the experimentally confirmed miR-375 target genes are involved in Hippo and focal adhesion related signaling (**Fig. 13c**), and both pathways are EMT related (Frisch et al., 2013).

3.3.4 Expression of genes involved in Hippo and EMT signaling slightly altered via miR-375 knockdown

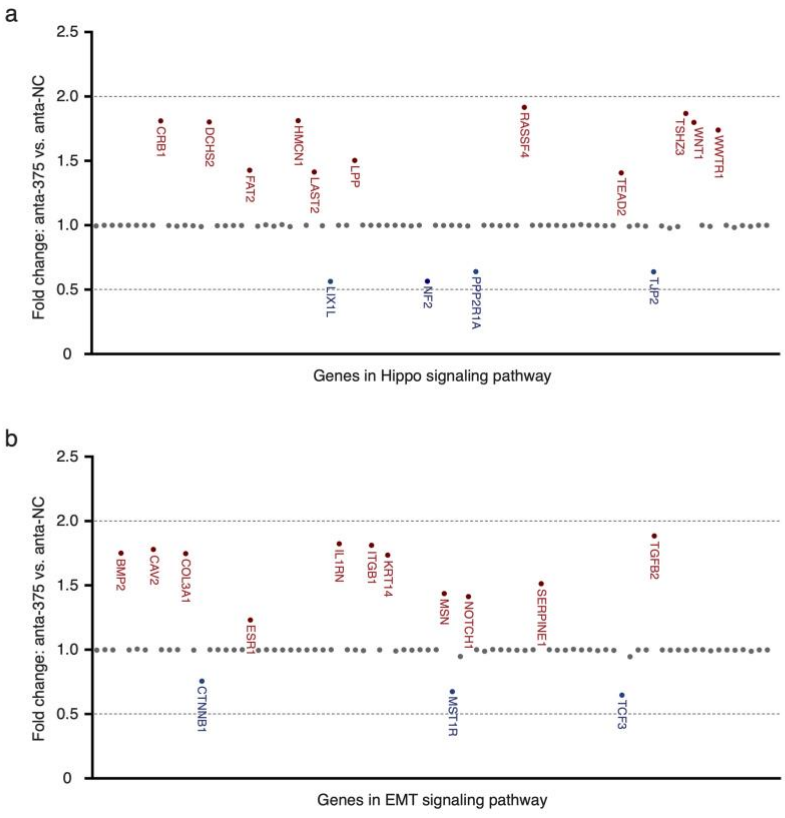

"Figure 14: Hippo and EMT signaling pathway related genes altered by miR-375 knockdown

Expression of genes related to Hippo (**a**) and EMT (**b**) signaling pathways were determined by multiplexed RT-qPCR expression array in WaGa cells transfected with anta-375 or anta-NC, normalized to the average of Ct values of housekeeping genes (GAPDH, HPRT and RPLP0) and calculated to the ΔCt of WaGa cells

transfected with anta-NC." The data shown above are from my preprint paper (Fan et al., 2019b), Paper III and reproduced here with the permission of bioRxiv.

Next, gene expression array was used to check the expression alteration of genes involved in Hippo and EMT signaling after miR-375 knockdown. Comparing to the MCC cells transfected with negative control antagomirs, expression of eleven genes upregulated and four genes downregulated in Hippo signaling pathway, also eleven genes upregulated and three downregulated in EMT related signaling pathway in MCC cells with miR-375 knockdown (**Fig. 14**). However, these alterations in gene expression are rather limited, not reaching a statistical relevance (less than two folds changes) (**Fig. 14**).

3.4 Merkel cell carcinoma derived exosomal miR-375 induces fibroblast polarization via inhibition of RBPJ and p53 (Paper IV)

We reported that knockdown of miR-375 in MCC cell lines, has at best minimal effects on cell survival, proliferation or cell morphology. Highly efficient knockdown did not alter any of the signaling pathways involving miR-375 target genes posing the question about the functional role of this highly abundant miRNA in MCC. Based on our observation that miR-375 is present in MCC conditioned cell culture medium as well as sera of MCC patients, it may function as exosomal shuttle miRNA. Here, we provide evidence that horizontally transferred exosomal miR-375 is substantial for polarization of fibroblasts towards CAFs in MCC.

3.4.1 Fibroblasts in MCC tumors exhibit a CAF like phenotype

Based on our previous results, we suggest that miR-375 acts in intercellular signaling process via exosomal shuttle and is able to polarize stromal cells of the tumor microenvironment. Thus, we characterized fibroblasts in the MCC microenvironment by evaluating the expression of CAF markers, including TE-7, Caveolin-1, α-SMA, and S100A4, using multiplexed immunofluorescence (IF) staining (n=10) (**Fig. 15A**). TE-7 was expressed at low levels in most stromal cells with a few exceptions. α-SMA was expressed by fibroblast-like cells and pericytes in the vicinity of blood vessels and was often colocalized with Caveolin-1. Unlike the expression pattern of the α-SMA, S100A4 was mainly expressed in single cells distributed throughout the tumor; only sometimes colocalizing with α-SMA (**Fig. 15A**). These morphological analyses demonstrate that MCC-associated fibroblasts are heterogeneous, but most of them exhibit a CAF-like phenotype.

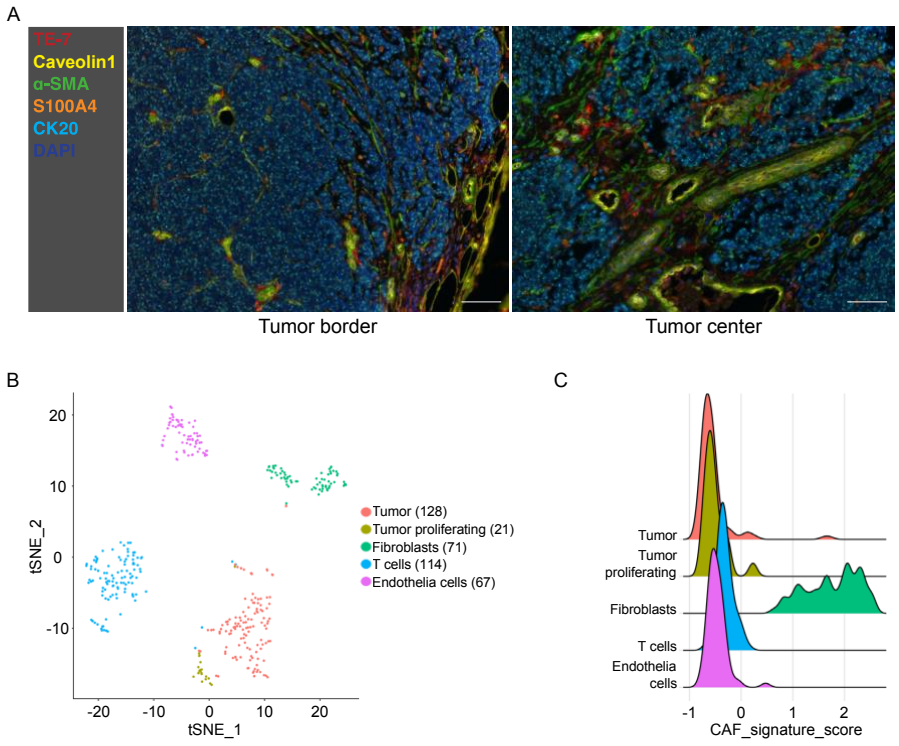

Fig. 15: Fibroblasts in MCC tumors exhibit a CAF like phenotype

A: FFPE sections of MCC tissues were stained by for fibroblast markers: TE-7 (red), Caveolin1 (yellow), a-SMA (green) and S100A4 (orange) as well as MCC tumor marker CK20 (light blue) and nuclear staining with DAPI (dark blue). A representative MCC tissue is depicted. Scale bar represents 50µm. **B**: t-SNE for mRNA expression obtained by scRNAseq of 401 cells isolated from MCC tumor. Cell clusters were annotated by mRNA expression profiles for known marker genes, numbers indicate the amount of cells in respective cell clusters. **C**: CAF signature score was generated for different cell clusters based on mRNA expression of selected CAF marker genes.

Next, we performed single cell RNA sequencing (scRNAseq) of a primary MCC tumor using 10x genomics chromium, in total 401 cells were analyzed. T-distributed stochastic neighbor embedding (tSNE) clustered them into MCC tumor cells (149, of which 21 were proliferating), fibroblasts (71), T lymphocytes (114) and endothelial cells (67) (**Fig. 15B**). Notably, tSNE separated the MCC associated fibroblasts roughly in two clusters based on their expression profile (**Fig. 15B**). In most of the fibroblasts expressed well-established CAF markers such as fibroblast activation protein (FAP), Thy-1 cell surface antigen (THY1), actin alpha 2, smooth muscle (ACAT2, encoding α-SMA), caveolin 1 (CAV1) and different collagenases, however, at different expression levels (**Fig. 16A**). Thus, we generated a CAF score based on the expression profile of these genes, which covered a large spectrum of values in the fibroblasts (**Fig. 15C**). Notably, several peaks within the spectrum represent groups of fibroblasts with different levels of CAF polarization (**Fig. 15C**). Besides that, two fibroblast clusters identified above were also classified as CAF_{low}

and CAF$_{high}$ groups according to respective CAF score values (**Fig. 16B, C**). In order to distinguish whether these two groups of fibroblasts were independently developed or just at different stages of CAF polarization, we calculated RNA velocity that predicts the future state of individual cells on a time scale of hours based on splicing transcripts ratios (La Manno et al., 2018). This revealed that these two fibroblasts clusters were directing towards different future states as indicated by RNA velocity vector in the principal component analysis (PCA) (**Fig. 16D**). In summary, MCC- associated fibroblasts showed a large heterogeneity and different polarization states in both IF studies as well as scRNAseq. On that basis we next analyzed if these observations are triggered by horizontal transfer of miR-375.

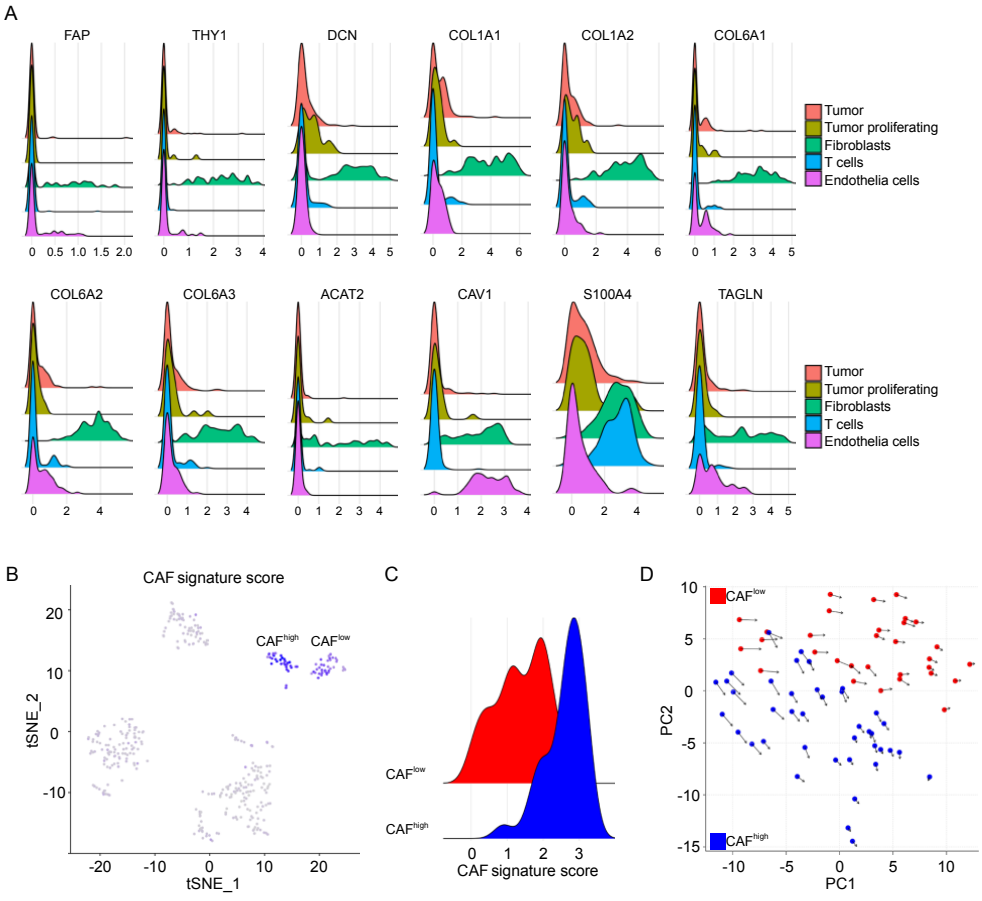

Figure 16: Heterogeneity of mRNA expression of gene related to fibroblast polarization in 401 individual cells obtained from a primary MCC tumor

A: mRNA expression levels of selected CAF markers in different identified cell clusters of MCC tumor. **B**: CAF signature score plotted on tSNE of all cell clusters, these two fibroblast clusters were annotated as CAF$_{high}$ and CAF$_{low}$. **C**: CAF signature score was generated for two fibroblast clusters based on mRNA expression of selected CAF marker genes. **D**: RNA velocity plotted in on tSNE of all cell clusters, arrows indicate the location of the estimated future cell state for each cell. **E**: RNA velocity plotted in principle component analysis (PCA) of the speed vector of two fibroblasts clusters, arrows indicate the location of the estimated future cell state for each cell.

3.4.2 miR-375 is enriched in MCC derived exosomes and transferred into fibroblasts

We confirmed the level of abundance of miR-375 and its function as exosomal shuttle miRNA in MCC cell lines by comparing the amount of previously reported highly expressed miRNAs (miR-19b, miR-106b, miR-375, miR-200c and miR-182) in WaGa cells and WaGa cell CM using RT-qPCR (**Fig 17A, B**) (Renwick et al., 2013, Fan et al., 2018). While all tested miRNAs were abundant in the cell lysate, only miR-375 was present in relevant amounts in CM. The strong predominance of miR-375 in cell free supernatant suggests an active and selective release of miR-375 by WaGa cells presumably by exosomal enrichment (Bhome et al., 2018). To test this hypothesis, we isolated exosomes from classical miR-375 expressing MCC cell lines (WaGa, PeTa, MKL-1, UM-MCC-13) conditioned medium, which exhibits the typical size between 30-100nm (**Fig. 17C**). miR-375 was strongly enriched in these exosomes as compared to the respective CM but it was not enriched in miR-375 negative cell lines MCC13 and SCL-2 (**Fig. 17D**). The MCC-derived exosomes were stained with ExoRed to investigate if they can be incorporated into the fibroblasts (**Fig. 17E**). The fibroblast cell line MRC-5 as well as primary skin fibroblast Fibro1.12 ingested the labelled exosomes within three hours (**Fig. 17F**). These observations strongly support the hypothesis that exosomal transfer of miR-375 from MCC cells to fibroblasts contribute to intercellular communication.

3.4.3 MCC derived factors polarize fibroblasts towards a CAF phenotype.

To explore the functional impact of MCC derived factors on fibroblasts, we performed a series of experiments co-culturing WaGa, PeTa or the miR-375 negative MCC13 cell line with fibroblasts. Three different co-culture conditions were tested: direct cell-cell contact (DC), transwell chamber system (TC) and MCC CM. For all subsequent experiments we used both the fibroblast cell line MRC-5 and primary fibroblasts. To ensure both reproducibility as well as biological relevance: while primary skin fibroblasts are biological more relevant, but they are characterized by a limited expansion capacity, thus primary skin fibroblasts from different donors had to be are used. Due to the different growth patterns of fibroblasts (adherent) and classical MCC cells (suspension), they could be easily separated before subsequent analysis. However, this does not apply for the variant MCC cell line MCC13 and therefore no DC experiment was performed for them.

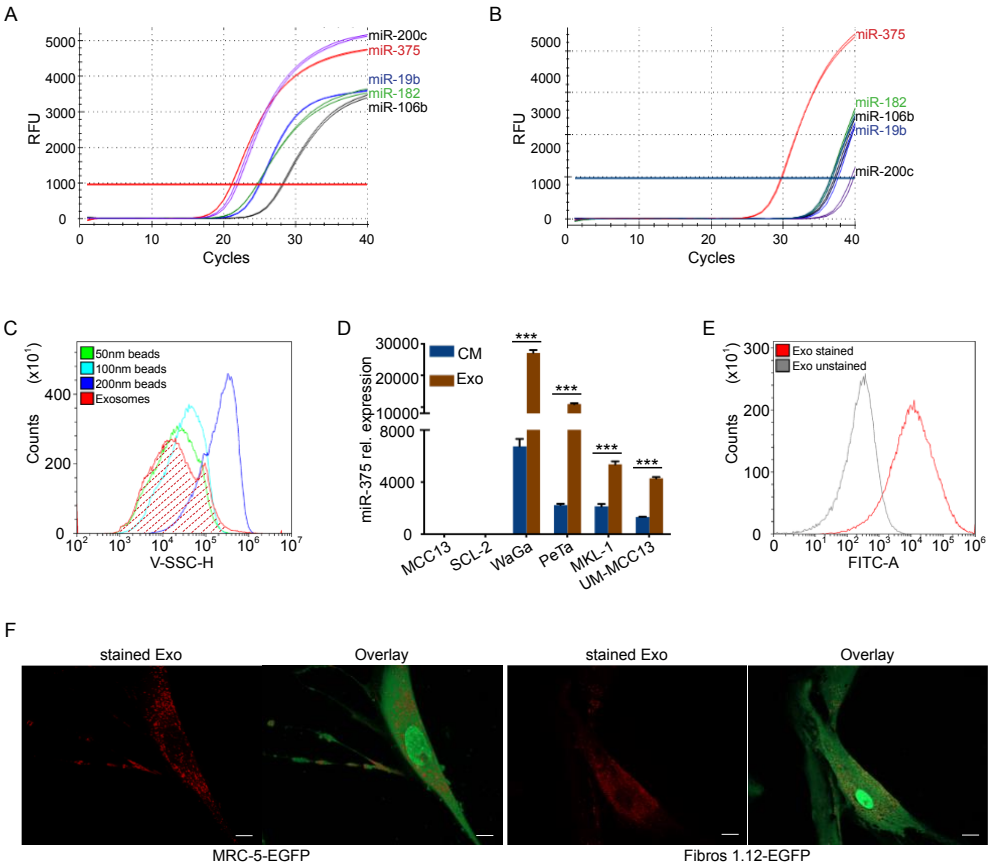

Fig. 17: Fibroblasts take up MCC derived exosomes containing miR-375.

A, B: Expression of miR-375, miR-182, miR-106b, miR-19b and miR-200c in WaGa cells (**A**) and conditioned medium (CM) of WaGa cells was determined by RT-qPCR. Depicted are the amplification curves of each micro-RNA in duplicates. **C**: Exosomes were isolated from WaGa CM. Size was determined by comparison to nanobeads of a defined size (50, 100 and 200nm). **D**: Relative miR-375 expression in exosomes derived from four classical MCC cell lines (WaGa, PeTa, MKL-1, UM-MCC13); a variant MCC cell line (MCC13), and cutaneous squamous cell carcinoma SCL-2 served as control, Ct values were normalized to a spike in cel-miR-39. **E**: Exosomes isolated from WaGa cells stained with Exo-Red, unstained exosomes served as negative control. **F**: EGFP expressing MRC-5 cells (left panels) or primary skin fibroblast (Fibro.1.12, right panels) were cultured alone or in presence of Exo-Red labeled WaGa derived exosomes. Representative overlay images are shown; scale bar represents 10µm. Error bars represent SD, *** indicates $p<0.001$.

The first discovery from these experiments was that either culture condition caused the newly occurring presence of miR-375 in MRC-5 and primary fibroblasts (**Fig. 18A, C**). The amount of detected miRNA varied substantially, with the largest amount in DC and the lowest in CM conditions (**Fig. 18A, C**). Since neither of the fibroblasts expressed miR-375 when cultured alone and none of the culture conditions induced pri-miR-375 (**Fig. 18B, D**), miR-375 expression was not induced, but it was rather transferred from MCC cells to fibroblasts.

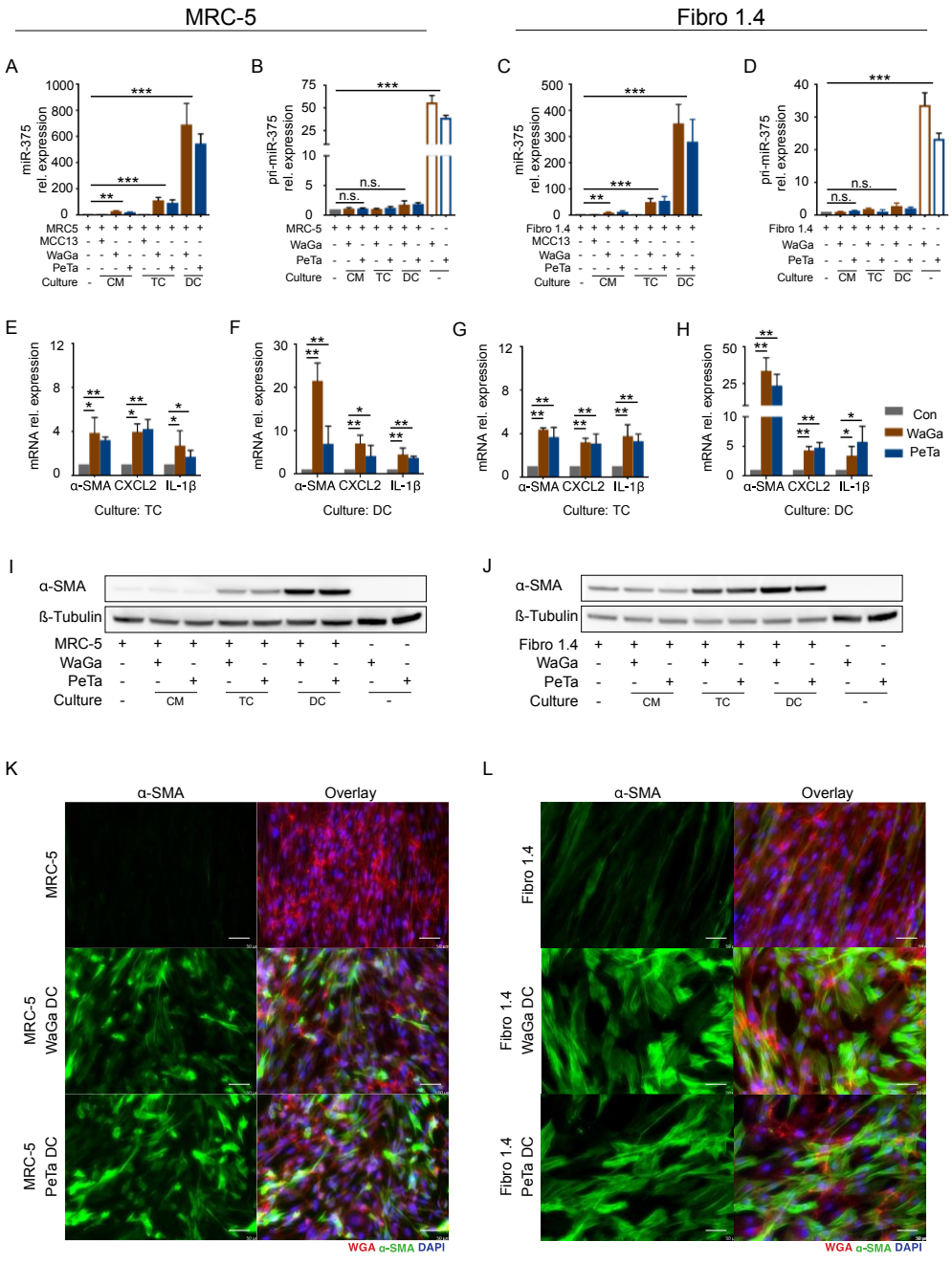

Fig. 18: mir-375 is horizontally transferred from MCC cells to fibroblasts induces a CAF-like phenotype

MRC-5 cells (A, B, E, F, I, K) or primary skin fibroblasts (Fibro1.4)(C, D, G, H, J, L) were treated with conditioned medium (CM), cultured in transwell (TC) or in direct (DC) co-culture with MCC13 (black), WaGa (red) or PeTa (blue) cells. **A- D**: Relative expression of miR-375 (A, C) and pri-miR-375 (B, D) in fibroblasts was determined by RT-q-PCR. **E- H**: Relative α-SMA, CXCL-2 and IL-1ß mRNA expression was determined in fibroblasts under TC conditions (**E, G**) or DC conditions (**F, H**) by RT-qPCR. **I, J**: α-SMA protein expression in fibroblasts co-cultured with MCC cells was determined by immunoblot, β-tubulin served as loading control. **K, L**: Immunofluorescence staining of α-SMA (green) in MRC-5 (**K**) and Fibro1.4 cells (**L**) after direct co-culture with MCC cells. Cellular membranes were stained with WGA (red) and nuclei with DAPI (blue). Scale bars represent 50µm. For RST-qPCR experiments, Ct values were

normalized to U6 or HPRT and calibrated to the ΔCt of untreated MRC-5 or Fibro1.4 cells respectively. All experiments were independently repeated three times. Error bars represent SD, *** indicates p<0.001.

Next, we analyzed the functional effects of the exosomal cargo transferred from MCC, including miR-375, on fibroblasts by measuring the mRNA expression of CAF markers, i.e. α-SMA, CXCL2 and IL-1β. In line with higher miR-375 uptake, CAF markers were also higher expressed in fibroblasts under DC conditions, especially α-SMA (**Fig. 18E-H**). α-SMA was also induced on protein level as evidenced by immunoblot of cell lysates and by IF staining (**Fig. 18I-L**). The latter also revealed substantial morphological changes of fibroblasts under co-culture conditions, like an elongated, stellate shape, which are in accordance with a CAF-like phenotype (**Fig. 18K, L**) (Kalluri, 2016).

3.4.4 miR-375 alone is sufficient for fibroblast polarization.

Since many factors transferred from MCC cells may cause fibroblasts polarization, we next tested to which extent miR-375 is responsible for the observed effect. Thus, we experimentally induced miR-375 in fibroblast (**Fig. 19A, C**). Ectopic expression of miR-375 resulted in an increased mRNA expression of CXCL2, IL-1β and predominately α-SMA (**Fig. 19B, D**), that was more pronounced in primary skin fibroblasts (Fibro 1.12) than in MRC-5 cells. α-SMA was also induced on protein level upon ectopic miR-375 expression as determined by immunoblot (**Fig. 19E, F**) and IF staining (**Fig. 19G, H**). In addition, the fibroblast morphology changed towards a CAF phenotype, but to a lesser extent compared to direct co-culture with miR-375 expressing MCC cells. Thus, these results provide conclusive evidence that miR-375 is sufficient for fibroblast polarization.

Most miRNAs exert their function by interfering with mRNA stability or inhibiting its translation. To this end, recombination signal binding protein for immunoglobulin kappa J region (RBPJ) and p53 are predicted and experimentally confirmed target genes of miR-375(Abraham et al., 2016a, Liu et al., 2013). Moreover, reduced expression of RBPJ and p53 has been reported to be associated with polarization of fibroblasts(Procopio et al., 2015, Kim et al., 2017, Goruppi et al., 2017, Arandkar et al., 2018). Upon experimentally induced expression of miR-375 in fibroblasts we indeed observed a significant downregulation of RBPJ and p53 mRNA and protein expression (**Fig. 19I- N**). With respect to CAF markers upregulation, this effect was more pronounced in primary skin fibroblasts comparing to MRC-5 cells (**Fig. 19B, D**). These observations indicate that miR-375 mediated inhibition of RBPJ and p53 is one of the mechanisms for MCC induced fibroblast polarization.

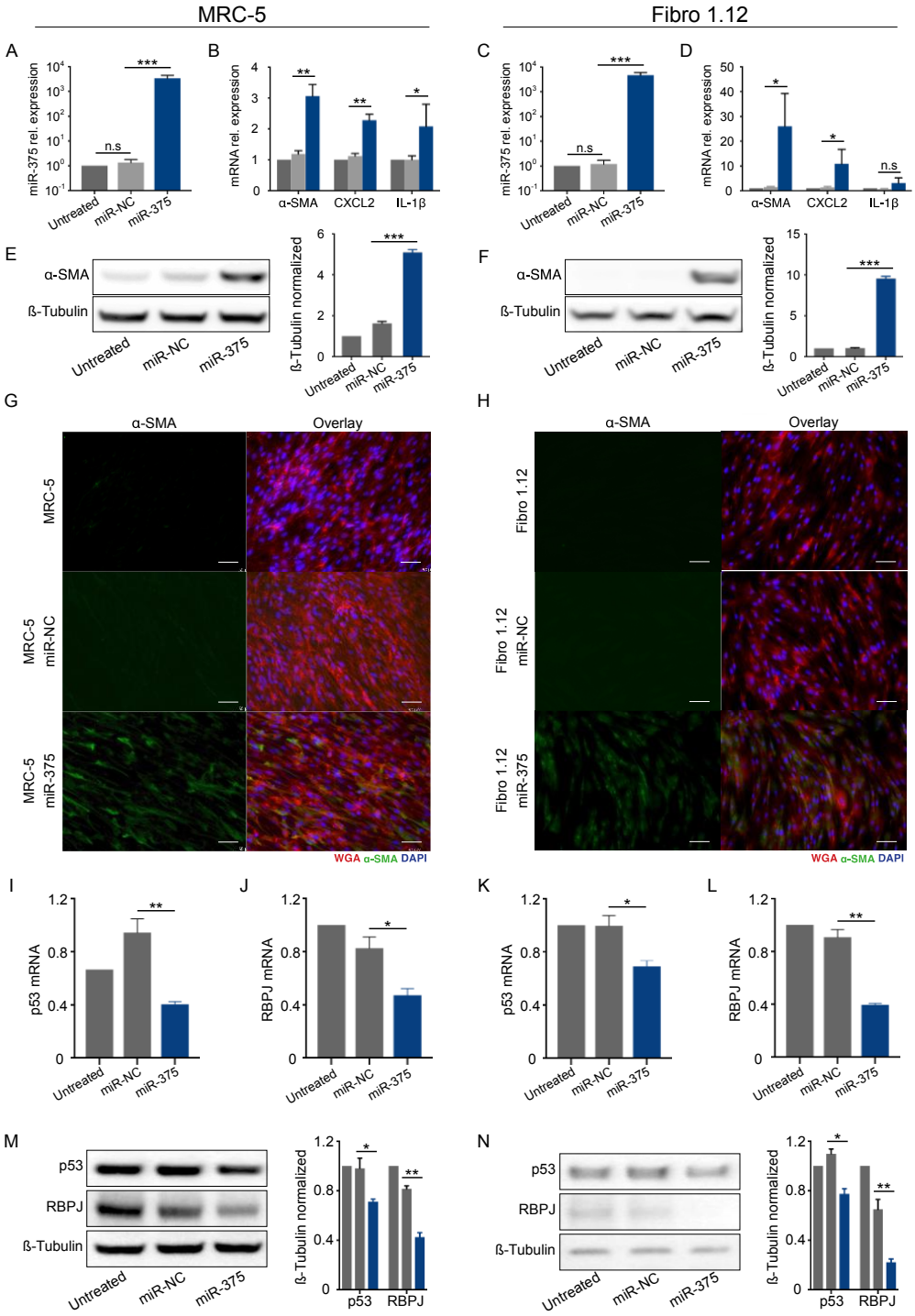

Fig. 19: Overexpression of mir-375 in MRC-5 and primary skin fibroblasts induces a CAF-like phenotype.

miR-375 was overexpressed in MRC-5 cells (**A, B, E, G, I, J**) or primary skin fibroblasts (Fibro1.12) (**C, D, F, H, L, N**). **A, C**: Relative miR-375 expression of untreated, miR-negative control (NC) and miR-375 mimic transfected fibroblasts was determined by RT-q-PCR. **B, D**: Relative α-SMA, CXCL-2 and IL-1ß mRNA expression of untreated, miR-NC and miR-375 mimic transfected fibroblasts by RT-qPCR. **E, F**: α-SMA protein expression in untreated, miR-NC and miR-375 mimic transfected fibroblasts was determined by immunoblot, β-tubulin served as loading control. Quantifications were performed using imageJ. **G, H**: Immunofluorescence staining for α-SMA (green) in untreated, miR-NC and miR-375 mimic transfected fibroblasts. Cellular membranes were stained with WGA (red) and nuclei with DAPI (blue). Scale bars represent 50µm. **I- L**: Relative p53 and RBPJ mRNA expression of untreated, miR-NC and miR-375 mimic

transfected fibroblasts were determined by RT-qPCR. **M, N**: p53 and RBPJ protein expression in untreated, miR-NC and miR-375 mimic transfected fibroblasts was determined by immunoblot, β-tubulin served as loading control. Quantifications were performed using imageJ. For RT-qPCR experiments, Ct values were normalized to U6 or HPRT and calibrated to the ΔCt of untreated MRC-5 or Fibro1.4 cells respectively. All experiments were independently repeated three times. Error bars represent SD, *** indicates p<0.001.

3.4.5 miR-375 antagomirs diminished MCC induced fibroblast polarization

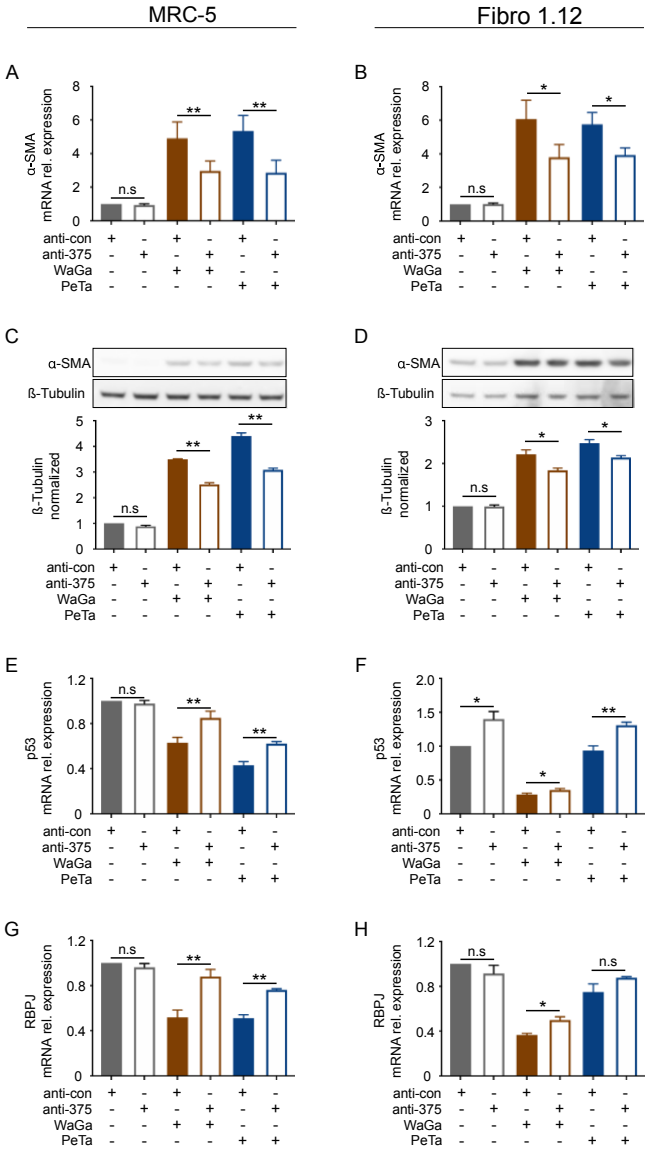

Fig. 20: miR-375 antagomirs diminish MCC cells co-culture induced fibroblast polarization

Fibroblasts MRC-5 (**A, C, E, G**) or primary skin fibroblasts Fibro 1.12 (**B, D, F, H**) were transfected with antagomirs against miR-375 or control prior to co-culture with WaGa or PeTa cells in transwell. **A, B**: Relative α-SMA expression in fibroblasts under indicated conditions was determined by RT-qPCR. **C, D**: α-SMA protein expression in in fibroblasts under indicated conditions was determined by immunoblot; β-tubulin served as loading control. **E- H**: Relative p53 and RBPJ mRNA expression of in fibroblasts under indicated conditions was determined by RT-qPCR. For all RT-qPCR experiments, Ct values were normalized to HPRT mRNA expression and calibrated to the ΔCt of untreated MRC-5 or Fibro.1.12 cells transfected with antagomirs control (anta-con) respectively. All experiments were independently repeated three times. Error bars represent SD, *** indicates p<0.001.

To further scrutinize the relevance of miR-375 in MCC induced fibroblast polarization, we repeated our co-culture experiments in the presence of miR-375 antagomirs. The antagomirs substantially reduced the detectable amount of miR-375 transferred into fibroblasts under TC or DC conditions. However, the transferred miR-375 was not completely abolished, indeed the reduced miR-375 amounts in DC conditions were still higher than the amounts under in TC conditions in absence of miR-375 antagomirs. Thus, we observed a significant reduction of induced miR-375 α-SMA expression on both mRNA and protein levels only for TC conditions (**Fig. 20A-D**). Notably, the effects of the miR-375 antagomirs on CXCL2 and IL-1β expression were more pronounced.

The effects of miR-375 antagomirs on miR-375 induced fibroblast polarization is directly explained by the observation that RBPJ and p53 mRNA is partly rescued by the miR-375 antagomirs (**Fig. 20E- H**). It should be noted that the rescue is more effective in MRC-5 cells. Due to the limited efficacy of antagomirs to inactivate miR-375, this effect was more evident under TC conditions.

3.4.6 Presence of miR-375 in tumor cells and CAFs of MCC tumor tissue *in situ*

To translate our *in vitro* observations into the clinical setting, we performed miRNA *in situ* hybridizations with miR-375 probe on a series of MCC tumors (n=6). miR-375 was predominantly expressed in MCC cells, but also present in stromal cells with fibroblast morphology (**Fig. 21A**). The miR-375 positive stromal cells were characterized by the same morphological appearance and distribution as the α-SMA expressing cells (**Fig. 21C**). Thus, we established a relative α-SMA staining score in 20 MCC lesions and correlated it with the miR-375 expression determined by qRT-PCR, demonstrating a significant positive correlation (**Fig. 21C, D**). Furthermore, expression of RBPJ and p53 were negatively correlated with miR-375 expression (**Fig. 21E, F**). GSEA of the scRNAseq data of a primary MCC described above comparing CAF_{high} and CAF_{low} fibroblast clusters based on the described CAF score demonstrated that p53 related pathway is more inhibited in the CAF_{high} fibroblasts (**Fig. 21G**). These *in situ* findings strongly support the notion that the horizontal transfer of miR-375 from MCC cells to fibroblast triggers the polarization of the latter towards a CAF phenotype by downregulation of p53 and RBPJ.

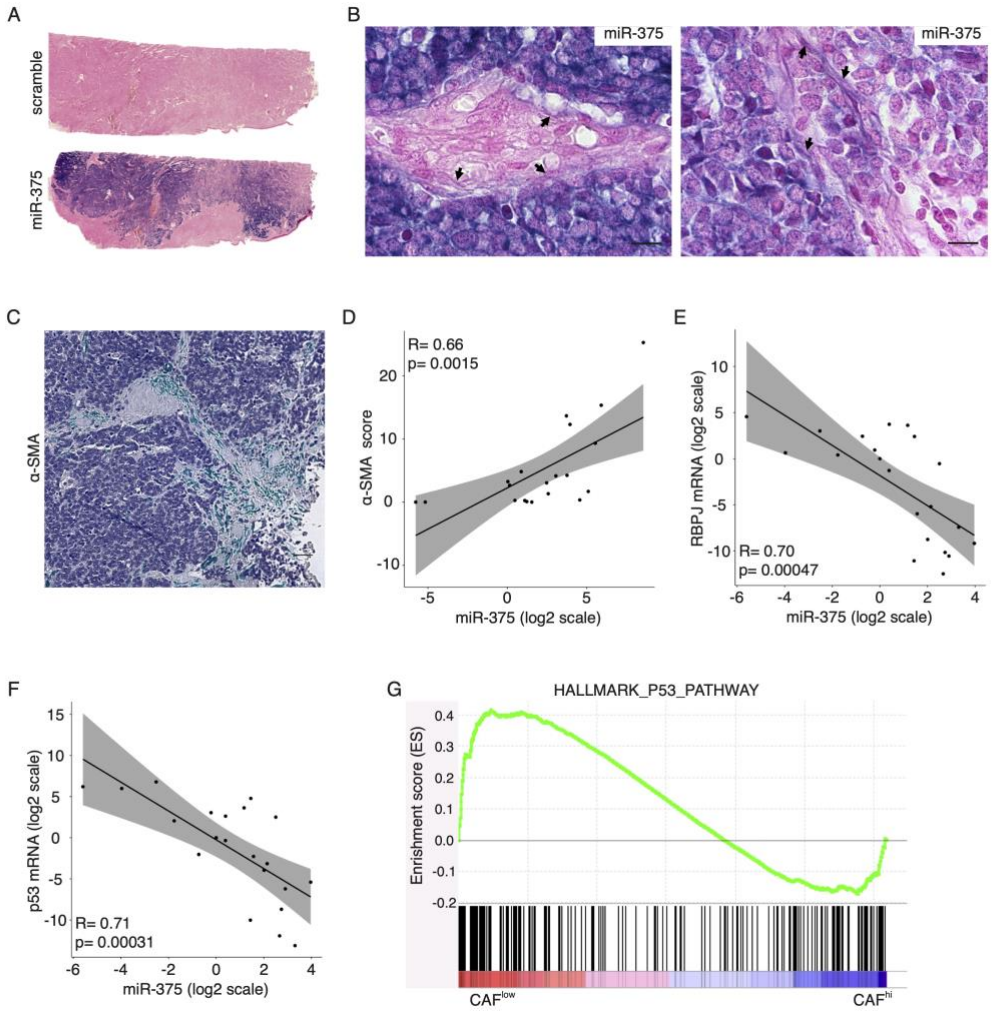

Fig. 21: miR-375 expression correlates with fibroblast polarization *in situ*.

A: FFPE fixed MCC tumor tissues were hybridized with a scrambled control probe (upper) or a miR-375 specific probe (lower). Whole slide scans of one representative MCC tissue are depicted. **B**: Two representative tumor areas are depicted at high resolution to demonstrate presence of miR-375 in fibroblasts (indicated by arrows); scale bars represent 10µm. **C**: MCC tissues (n=20) were stained for α-SMA, one representative MCC tissue are depicted. **D**: Spearman rank correlation of α-SMA staining scores and miR-375 expression level. **E, F**: Spearman rank correlation of p53 and RBPJ mRNA expression level with miR-375 expression level. Statistical analyses were performed in R using the "ggpubr" package. Error bars represent SD. *** indicates $p<0.001$. **G**: GSEA was performed using scRNA data of two fibroblasts clusters, p53 related signaling was manifested.

4. Discussion

Part of the discussion may resemble the discussion sections from my published papers (Fan et al., 2019a, Fan et al., 2018, Fan et al., 2019b).

In this thesis, we discovery that miR-375 is highly expressed in MCC cells and tissues, present in MCC conditioned medium as well as serum of two preclinical animal models bearing MCC tumor xenotransplantation. More importantly, data from four independent MCC patient cohorts clearly indicate that miR-375 serum levels not only distinguish MCC patients with tumor from MCC patients of NED, but also could be used as a powerful tool to monitor tumor progression or treatment. Besides miR-375 as a biomarker, we also explored the transcriptional mechanism of miR-375. We demonstrate that forced expression of truncated MCPyV LT in fibroblasts triggers expression of ATOH1, a BHLH transcriptional factor, which binds to E-boxes and directly activates transcription of miR-375. To determine the functional role of miR-375 in MCC cells, knockdown of miR-375 was performed in cMCC cell lines. However, nearly miR-375 knockdown did not change cell viability, morphology as well as growth pattern, two oncogenic pathways (Hippo and EMT) were only slightly altered. Based on the facts showed above, we hypotheses that miR-375 might an intercellular factor, rather than an intracellular oncogenic factor. Indeed, horizontally transferred exosomal miR-375 polarizes fibroblasts into CAF phenotype via targeting RBPJ and p53.

MCC is highly metastatic cancer type in the skin, however, the treatment methods for metastatic MCC are rather limited, i.e. surgery and radiation, and these methods are not usually effective enough to benefit the pat. The appearance of immunotherapy using immune checkpoint inhibitors dramatically changed the landscape of MCC treatment (Kaufman et al., 2016, Nghiem et al., 2016, Terheyden and Becker, 2017). Nevertheless, part of the patients doesn't respond to the therapy or develop resistance to it. As we learned from the reports of previous clinical trials, around 2/3 patients responded to the therapy in the first-line treatment and only 1/3 patients in the second-line treatment (Kaufman et al., 2016, Nghiem et al., 2016, Terheyden and Becker, 2017). These data showed that MCC patients bearing limited tumor burden benefited more from the immunotherapy, thus we need a method for detection of early MCC tumor recurrence or progression after treatment. Obviously, tumor tissue-based techniques are not feasible for metastatic MCC tumors. Regarding imaging technologies, such as PET/CT or MR imaging, they are effective but

rather costly, moreover, documented risks are involved (Huntington et al., 2015). Thus, blood-based biomarkers have advantages, they could be repeatedly collected in a non-invasive way and monitoring the whole clinical course of the patients. More importantly, they could provide evidence when the imaging step is required for localizing the tumor (Wong et al., 2017). Another advantage of using miRNA as a marker is that tumor burden information can be revealed without knowing the exact locations of metastatic or recurrent lesions, which is essential for highly metastatic cancer types.

Blood-based tumor markers have been identified and applied in many tumor types, in MCC, different molecules had been investigated by several research groups. Since MCC is the NE tumor of the skin, established biomarkers for other NE tumors are rational candidates to be tested. For example, chromogranin A (CGA) and neuron-specific enolase (NSE) serum levels serve as circulating biomarkers for small cell lung cancer (SCLC) (Isgro et al., 2015). However, when tested in MCC patients, neither CGA nor NSE was able to distinguish MCC patients bearing tumor burden or not effectively according to their serum levels (Gaiser et al., 2015). On the other hand, more than 80% MCC tumors are associated with MCPyV integration, thus the presence of oncoproteins encoded by MCPyV might serve as surrogate markers for MCC tumor burden (Paulson et al., 2010, Touzé et al., 2011, Paulson et al., 2017). Antibodies against these virus coded oncoproteins (antibody titer) were used to demonstrate their serum levels of MCC patients. As expected, oncoprotein antibody titers significantly correlated with MCC tumor burden, low antibody titers in the patients with tumor remission and high titers in patients with tumor recurrence were detected. In cohort from Seattle, antibody titers of MCPyV ST data were also provided by collaborators, which allow us to compare miR-375 and MCPyV ST serum level in the same samples. Indeed, ROC analysis revealed the almost identical results of miR-375 and MCPyV ST in MCC patients with the presence of MCPyV ST in the serum. However, MCPyV oncoproteins are not present in the serum of MCC patients carrying MCPyV negative tumors, then this method is not feasible in these patients. Moreover, no MCPyV oncoproteins is not detected in half of the patients carrying MCPyV associated MCC tumors at baseline (Paulson et al., 2017), which indicates that these antibody titers could not be set at baseline and not applicable to monitor the tumor progression. To date, miR-375 is the only applicable circulating biomarker for MCC tumor burden in virus negative and positive MCC patients.

As mentioned in the introduction section, at beginning miR-375 was described as a pancreatic specific miRNA, which functioned in insulin secretion regulation and was required for pancreatic islet development (Poy et al., 2004). Later on, miR-375 dysregulation was found in different tumor types, downregulated in gastric (Ding et al., 2010, Tsukamoto et al., 2010), pancreatic (Zhou et al., 2012), colon (Dai et al., 2012, Faltejskova et al., 2012) and liver cancer (He et al., 2012), indicating miR-375 was playing a role of oncogene in these cancer types. In prostate cancer (Szczyrba et al., 2011), medullary thyroid carcinoma (Hudson et al., 2013), NE lung cancer (Nishikawa et al., 2011) and MCC (Renwick et al., 2013, Xie et al., 2014), miR-375 expression was found upregulated. In line with these studies, we confirmed here miR-375 was strongly expressed in the largest MCC cell lines panel to date *in vitro*, MCC tissues samples *in vivo* and miR-375 hybridization on MCC tissue *in situ*. To be noted, high expression of miR-375 was not virus dependent in MCC cell lines and tumor tissues. Moreover, a substantial amount of miR-375 was detected in MCC conditioned medium, but not other miRNAs which were also highly expressed in MCC cells (miR-106b, miR-182, miR-19b, miR-200c). miR-375 was reported as exosomal miRNA, which explains miR-375 was readily in conditioned medium. Moreover, in our following research, we indeed found that miR-375 was enriched in exosomes derived from MCC cells.

According to our data, we infer that miR-375 in the serum of MCC patients is secreted from MCC cells, then miR-375 expressed in blood cells might impair the function of miR-375 as a biomarker. As we checked published investigations, miR-375 is not expressed in blood cells (Pritchard et al., 2012), such as red blood cells or platelets (Mitchell et al., 2016). Moreover, miR-375 is not differentially expressed in serum and plasma (Wang et al., 2012a), which allows us to use both blood materials for miR-375 detection.

To shortly summarize, miR-375 is highly expressed in MCCs and present in MCC derived CMs as well as sera of two preclinical animal models carrying MCC tumors. These facts allow us to check if miR-375 is present in the serum of MCC patients and serves as a circulating tumor marker for MCC tumor burden. Indeed, miR-375 serum levels not only distinguish MCC patients with or without tumor burden but also correlated with tumor stages. Moreover, miR-375 is a promising tool for monitoring the response to different therapies, especially immunotherapy. In the future, miR-375 will be validated in the clinical trials for MCC treatment.

MCC development is strongly associated with MCPyV integration in the genome, more than 80% MCC are MCPyV positive. Now it is known that viruses integrated into the host genome manipulate the expression of host genes via multiple means, one is that virus encoded proteins or short RNA molecules (such as miRNAs) could hijack the epigenetic machinery of the host cells (Engdahl et al., 2017, Kuss-Duerkop et al., 2018). Take the methylation machinery as an example, viruses could foster hypermethylation in the promoter regions of certain immune related genes in order to avoid the detection of host immune system, which a common mechanism applied by different viruses (Kuss-Duerkop et al., 2018). More specific, DNA methyltransferases (DNMTs) are strongly associated with DNA methylation status, which could be exploited by different viruses, such as KSHV recruits DNMT3A to host genes (Shamay et al., 2006), and HPV E6 and E7 upregulate DNMT1 expression level (Burgers et al., 2007). Another example, human herpesvirus 6B (HHV-6B) infection often result in hypomethylation of telomere regions as their accessible integration site (Engdahl et al., 2017). In MCC cells, MCPyV might be also associated with epigenetic modification during MCC development. According to our data, truncated MCPyV LTs likely induce hypomethylation of promoter regions of ATOH1 and miR-375, thus increase their expression levels. On the other hand, LTs might induce ATOH1 or miR-375 expression in different manners, as reported recently ATOH1 is directly activated by SOX2, which as induced by MCPyV LTs (Harold et al., 2019). However, deeper investigations are required to fully understand the mechanism.

Nevertheless, highly expressed ATOH1 and miR-375 is observed in MCPyV negative MCC tissues and classical MCC cell lines, the regulation mechanism of ATOH1 and miR-375 in these cells cannot explained by MCPyV LTs associated inductions. To date, virus negative MCCs are more associated with UV induced mutations, however, shared activated oncogenic signaling pathways were discovered in both virus positive and negative MCCs (Gonzalez-Vela et al., 2017). Although the genetic landscape of those two groups of MCCs is quite different from each, higher mutation burden is associated with virus negative MCCs, same transcription factors, i.e. STAT3, is found accumulated in the nuclear of MCC cells (Gonzalez-Vela et al., 2017). More important, STAT3 was reported as an inducer of ATOH1 in epithelial cells (Zhang et al., 2012).

In the ATOH1 overexpression experiments in vMCC cell lines as well as in skin fibroblasts, we reveal ATOH1 as transcription factor inducing miR-375 expression. To be noted, forced expression of ATOH1 in these cells not only upregulate miR-375 expression

but also changed their growth pattern from adherent cells into a NE like pattern, like suspension growing cells. In general, suspension cells derived from adherent cells are considered as apoptotic or dying cells, however, a substantial amount of those suspension growing cells induced by ATOH1 expression are living cells. Moreover, expression levels of ATOH1 and miR-375 are much higher comparing to those adherent cells transfected with ATOH1. Someone might argue that ATOH1 induces cell morphology change and miR-375 induction is likely an accompanying event during cell morphology change, such as suspension growing. To clear the doubt, we also checked the expression of miR-375 in vMCC cell lines growing in ultra-low attachment plates as well as hanging drops, miR-375 expression was not altered in such forced suspension growing conditions, which indicate miR-375 induction is not an accompanying event via suspension growing. Moreover, overexpression of miR-375 in vMCC cell lines promoted NE differentiation phenotype (Abraham et al., 2016a). Taken these observations and notions together, augmented expression of ATOH1 and miR-375 are associated with NE like growth pattern change, and we even conjecture that ectopic expression of ATOH1 and miR-375 caused the morphology changes. To verify if this hypothesis is supported in other NE cancers, we checked previously published papers about ATOH1 and miR-375 expression levels. The fact that high expression of both ATOH1 and miR-375 are found in these cancers indeed supports this hypothesis (Park et al., 2006, Northcott et al., 2009, Flora et al., 2009, Arvidsson et al., 2018).

ATOH1, also called Hath1 as a human gene or Math1 as a mouse gene, is a BHLH transcription factor, often involved in NE differentiation. As reported, it is required for Merkel cells and inner ear hair cell development (Ostrowski et al., 2015, Chen et al., 2018). Dysregulation of ATOH1 was found in multiple cancer types. Downregulation of ATOH1 in gastric cancer (Han et al., 2015) hepatocellular cancer (Gao et al., 2017) and colon cancer (Bossuyt et al., 2009, Fukushima et al., 2015) indicates that it might function as a tumor suppressor, while high expression of ATOH1 in medulloblastoma (Briggs et al., 2008, Grausam et al., 2017) reflects that it might play a role as oncogene. As we learned from this paper, ATOH1 is highly expressed in cMCC cell lines and tissues, and it might function as an oncogene. However, ATOH1 knockdown in cMCC cell lines did not result in cell viability /proliferation alteration. Therefore, we speculate that ATOH1 may rather be a lineage dependent oncogene, but not a lineage survival oncogene in MCCs (Garraway and Sellers, 2006). However, besides proliferation ability, migration/ invasion ability or

drug resistance was not investigated after ATOH1 knockdown. Another evidence that supports the idea that ATOH1 functions as lineage dependent oncogene is from a recent reported MCC transgenic mice model. Only co-expressing ATOH1 together with MCPyV LTs induces MCC-like lesions in the mice indicate that ATOH1 is an essential factor for MCC development. In our experiments of overexpressing different truncated MCPyV LTs in MRC-5 cells, we indeed observed that ATOH1 expression was induced by LTs. Moreover, this induction was stronger in the cells changed their morphology into NE growth pattern comparing to the unchanged adherent cells. In line with our hypothesis, a recently published paper demonstrates that knockdown of MCPyV T antigen directly inhibited ATOH1 expression (Harold et al., 2019).

Next, we investigated the function of miR-375 in cMCC cells via miR-373 knockdown. As introduced in previous papers, miR-375 abundantly expressed in cMCC cell lines and MCC tissues, however, the function of miR-375 is still not clear in MCC. Thus, knockdown experiments using specific antagomirs against miR-375 or NC were applied to demolish miR-375 in cMCC cell lines. To our surprise, nearly complete miR-375 knockdown did not change cell proliferation ability, morphology or growth pattern. Accordingly, two oncogenic signaling pathways, i.e. Hippo and EMT, which is predicted as miR-375 regulating pathways in MCC cells, are only marginally affected by miR-375 knockdown. Moreover, we have demonstrated in the previous paper that the presence of miR-375 was readily detected in CM derived from cMCC cells culture, serum of two MCC xenotransplantation animal models as well as serum of MCC patients with tumor burden (Fan et al., 2018). Taken together, miR-375 might function as intercellular signaling molecule interacting with stromal cells in the MTE of MCCs, but not serve in intracellular signaling. Furthermore, miR-375 was reported as exosomal miRNA recently (Huang et al., 2015, Su et al., 2019), and we indeed confirmed that miR-375 was enriched in exosomes derived from MCC cells in a subsequent project.

Regarding the function of miR-375 in MCC cells, several reports have been published, however, the results are not consistence in cMCC cells. In vMCC cell lines, miR-375 is lowly expressed and overexpression of miR-375 decreased cell proliferation and migration ability, thus it is considered as a tumor suppressor (Abraham et al., 2016b, Kumar et al., 2018). However, in cMCC cells knockdown or inhibition of miR-375 resulted in different outcomes. Abraham et al demonstrated that miR-375 knockdown by antagomis did not change cell growth properties (Abraham et al., 2016b), while according to Kumar's study,

miRNA sponge induced miR-375 inhibition resulted in decreased cell proliferation ability, upregulated cell death via targeting to LDHB gene (Kumar et al., 2018). Moreover, another function of miR-375 was revealed by Kumar's another published paper, miR-375 inhibits autophagy via targeting to ATG7 (Kumar et al., 2019). The conflicting results in cMCC cells might be due to the limited specificity of used antagomirs or miRNA sponge, or different effectivity of transfection methods.

To knockdown highly expressed miRNAs could be a demanding task (Krutzfeldt et al., 2005), especially in certain cells difficult to be transfected. In this study, two transfection methods were applied to introduce antagomirs into cMCC cells, one is common lipofectamine based transfection and another is nucleofection. The result revealed that nucleofection using antagomirs lead to a nearly complete miR-375 knockdown. To be noted here, nucleofection is also associated with half of the cell death, thus for some primary cell with limited amount, it is might not applicable. As mentioned before, other than antagomirs, miRNA sponge was applied to inhibit the function of miR-375 in cMCC cells (Kumar et al., 2018). To specify here, the miR-375 expression could remain the same after the miRNA sponge was introduced.

To date, more than ten online tools have been released for miRNA target genes prediction, but the results from those tools are highly incompatible. ENCORI we used in the study could provide comprehensive results from online tools, such as TargetScan, miRanda, microT, PITA, miRmap, and PicTar (Li et al., 2014). More practically, Argonaute crosslinking and immunoprecipitation data of all tested miRNAs were also integrated into the results (Li et al., 2014). Using ENCORI, miR-375 target genes were predicted in this study. Then those selected target genes were used for Gene Ontology (GO) enrichment analysis in Metascape, signaling pathways possibly targeted or regulated by miR-375 were determined. Together with the GSEA using published transcriptome microarray data of MCC cell lines, EMT and Hippo were determined as miR-375 regulating signaling pathway in MCC cells.

RT-qPCR based profiler arrays were applied to check the expression of Hippo and EMT related signaling molecules after miR-375 knockdown, up 84 genes of each signaling pathway were tested. According to our data, only a few genes were upregulated after miR-375 knockdown and even less gene downregulated, and more importantly, all of these changes are smaller than two-fold changes. Even Hippo and EMT were predicted as miR-375 regulating signaling pathways in MCCs, however, the effect of miR-375 knockdown

on them was rather very limited. Actually, the gap is not too difficult to understand. Recent studies about long non-coding RNAs (lncRNAs) offered possible explanations: lncRNAs, like HNGA1, TINCR and CircFAT1 are reported as miR-375 sponge in different cancer types (Chen et al., 2017b, Liu et al., 2018, Wang, 2016). Thus, it is possible that one or more than one lncRNAs are highly expressed in MCC cells and abundant miR-375 is trapped and not functional. On the other hand, miR-375 might act in a redundant manner in MCC cells because other miRNAs which are homologues to it are also expressed and targeting to similar genes. More investigations are required to solve this question.

In solid cancers, stromal cells have an impact at all stages of cancer progression. To date, fibroblasts in MCC tumors have not been scrutinized in detail. Here, we reveal the heterogeneity of fibroblasts in the stroma of MCC lesions, reflecting a spectrum of polarization towards a CAF phenotype. In most cancers, fibroblast polarization is triggered by tumor derived factors such as TGF-β, PDGF or IL-6 that are only lowly expressed or absent in tested cMCC cell lines and MCC tumors (data not shown). Moreover, these molecules are not present in the exosomes derived from cMCC cell lines (Konstantinell et al., 2016). Thus, the question of alternative ways of fibroblasts polarization in MCCs is raised.

To this end, horizontal transfer of miRNAs within exosomes has been reported to promote functional and metabolic reprogramming of fibroblasts (Mitra et al., 2012, Yan et al., 2018a). Here we demonstrate that exosomal transferred miR-375 from MCC cells to fibroblasts targets RBPJ and p53 causing downregulation of their expression that is associated with fibroblast polarization. RBPJ, *aka* CSL, is a Notch mediator which suppresses CAF polarization (Procopio et al., 2015, Goruppi et al., 2017, Kim et al., 2017). p53 downregulation allows fibroblasts to overcome cell senescence that is induced by RBPJ downregulation and thus boosts CAF polarization (Procopio et al., 2015, Arandkar et al., 2018). Both RBPJ and p53 were previously reported as target genes of miR-375 (Abraham et al., 2016a, Liu et al., 2013), a notion which was confirmed by our study. Indeed, expression of miR-375 was inversely correlated with RBPJ and p53 expression in MCC tumor tissues. Unfortunately, mRNA expression of RBPJ and p53 in fibroblasts from MCC tumor was below detection line in scRNAseq. However, p53 related signaling pathways are strongly inhibited in those fibroblasts manifesting a high CAF score.

Different MCC/ fibroblast co-culture conditions, *i.e.*, CM, TC or DC resulted in increasing effects on CAF polarization. This phenomenon can be explained by the amount of miR-

375 transferred to fibroblasts via exosomes or direct contact. In addition, DC conditions may also allow material transfer, such as miRNAs, through tunneling nanotubes between tumor cells and fibroblasts (Thayanithy et al., 2014). Besides miR-375, other factors horizontally transferred by exosomes or nanotubes from MCC cells to fibroblasts may cause their polarization. Secretomic analysis of MCC derived exosomes revealed more than 160 proteins are present (Konstantinell et al., 2016). Hence, it is important to note that the ectopic expression of miR-375 alone was sufficient to polarize fibroblasts and that miR-375 antagomirs decreased MCC co-culture triggered phenotype changes in fibroblasts. Thus, it is safe to conclude that miR-375 plays a major role in MCC mediated CAF polarization.

We further demonstrate the presence of miR-375 in stromal cells with the appearance of fibroblasts of MCC by *in situ* hybridization. Quantitative differences of miR-375 might be one of the causes for CAFs' heterogeneity in MCC as observed by multiplexed IF staining and scRNAseq. However, different origins, *e.g.*, tissue resident fibroblasts or recruited mesodermal stem cells, prior activation stages or additional environmental factors may contribute to this fibroblast heterogeneity in MCC (Kalluri, 2016, Chen and Song, 2019). We demonstrated uptake of exosomes by fibroblasts, but other stromal cells, such as lymphocytes, macrophages and endothelial cells in the microenvironment are likely to be affected as well. As reported previously, mesenchymal stromal cell-derived exosomes altered mRNA expression and function of B-Lymphocytes (Khare et al., 2018) and endothelial cells (Liang et al., 2016). Notably, transferred miR-375 enhanced tumor-associated macrophages migration and infiltration into tumor spheroids in breast cancer (Frank et al., 2019).

Until now, we have established the role of miR-375 for intercellular communication between MCC tumor cells and stromal fibroblasts. We demonstrate that miR-375 derived from MCC cells or miR-375 alone can induce fibroblast polarization *in vitro* and that this probably also occurs *in situ* MCC patients. These observations suggest that miR-375 constitutes an attractive target for therapeutic interventions, as the feasibility of the therapeutic role of miRNA is currently investigated in cutaneous T cell lymphoma for miR-155 (Seto et al., 2018).

To summarize all these four papers, we confirm that miR-375 is highly expressed in MCCs and present in CM and sera of MCC animal models and patients. It is identified as a reliable circulating biomarker for MCC tumor burden and promising monitor for disease

progression or treatment. On the other hand, the mechanism of high miR-375 expression is also explored. ATOH1 binds to E-boxes of miR-375 promoter and induce its transcription. Moreover, ectopic ATOH1 also induces morphology change of vMCC cell lines and fibroblast into NE like growing pattern. Both ATOH1 and miR-375 are induced by truncated MCPyV LTs partial disclose the mechanism of MCPyV associated MCC carcinogenesis. Regarding the function of miR-375 in MCC cells, knockdown experiments were performed. To our surprise, nearly complete miR-375 knockdown does not alter cell proliferation/ viability, nor cell morphology change. Two oncogenic signaling pathways predicted as targets of miR-375 are only weakly altered. However, as an exosomal miRNA, miR-375 is found enriched in MCC derived exosomes, together with the observations described above, we indicate that miR-375 could be an important regulator in the cell-cell communication. Next, we discover that fibroblasts in MCC TME exhibit heterogeneous CAF phenotype, and this phenomenon is likely associated with miR-375. MCC co-culture and miR-375 overexpression /knockdown experiments with/ in different fibroblasts reveal miR-375 horizontally transferred from MCC cells to fibroblasts or alone induces fibroblast polarization. All in all, in this thesis, we not only identify miR-375 as a serum marker but also reveal miR-375 expression mechanism and its function in CAF polarization in TME of MCC.

5. Bibliography

ABRAHAM, K. J., ZHANG, X., VIDAL, R., PARE, G. C., FEILOTTER, H. E. & TRON, V. A. 2016a. Roles for miR-375 in neuroendocrine differentiation and tumor suppression via Notch pathway suppression in Merkel cell carcinoma. *The American Journal of Pathology,* 186**,** 1025-1035.

ABRAHAM, K. J., ZHANG, X., VIDAL, R., PARE, G. C., FEILOTTER, H. E. & TRON, V. A. 2016b. Roles for miR-375 in neuroendocrine differentiation and tumor suppression via Notch pathway suppression in Merkel cell carcinoma. *Am J Pathol,* 186**,** 1025-1035.

AGELLI, M. & CLEGG, L. X. 2003. Epidemiology of primary Merkel cell carcinoma in the United States. *Journal of the American Academy of Dermatology,* 49**,** 832-41.

AGELLI, M., CLEGG, L. X., BECKER, J. C. & ROLLISON, D. E. 2010. The etiology and epidemiology of merkel cell carcinoma. *Current Problems in Cancer,* 34**,** 14-37.

AGUADO-LLERA, D., GOORMAGHTIGH, E., DE GEEST, N., QUAN, X. J., PRIETO, A., HASSAN, B. A., GOMEZ, J. & NEIRA, J. L. 2010. The basic helix-loop-helix region of human neurogenin 1 is a monomeric natively unfolded protein which forms a “fuzzy" complex upon DNA binding. *Biochemistry,* 49**,** 1577-1589.

AHIRWAR, D. K., NASSER, M. W., OUSEPH, M. M., ELBAZ, M., CUITINO, M. C., KLADNEY, R. D., VARIKUTI, S., KAUL, K., SATOSKAR, A. R., RAMASWAMY, B., ZHANG, X. L., OSTROWSKI, M. C., LEONE, G. & GANJU, R. K. 2018. Fibroblast-derived CXCL12 promotes breast cancer metastasis by facilitating tumor cell intravasation. *Oncogene,* 37**,** 4428-4442.

AKERS, J. C., GONDA, D., KIM, R., CARTER, B. S. & CHEN, C. C. 2013. Biogenesis of extracellular vesicles (EV): exosomes, microvesicles, retrovirus-like vesicles, and apoptotic bodies. *Journal of Neuro-Oncology,* 113**,** 1-11.

ALKASALIAS, T., FLABERG, E., KASHUBA, V., ALEXEYENKO, A., PAVLOVA, T., SAVCHENKO, A., SZEKELY, L., KLEIN, G. & GUVEN, H. 2014. Inhibition of tumor cell proliferation and motility by fibroblasts is both contact and soluble factor dependent. *Proceedings of the National Academy of Sciences of the United States of America,* 111**,** 17188-17193.

ARANDKAR, S., FURTH, N., ELISHA, Y., NATARAJ, N. B., VAN DER KUIP, H., YARDEN, Y., AULITZKY, W., ULITSKY, I., GEIGER, B. & OREN, M. 2018. Altered p53 functionality in cancer-associated fibroblasts contributes to their cancer-supporting features. *Proceedings of the National Academy of Sciences of the United States of America,* 115**,** 6410-6415.

ARAVIN, A. A., LAGOS-QUINTANA, M., YALCIN, A., ZAVOLAN, M., MARKS, D., SNYDER, B., GAASTERLAND, T., MEYER, J. & TUSCHL, T. 2003. The small RNA profile during Drosophila melanogaster development. *Developmental Cell,* 5**,** 337-350.

ARNOLD, J. N., MAGIERA, L., KRAMAN, M. & FEARON, D. T. 2014. Tumoral immune suppression by macrophages expressing fibroblast activation protein-alpha and heme oxygenase-1. *Cancer Immunology Research,* 2**,** 121-6.

ARROYO, J. D., CHEVILLET, J. R., KROH, E. M., RUF, I. K., PRITCHARD, C. C., GIBSON, D. F., MITCHELL, P. S., BENNETT, C. F., POGOSOVA-AGADJANYAN, E. L., STIREWALT, D. L., TAIT, J. F. & TEWARI, M. 2011. Argonaute2 complexes carry a population of circulating microRNAs independent of vesicles in human plasma. *Proceedings of the National Academy of Sciences of the United States of America,* 108**,** 5003-5008.

ARVIDSSON, Y., REHAMMAR, A., BERGSTRÖM, A., ANDERSSON, E., ALTIPARMAK, G., SWÄRD, C., WÄNGBERG, B., KRISTIANSSON, E. & NILSSON, O. 2018. miRNA profiling of small intestinal neuroendocrine tumors defines novel molecular subtypes and identifies miR-375 as a biomarker of patient survival. *Modern Pathology,* 31**,** 1302-1317.

AYALA, G., TUXHORN, J. A., WHEELER, T. M., FROLOV, A., SCARDINO, P. T., OHORI, M., WHEELER, M., SPITLER, J. & ROWLEY, D. R. 2003. Reactive stroma as a predictor of biochemical-free recurrence in prostate cancer. *Clinical Cancer Research,* 9**,** 4792-4801.

BABIARZ, J. E., RUBY, J. G., WANG, Y. M., BARTEL, D. P. & BLELLOCH, R. 2008. Mouse ES cells express endogenous shRNAs, siRNAs, and other Microprocessor-independent, Dicer-dependent small RNAs. *Genes & Development,* 22**,** 2773-2785.

BARTEL, D. P. 2004. MicroRNAs: Genomics, biogenesis, mechanism, and function. *Cell,* 116**,** 281-297.

BARTEL, D. P. 2009. MicroRNAs: target recognition and regulatory functions. *Cell,* 136**,** 215-233.

BECKER, J. C., HOUBEN, R., UGUREL, S., TREFZER, U., PFOHLER, C. & SCHRAMA, D. 2009. MC polyomavirus is frequently present in Merkel cell carcinoma of European patients. *Journal of Investigative Dermatology,* 129**,** 248-250.

BECKER, J. C., STANG, A., DECAPRIO, J. A., CERRONI, L., LEBBE, C., VENESS, M. & NGHIEM, P. 2017. Merkel cell carcinoma. *Nature Reviews Disease Primers,* 3**,** 17077.

BEHM-ANSMANT, I., REHWINKEL, J., DOERKS, T., STARK, A., BORK, P. & IZAURRALDE, E. 2006. MRNA degradation by miRNAs and GW182 requires both CCR4 : NOT deadenylase and DCP1 : DCP2 decapping complexes. *Genes & Development,* 20**,** 1885-1898.

BHATIA, K., GOEDERT, J. J., MODALI, R., PREISS, L. & AYERS, L. W. 2010. Merkel cell carcinoma subgroups by Merkel cell polyomavirus DNA relative abundance and oncogene expression. *International Journal of Cancer,* 126**,** 2240-6.

BHOME, R., DEL VECCHIO, F., LEE, G. H., BULLOCK, M. D., PRIMROSE, J. N., SAYAN, A. E. & MIRNEZAMI, A. H. 2018. Exosomal microRNAs (exomiRs): Small molecules with a big role in cancer. *Cancer Letter,* 420**,** 228-235.

BINNEWIES, M., ROBERTS, E. W., KERSTEN, K., CHAN, V., FEARON, D. F., MERAD, M., COUSSENS, L. M., GABRILOVICH, D. I., OSTRAND-ROSENBERG, S., HEDRICK, C. C., VONDERHEIDE, R. H., PITTET, M. J., JAIN, R. K., ZOU, W. P., HOWCROFT, T. K., WOODHOUSE, E. C., WEINBERG, R. A. & KRUMMEL, M. F. 2018. Understanding the tumor immune microenvironment (TIME) for effective therapy. *Nature Medicine,* 24**,** 541-550.

BOHNSACK, M. T., CZAPLINSKI, K. & GORLICH, D. 2004. Exportin 5 is a RanGTP-dependent dsRNA-binding protein that mediates nuclear export of pre-miRNAs. *RNA,* 10**,** 185-191.

BORCHERT, G. M., LANIER, W. & DAVIDSON, B. L. 2006. RNA polymerase III transcribes human microRNAs. *Nature Structural & Molecular Biology,* 13**,** 1097-1101.

BOSSUYT, W., KAZANJIAN, A., DE GEEST, N., VAN KELST, S., DE HERTOGH, G., GEBOES, K., BOIVIN, G. P., LUCIANI, J., FUKS, F., CHUAH, M., VANDENDRIESSCHE, T., MARYNEN, P., COOLS, J., SHROYER, N. F. & HASSAN, B. A. 2009. Atonal homolog 1 is a tumor suppressor gene. *Plos Biology,* 7**,** 311-326.

BRACKEN, C. P., GREGORY, P. A., KOLESNIKOFF, N., BERT, A. G., WANG, J., SHANNON, M. F. & GOODALL, G. J. 2008. A double-negative feedback loop between ZEB1-SIP1 and the microRNA-200 family regulates epithelial-mesenchymal transition. *Cancer Research,* 68**,** 7846-7854.

BRECHBUHL, H. M., FINLAY-SCHULTZ, J., YAMAMOTO, T. M., GILLEN, A. E., CITTELLY, D. M., TAN, A. C., SAMS, S. B., PILLAI, M. M., ELIAS, A. D., ROBINSON, W. A., SARTORIUS, C. A. & KABOS, P. 2017. Fibroblast subtypes regulate responsiveness of Luminal breast cancer to Estrogen. *Clinical Cancer Research,* 23**,** 1710-1721.

BRIGGS, K. J., EBERHART, C. G. & WATKINS, D. N. 2008. Just say no to ATOH: how HIC1 methylation might predispose medulloblastoma to lineage addiction. *Cancer Research,* 68**,** 8654-8656.

BURGERS, W. A., BLANCHON, L., PRADHAN, S., DE LAUNOIT, Y., KOUZARIDES, T. & FUKS, F. 2007. Viral oncoproteins target the DNA methyltransferases. *Oncogene,* 26**,** 1650-1655.

BUTLER, A., HOFFMAN, P., SMIBERT, P., PAPALEXI, E. & SATIJA, R. 2018. Integrating single-cell transcriptomic data across different conditions, technologies, and species. *Nature Biotechnology,* 36**,** 411-420.

CAMPS, C., BUFFA, F. M., COLELLA, S., MOORE, J., SOTIRIOU, C., SHELDON, H., HARRIS, A. L., GLEADLE, J. M. & RAGOUSSIS, J. 2008. hsa-miR-210 is induced by hypoxia and is an independent prognostic factor in breast cancer. *Clinical Cancer Research,* 14**,** 1340-1348.

CHANG, T. C., YU, D. N., LEE, Y. S., WENTZEL, E. A., ARKING, D. E., WEST, K. M., DANG, C. V., THOMAS-TIKHONENKO, A. & MENDELL, J. T. 2008. Widespread microRNA repression by Myc contributes to tumorigenesis. *Nature Genetics,* 40**,** 43-50.

CHEN, X. & SONG, E. 2019. Turning foes to friends: targeting cancer-associated fibroblasts. *Nature Reviews Drug Discovery,* 18**,** 99-115.

CHEN, Y., ZENG, C., ZHAN, Y., WANG, H., JIANG, X. & LI, W. 2017a. Aberrant low expression of p85α in stromal fibroblasts promotes breast cancer cell metastasis through exosome-mediated paracrine Wnt10b. *Oncogene,* 36**,** 4692.

CHEN, Y. C., TSAI, C. L., WEI, Y. H., WU, Y. T., HSU, W. T., LIN, H. C. & HSU, Y. C. 2018. ATOH1/RFX1/RFX3 transcription factors facilitate the differentiation and characterisation of inner ear hair cell-like cells from patient-specific induced

pluripotent stem cells harbouring A8344G mutation of mitochondrial DNA. *Cell Death & Disease,* 9**,** 437.

CHEN, Z., LIU, H., YANG, H., GAO, Y., ZHANG, G. & HU, J. 2017b. The long noncoding RNA, TINCR, functions as a competing endogenous RNA to regulate PDK1 expression by sponging miR-375 in gastric cancer. *OncoTargets and Therapy,* 10**,** 3353-3362.

CHENDRIMADA, T. P., GREGORY, R. I., KUMARASWAMY, E., NORMAN, J., COOCH, N., NISHIKURA, K. & SHIEKHATTAR, R. 2005. TRBP recruits the Dicer complex to Ago2 for microRNA processing and gene silencing. *Nature,* 436**,** 740-744.

CHENG, J. W., ROZENBLATT-ROSEN, O., PAULSON, K. G., NGHIEM, P. & DECAPRIO, J. A. 2013. Merkel cell polyomavirus large T antigen has growth-promoting and inhibitory activities. *Journal of Virology,* 87**,** 6118-6126.

CHIM, S. S. C., SHING, T. K. F., HUNG, E. C. W., LEUNG, T. Y., LAU, T. K., CHIU, R. W. K. & LO, Y. M. D. 2008. Detection and characterization of placental MicroRNAs in maternal plasma. *Clinical Chemistry,* 54**,** 482-490.

CHOY, E. Y. W., SIU, K. L., KOK, K. H., LUNG, R. W. M., TSANG, C. M., TO, K. F., KWONG, D. L. W., TSAO, S. W. & JIN, D. Y. 2008. An Epstein-Barr virus-encoded microRNA targets PUMA to promote host cell survival. *Journal of Experimental Medicine,* 205**,** 2551-2560.

CHTEINBERG, E., SAUER, C. M., RENNSPIESS, D., BEUMERS, L., SCHIFFELERS, L., EBEN, J., HAUGG, A., WINNEPENNINCKX, V., KURZ, A. K., SPEEL, E. J., ZENKE, M. & ZUR HAUSEN, A. 2018. Neuroendocrine key regulator gene expression in Merkel cell carcinoma. *Neoplasia,* 20**,** 1227-1235.

CIMINO, P. J., ROBIRDS, D. H., TRIPP, S. R., PFEIFER, J. D., ABEL, H. J. & DUNCAVAGE, E. J. 2014. Retinoblastoma gene mutations detected by whole exome sequencing of Merkel cell carcinoma. *Modern Pathology,* 27**,** 1073-1087.

CIMMINO, A., CALIN, G. A., FABBRI, M., IORIO, M. V., FERRACIN, M., SHIMIZU, M., WOJCIK, S. E., AQEILAN, R. I., ZUPO, S., DONO, M., RASSENTI, L., ALDER, H., VOLINIA, S., LIU, C. G., KIPPS, T. J., NEGRINI, M. & CROCE, C. M. 2005. miR-15 and miR-16 induce apoptosis by targeting BCL2. *Proceedings of the National Academy of Sciences of the United States of America,* 102**,** 13944-13949.

COENEN-STASS, A. M. L., MAGEN, I., BROOKS, T., BEN-DOV, I. Z., GREENSMITH, L., HORNSTEIN, E. & FRATTA, P. 2018. Evaluation of methodologies for microRNA biomarker detection by next generation sequencing. *Rna Biology,* 15**,** 1133-1145.

COLLER, H. A., FORMAN, J. J. & LEGESSE-MILLER, A. 2007. "Myc'ed messages": myc induces transcription of E2F1 while inhibiting its translation via a microRNA polycistron. *Plos Genetics,* 3**,** e146.

DAI, X., CHIANG, Y., WANG, Z., SONG, Y., LU, C., GAO, P. & XU, H. 2012. Expression levels of microRNA-375 in colorectal carcinoma. *Mol Med Rep,* 5**,** 1299-304.

DE PALMA, M., BIZIATO, D. & PETROVA, T. V. 2017. Microenvironmental regulation of tumour angiogenesis. *Nature Reviews Cancer,* 17**,** 457-474.

DE SOUZA, M. F., KUASNE, H., BARROS, M. D., CILIAO, H. L., MARCHI, F. A., FUGANTI, P. E., PASCHOAL, A. R., ROGATTO, S. R. & COLUS, I. M. D. 2017. Circulating mRNAs and miRNAs as candidate markers for the diagnosis and prognosis of prostate cancer. *Plos One,* 12**,** e0184094.

DENLI, A. M., TOPS, B. B. J., PLASTERK, R. H. A., KETTING, R. F. & HANNON, G. J. 2004. Processing of primary microRNAs by the Microprocessor complex. *Nature,* 432**,** 231-235.

DING, L., XU, Y., ZHANG, W., DENG, Y., SI, M., DU, Y., YAO, H., LIU, X., KE, Y., SI, J. & ZHOU, T. 2010. MiR-375 frequently downregulated in gastric cancer inhibits cell proliferation by targeting JAK2. *Cell Research,* 20**,** 784-93.

DONG, H., GAO, Q., PENG, X. W., SUN, Y., HAN, T., ZHAO, B. L., LIU, Y. F., WANG, C. B., SONG, X. H., WU, J. J. & YANG, L. 2017. Circulating microRNAs as potential biomarkers for veterinary infectious diseases. *Frontiers in Veterinary Science,* 4**,** 186.

DONNARUMMA, E., FIORE, D., NAPPA, M., ROSCIGNO, G., ADAMO, A., IABONI, M., RUSSO, V., AFFINITO, A., PUOTI, I., QUINTAVALLE, C., RIENZO, A., PISCUOGLIO, S., THOMAS, R. & CONDORELLI, G. 2017. Cancer-associated fibroblasts release exosomal microRNAs that dictate an aggressive phenotype in breast cancer. *Oncotarget,* 8**,** 19592-19608.

DONZELLI, S., MORI, F., BELLISSIMO, T., SACCONI, A., CASINI, B., FRIXA, T., ROSCILLI, G., AURISICCHIO, L., FACCIOLO, F., POMPILI, A., CAROSI, M. A., PESCARMONA, E., SEGATTO, O., POND, G., MUTI, P., TELERA, S.,

STRANO, S., YARDEN, Y. & BLANDINO, G. 2015. Epigenetic silencing of miR-145-5p contributes to brain metastasis. *Oncotarget,* 6**,** 35183-35201.

DOWLATSHAHI, M., HUANG, V., GEHAD, A. E., JIANG, Y., CALARESE, A., TEAGUE, J. E., DOROSARIO, A. A., CHENG, J. W., NGHIEM, P., SCHANBACHER, C. F., THAKURIA, M., SCHMULTS, C. D., WANG, L. C. & CLARK, R. A. 2013. Tumor-specific T cells in human Merkel cell carcinomas: a possible role for Tregs and T-cell exhaustion in reducing T-cell responses. *Journal of Investigative Dermatology,* 133**,** 1879-1889.

DUNCAVAGE, E. J., MAGRINI, V., BECKER, N., ARMSTRONG, J. R., DEMETER, R. T., WYLIE, T., ABEL, H. J. & PFEIFER, J. D. 2011. Hybrid capture and next-generation sequencing identify viral integration sites from formalin-fixed, paraffin-embedded tissue. *The Journal of Molecular Diagnostics,* 13**,** 325-33.

DUPRAT, J. P., LANDMAN, G., SALVAJOLI, J. V. & BRECHTBUHL, E. R. 2011. A review of the epidemiology and treatment of Merkel cell carcinoma. *Clinics (Sao Paulo),* 66**,** 1817-23.

ELHAMAMSY, A. R., EL SHARKAWY, M. S., ZANATY, A. F., MAHROUS, M. A., MOHAMED, A. E. & ABUSHAABAN, E. A. 2017. Circulating miR-92a, miR-143 and miR-342 in plasma are novel potential biomarkers for acute myeloid leukemia. *International Journal of Molecular and Cellular Medicine,* 6**,** 77-86.

ENGDAHL, E., DUNN, N., NIEHUSMANN, P., WIDEMAN, S., WIPFLER, P., BECKER, A. J., EKSTROM, T. J., ALMGREN, M. & FOGDELL-HAHN, A. 2017. Human herpesvirus 6B induces hypomethylation on chromosome 17p13.3, correlating with increased gene expression and virus integration. *Journal of Virology,* 91**,** e02105-16.

EREZ, N., TRUITT, M., OLSON, P., ARRON, S. T. & HANAHAN, D. 2010. Cancer-associated fibroblasts are activated in incipient neoplasia to orchestrate tumor-promoting inflammation in an NF-kappaB-dependent manner. *Cancer Cell,* 17**,** 135-47.

FALTEJSKOVA, P., SVOBODA, M., SRUTOVA, K., MLCOCHOVA, J., BESSE, A., NEKVINDOVA, J., RADOVA, L., FABIAN, P., SLABA, K., KISS, I., VYZULA, R. & SLABY, O. 2012. Identification and functional screening of microRNAs highly deregulated in colorectal cancer. *Journal of Cellular and Molecular Medicine,* 16**,** 2655-66.

FAN, K., GRAVEMEYER, J., RITTER, C., RASHEED, K., GAMBICHLER, T., MOENS, U., SHUDA, M., SCHRAMA, D. & BECKER, J. C. 2019a. MCPyV large T antigen-induced Atonal homolog 1 Is a lineage-dependency oncogene in Merkel cell carcinoma. *Journal of Investigative Dermatology*.

FAN, K., RITTER, C., NGHIEM, P., BLOM, A., VERHAEGEN, M. E., DLUGOSZ, A., ODUM, N., WOETMANN, A., TOTHILL, R. W. & HICKS, R. J. 2018. Circulating cell-free miR-375 as surrogate marker of tumor burden in Merkel cell carcinoma. *Clinical Cancer Research,* 24**,** 5873-5882.

FAN, K., ZEBISCH, A., HORNY, K., SCHRAMA, D. & BECKER, J. C. 2019b. Highly expressed miR-375 is not an intracellular oncogene in Merkel cell polyomavirus-associated Merkel cell carcinoma. *bioRxiv***,** 813378.

FANG, T., LV, H. W., LV, G. S., LI, T., WANG, C. Z., HAN, Q., YU, L. X., SU, B., GUO, L. N., HUANG, S. N., CAO, D., TANG, L., TANG, S. H., WU, M. C., YANG, W. & WANG, H. Y. 2018. Tumor-derived exosomal miR-1247-3p induces cancer-associated fibroblast activation to foster lung metastasis of liver cancer. *Nature Communications,* 9**,** 191.

FEEDERLE, R., HAAR, J., BERNHARDT, K., LINNSTAEDT, S. D., BANNERT, H., LIPS, H., CULLEN, B. R. & DELECLUSE, H. J. 2011. The members of an Epstein-Barr virus microRNA cluster cooperate to transform B lymphocytes. *Journal of Virology,* 85**,** 9801-9810.

FENG, H., SHUDA, M., CHANG, Y. & MOORE, P. S. 2008. Clonal integration of a polyomavirus in human Merkel cell carcinoma. *Science,* 319**,** 1096-1100.

FLORA, A., KLISCH, T. J., SCHUSTER, G. & ZOGHBI, H. Y. 2009. Deletion of Atoh1 disrupts Sonic Hedgehog signaling in the developing cerebellum and prevents medulloblastoma. *Science,* 326**,** 1424-1427.

FONG, M. Y., ZHOU, W., LIU, L., ALONTAGA, A. Y., CHANDRA, M., ASHBY, J., CHOW, A., O'CONNOR, S. T. F., LI, S. & CHIN, A. R. 2015. Breast-cancer-secreted miR-122 reprograms glucose metabolism in premetastatic niche to promote metastasis. *Nature Cell Biology,* 17**,** 183.

FRANK, A. C., EBERSBERGER, S., FINK, A. F., LAMPE, S., WEIGERT, A., SCHMID, T., EBERSBERGER, I., SYED, S. N. & BRUNE, B. 2019. Apoptotic tumor cell-derived microRNA-375 uses CD36 to alter the tumor-associated macrophage phenotype. *Nature Communications,* 10**,** 1135.

FRISCH, S. M., SCHALLER, M. & CIEPLY, B. 2013. Mechanisms that link the oncogenic epithelial–mesenchymal transition to suppression of anoikis. *J Cell Sci,* 126**,** 21-29.

FUKAO, A., MISHIMA, Y., TAKIZAWA, N., OKA, S., IMATAKA, H., PELLETIER, J., SONENBERG, N., THOMA, C. & FUJIWARA, T. 2014. MicroRNAs trigger dissociation of eIF4AI and eIF4AII from target mRNAs in humans. *Molecular Cell,* 56**,** 79-89.

FUKUSHIMA, K., TSUCHIYA, K., KANO, Y., HORITA, N., HIBIYA, S., HAYASHI, R., KITAGAKI, K., NEGI, M., ITOH, E., AKASHI, T., EISHI, Y., OSHIMA, S., NAGAISHI, T., OKAMOTO, R., NAKAMURA, T. & WATANABE, M. 2015. Atonal homolog 1 protein stabilized by tumor necrosis factor alpha induces high malignant potential in colon cancer cell line. *Cancer Science,* 106**,** 1000-1007.

GAGGIOLI, C., HOOPER, S., HIDALGO-CARCEDO, C., GROSSE, R., MARSHALL, J. F., HARRINGTON, K. & SAHAI, E. 2007. Fibroblast-led collective invasion of carcinoma cells with differing roles for RhoGTPases in leading and following cells. *Nature Cell Biology,* 9**,** 1392-U92.

GAISER, M. R., DAILY, K., HOFFMANN, J., BRUNE, M., ENK, A. & BROWNELL, I. 2015. Evaluating blood levels of neuron specific enolase, chromogranin A, and circulating tumor cells as Merkel cell carcinoma biomarkers. *Oncotarget,* 6**,** 26472-82.

GALLO, A., TANDON, M., ALEVIZOS, I. & ILLEI, G. G. 2012. The majority of microRNAs detectable in serum and saliva is concentrated in exosomes. *Plos One,* 7**,** e30679.

GAO, Q., WANG, K., CHEN, K., LIANG, L., ZHENG, Y., ZHANG, Y., XIANG, J. & TANG, N. 2017. HBx protein-mediated ATOH1 downregulation suppresses ARID2 expression and promotes hepatocellular carcinoma. *Cancer Science,* 108**,** 1328-1337.

GARCIA-ELIAS, A., ALLOZA, L., PUIGDECANET, E., NONELL, L., TAJES, M., CURADO, J., ENJUANES, C., DIAZ, O., BRUGUERA, J., MARTI-ALMOR, J., COMIN-COLET, J. & BENITO, B. 2017. Defining quantification methods and optimizing protocols for microarray hybridization of circulating microRNAs. *Scientific Reports,* 7.

GARRAWAY, L. A. & SELLERS, W. R. 2006. Lineage dependency and lineage-survival oncogenes in human cancer. *Nature Reviews Cancer,* 6**,** 593-602.

GEBERT, L. F. R. & MACRAE, I. J. 2019. Regulation of microRNA function in animals. *Nature Reviews Molecular Cell Biology,* 20**,** 21-37.

GHEIT, T., DUTTA, S., OLIVER, J., ROBITAILLE, A., HAMPRAS, S., COMBES, J. D., MCKAY-CHOPIN, S., LE CALVEZ-KELM, F., FENSKE, N., CHERPELIS, B., GIULIANO, A. R., FRANCESCHI, S., MCKAY, J., ROLLISON, D. E. & TOMMASINO, M. 2017. Isolation and characterization of a novel putative human polyomavirus. *Virology,* 506**,** 45-54.

GIANNONI, E., BIANCHINI, F., MASIERI, L., SERNI, S., TORRE, E., CALORINI, L. & CHIARUGI, P. 2010. Reciprocal activation of prostate cancer cells and cancer-associated fibroblasts stimulates epithelial-mesenchymal transition and cancer stemness. *Cancer Research,* 70**,** 6945-6956.

GIBBINGS, D. J., CIAUDO, C., ERHARDT, M. & VOINNET, O. 2009. Multivesicular bodies associate with components of miRNA effector complexes and modulate miRNA activity. *Nature Cell Biology,* 11**,** 1143-U223.

GILLIES, J. K. & LORIMER, I. A. 2007. Regulation of p27Kip1 by miRNA 221/222 in glioblastoma. *Cell Cycle,* 6**,** 2005-9.

GIRSCHIK, J., THORN, K., BEER, T. W., HEENAN, P. J. & FRITSCHI, L. 2011. Merkel cell carcinoma in Western Australia: a population-based study of incidence and survival. *British Journal of Dermatology,* 165**,** 1051-7.

GLENTIS, A., OERTLE, P., MARIANI, P., CHIKINA, A., EL MARJOU, F., ATTIEH, Y., ZACCARINI, F., LAE, M., LOEW, D., DINGLI, F., SIRVEN, P., SCHOUMACHER, M., GURCHENKOV, B. G., PLODINEC, M. & VIGNJEVIC, D. M. 2017. Cancer-associated fibroblasts induce metalloprotease-independent cancer cell invasion of the basement membrane. *Nature Communications,* 8**,** 924.

GOH, G., WALRADT, T., MARKAROV, V., BLOM, A., RIAZ, N., DOUMANI, R., STAFSTROM, K., MOSHIRI, A., YELISTRATOVA, L., LEVINSOHN, J., CHAN, T. A., NGHIEM, P., LIFTON, R. P. & CHOI, J. 2016. Mutational landscape of MCPyV-positive and MCPyV-negative Merkel cell carcinomas with implications for immunotherapy. *Oncotarget,* 7**,** 3393-3405.

GOLDIE, B. J., DUN, M. D., LIN, M. J., SMITH, N. D., VERRILLS, N. M., DAYAS, C. V. & CAIRNS, M. J. 2014. Activity-associated miRNA are packaged in Map1b-enriched exosomes released from depolarized neurons. *Nucleic Acids Research,* 42**,** 9195-9208.

GONZALEZ-VELA, M. D. C., CURIEL-OLMO, S., DERDAK, S., BELTRAN, S., SANTIBANEZ, M., MARTINEZ, N., CASTILLO-TRUJILLO, A., GUT, M., SANCHEZ-PACHECO, R., ALMARAZ, C., CERECEDA, L., LLOMBART, B., AGRAZ-DOBLAS, A., REVERT-ARCE, J., GUERRERO, J. A. L., MOLLEJO, M., MARRON, P. I., ORTIZ-ROMERO, P., FERNANDEZ-CUESTA, L., VARELA, I., GUT, I., CERRONI, L., PIRIS, M. A. & VAQUE, J. P. 2017. Shared oncogenic pathways implicated in both virus-positive and UV-Induced Merkel cell carcinomas. *Journal of Investigative Dermatology,* 137**,** 197-206.

GORUPPI, S., PROCOPIO, M. G., JO, S., CLOCCHIATTI, A., NEEL, V. & DOTTO, G. P. 2017. The ULK3 kinase is critical for convergent control of cancer-associated fibroblast activation by CSL and GLI. *Cell Reports,* 20**,** 2468-2479.

GOULET, C. R., BERNARD, G., TREMBLAY, S., CHABAUD, S., BOLDUC, S. & POULIOT, F. 2018. Exosomes induce fibroblast differentiation into Cancer-associated fibroblasts through TGFβ signaling. *Molecular Cancer Research,* 16**,** 1196-1204.

GRAUSAM, K. B., DOOYEMA, S. D. R., BIHANNIC, L., PREMATHILAKE, H., MORRISSY, A. S., FORGET, A., SCHAEFER, A. M., GUNDELACH, J. H., MACURA, S., MAHER, D. M., WANG, X., HEGLIN, A. H., GE, X., ZENG, E., PUGET, S., CHANDRASEKAR, I., SURENDRAN, K., BRAM, R. J., SCHULLER, U., TALYOR, M. D., AYRAULT, O. & ZHAO, H. 2017. ATOH1 promotes leptomeningeal dissemination and metastasis of Sonic Hedgehog subgroup medulloblastomas. *Cancer Research,* 77**,** 3766-3777.

GREGORY, P. A., BERT, A. G., PATERSON, E. L., BARRY, S. C., TSYKIN, A., FARSHID, G., VADAS, M. A., KHEW-GOODALL, Y. & GOODALL, G. J. 2008. The mir-200 family and mir-205 regulate epithelial to mesenchymal transition by targeting ZEB1 and SIP1. *Nature Cell Biology,* 10**,** 593-601.

GREGORY, R. I., YAN, K. P., AMUTHAN, G., CHENDRIMADA, T., DORATOTAJ, B., COOCH, N. & SHIEKHATTAR, R. 2004. The Microprocessor complex mediates the genesis of microRNAs. *Nature,* 432**,** 235-240.

HAFNER, C., HOUBEN, R., BAEURLE, A., RITTER, C., SCHRAMA, D., LANDTHALER, M. & BECKER, J. C. 2012. Activation of the PI3K/AKT pathway in Merkel cell carcinoma. *Plos One,* 7**,** e31255.

HAMAM, R., HAMAM, D., ALSALEH, K. A., KASSEM, M., ZAHER, W., ALFAYEZ, M., ALDAHMASH, A. & ALAJEZ, N. M. 2017. Circulating microRNAs in breast

cancer: novel diagnostic and prognostic biomarkers. *Cell Death & Disease,* 8**,** e3045.

HAN, J. J., LEE, Y., YEOM, K. H., NAM, J. W., HEO, I., RHEE, J. K., SOHN, S. Y., CHO, Y. J., ZHANG, B. T. & KIM, V. N. 2006. Molecular basis for the recognition of primary microRNAs by the Drosha-DGCR8 complex. *Cell,* 125**,** 887-901.

HAN, M. E., BAEK, S. J., KIM, S. Y., KANG, C. D. & OH, S. O. 2015. ATOH1 can regulate the tumorigenicity of gastric cancer cells by inducing the differentiation of cancer stem cells. *PloS One,* 10**,** e0126085.

HANAHAN, D. & WEINBERG, R. A. 2011. Hallmarks of cancer: the next generation. *Cell,* 144**,** 646-674.

HARDIKAR, A. A., FARR, R. J. & JOGLEKAR, M. V. 2014. Circulating microRNAs: understanding the limits for quantitative measurement by real‐time PCR. *Journal of the American Heart Association,* 3**,** e000792.

HARMS, P. W., HARMS, K. L., MOORE, P. S., DECAPRIO, J. A., NGHIEM, P., WONG, M. K. K., BROWNELL, I. & INTERNATIONAL WORKSHOP ON MERKEL CELL CARCINOMA RESEARCH WORKING, G. 2018. The biology and treatment of Merkel cell carcinoma: current understanding and research priorities. *Nature Reviews Clinical Oncology,* 15**,** 763-776.

HARMS, P. W., VATS, P., VERHAEGEN, M. E., ROBINSON, D. R., WU, Y. M., DHANASEKARAN, S. M., PALANISAMY, N., SIDDIQUI, J., CAO, X. H., SU, F. Y., WANG, R., XIAO, H., KUNJU, L. P., MEHRA, R., TOMLINS, S. A., FULLEN, D. R., BICHAKJIAN, C. K., JOHNSON, T. M., DLUGOSZ, A. A. & CHINNAIYAN, A. M. 2015. The distinctive mutational spectra of polyomavirus-negative Merkel Cell Carcinoma. *Cancer Research,* 75**,** 3720-3727.

HAROLD, A., AMAKO, Y., HACHISUKA, J., BAI, Y., LI, M. Y., KUBAT, L., GRAVEMEYER, J., FRANKS, J., GIBBS, J. R., PARK, H. J., EZHKOVA, E., BECKER, J. C. & SHUDA, M. 2019. Conversion of Sox2-dependent Merkel cell carcinoma to a differentiated neuron-like phenotype by T antigen inhibition. *Proceedings of the National Academy of Sciences of the United States of America,* 116**,** 20104-20114.

HASSONA, Y., CIRILLO, N., HEESOM, K., PARKINSON, E. K. & PRIME, S. S. 2014. Senescent cancer-associated fibroblasts secrete active MMP-2 that promotes keratinocyte dis-cohesion and invasion. *British Journal of Cancer,* 111**,** 1230-1237.

HAVEL, J. J., CHOWELL, D. & CHAN, T. A. 2019. The evolving landscape of biomarkers for checkpoint inhibitor immunotherapy. *Nature Reviews Cancer,* 19**,** 133-150.

HE, X. X., CHANG, Y., MENG, F. Y., WANG, M. Y., XIE, Q. H., TANG, F., LI, P. Y., SONG, Y. H. & LIN, J. S. 2012. MicroRNA-375 targets AEG-1 in hepatocellular carcinoma and suppresses liver cancer cell growth in vitro and in vivo. *Oncogene,* 31**,** 3357-69.

HODGSON, N. C. 2005. Merkel cell carcinoma: changing incidence trends. *Journal of Surgical Oncology,* 89**,** 1-4.

HOUBEN, R., ADAM, C., BAEURLE, A., HESBACHER, S., GRIMM, J., ANGERMEYER, S., HENZEL, K., HAUSER, S., ELLING, R., BROCKER, E. B., GAUBATZ, S., BECKER, J. C. & SCHRAMA, D. 2012. An intact retinoblastoma protein-binding site in Merkel cell polyomavirus large T antigen is required for promoting growth of Merkel cell carcinoma cells. *International Journal of Cancer,* 130**,** 847-856.

HOUBEN, R., SHUDA, M., WEINKAM, R., SCHRAMA, D., FENG, H., CHANG, Y., MOORE, P. S. & BECKER, J. C. 2010. Merkel cell polyomavirus-infected Merkel cell carcinoma cells require expression of viral T antigens. *Journal of Virology,* 84**,** 7064-7072.

HUANG, M. Z., LI, Y. Q., ZHANG, H. L. & NAN, F. F. 2010. Breast cancer stromal fibroblasts promote the generation of CD44(+)CD24(-) cells through SDF-1/CXCR4 interaction. *Journal of Experimental & Clinical Cancer Research,* 29.

HUANG, X. Y., YUAN, T. Z., LIANG, M. H., DU, M. J., XIA, S., DITTMAR, R., WANG, D., SEE, W., COSTELLO, B. A., QUEVEDO, F., TAN, W., NANDY, D., BEVAN, G. H., LONGENBACH, S., SUN, Z. F., LU, Y., WANG, T., THIBODEAU, S. N., BOARDMAN, L., KOHLI, M. & WANG, L. 2015. Exosomal miR-1290 and miR-375 as prognostic markers in castration-resistant prostate cancer. *European Urology,* 67**,** 33-41.

HUDSON, J., DUNCAVAGE, E., TAMBURRINO, A., SALERNO, P., XI, L., RAFFELD, M., MOLEY, J. & CHERNOCK, R. D. 2013. Overexpression of miR-10a and miR-375 and downregulation of YAP1 in medullary thyroid carcinoma. *Exp Mol Pathol,* 95**,** 62-7.

HUNTINGTON, S. F., SVOBODA, J. & DOSHI, J. A. 2015. Cost-effectiveness analysis of routine surveillance imaging of patients with diffuse large B-cell lymphoma in first remission. *Journal of Clinical Oncology,* 33**,** 1467-74.

HUTVAGNER, G., MCLACHLAN, J., PASQUINELLI, A. E., BALINT, E., TUSCHL, T. & ZAMORE, P. D. 2001. A cellular function for the RNA-interference enzyme Dicer in the maturation of the let-7 small temporal RNA. *Science,* 293**,** 834-838.

IORIO, M. V., FERRACIN, M., LIU, C. G., VERONESE, A., SPIZZO, R., SABBIONI, S., MAGRI, E., PEDRIALI, M., FABBRI, M., CAMPIGLIO, M., MENARD, S., PALAZZO, J. P., ROSENBERG, A., MUSIANI, P., VOLINIA, S., NENCI, I., CALIN, G. A., QUERZOLI, P., NEGRINI, M. & CROCE, C. M. 2005. MicroRNA gene expression deregulation in human breast cancer. *Cancer Research,* 65**,** 7065-7070.

ISGRO, M. A., BOTTONI, P. & SCATENA, R. 2015. Neuron-specific enolase as a biomarker: biochemical and clinical aspects. *Advances in Experimental Medicine and Biology,* 867**,** 125-43.

IWANO, M., PLIETH, D., DANOFF, T. M., XUE, C., OKADA, H. & NEILSON, E. G. 2002. Evidence that fibroblasts derive from epithelium during tissue fibrosis. *Journal of Clinical Investigation,* 110**,** 341-350.

JOHNSTONE, R. M., ADAM, M., HAMMOND, J. R., ORR, L. & TURBIDE, C. 1987. Vesicle Formation during Reticulocyte Maturation - Association of Plasma-Membrane Activities with Released Vesicles (Exosomes). *Journal of Biological Chemistry,* 262**,** 9412-9420.

JOPLING, C. L. 2008. Regulation of hepatitis C virus by microRNA-122. *Biochemical Society Transactions,* 36**,** 1220-1223.

JOPLING, C. L., YI, M. K., LANCASTER, A. M., LEMON, S. M. & SARNOW, P. 2005. Modulation of hepatitis C virus RNA abundance by a liver-specific microRNA. *Science,* 309**,** 1577-1581.

KAAE, J., HANSEN, A. V., BIGGAR, R. J., BOYD, H. A., MOORE, P. S., WOHLFAHRT, J. & MELBYE, M. 2010. Merkel cell carcinoma: incidence, mortality, and risk of other cancers. *Journal of the National Cancer Institute,* 102**,** 793-801.

KALLURI, R. 2016. The biology and function of fibroblasts in cancer. *Nature Reviews Cancer,* 16**,** 582-598.

KAUFMAN, H. L., RUSSELL, J., HAMID, O., BHATIA, S., TERHEYDEN, P., D'ANGELO, S. P., SHIH, K. C., LEBBE, C., LINETTE, G. P., MILELLA, M., BROWNELL, I., LEWIS, K. D., LORCH, J. H., CHIN, K., MAHNKE, L., VON HEYDEBRECK, A., CUILLEROT, J. M. & NGHIEM, P. 2016. Avelumab in patients with chemotherapy-refractory metastatic Merkel cell carcinoma: a multicentre, single-group, open-label, phase 2 trial. *Lancet Oncology,* 17**,** 1374-1385.

KHARE, D., OR, R., RESNICK, I., BARKATZ, C., ALMOGI-HAZAN, O. & AVNI, B. 2018. Mesenchymal stromal cell-derived exosomes affect mRNA expression and function of B-lymphocytes. *Frontiers in Immunology,* 9**,** 3053.

KIM, D. E., PROCOPIO, M. G., GHOSH, S., JO, S. H., GORUPPI, S., MAGLIOZZI, F., BORDIGNON, P., NEEL, V., ANGELINO, P. & DOTTO, G. P. 2017. Convergent roles of ATF3 and CSL in chromatin control of cancer-associated fibroblast activation. *Journal of Experimental Medicine,* 214**,** 2349-2368.

KONSTANTINELL, A., BRUUN, J. A., OLSEN, R., ASPAR, A., SKALKO-BASNET, N., SVEINBJORNSSON, B. & MOENS, U. 2016. Secretomic analysis of extracellular vesicles originating from polyomavirus-negative and polyomavirus-positive Merkel cell carcinoma cell lines. *Proteomics,* 16**,** 2587-2591.

KOSAKA, N., IGUCHI, H., YOSHIOKA, Y., TAKESHITA, F., MATSUKI, Y. & OCHIYA, T. 2010. Secretory mechanisms and intercellular transfer of microRNAs in living cells. *Journal of Biological Chemistry,* 285**,** 17442-17452.

KRUTZFELDT, J., RAJEWSKY, N., BRAICH, R., RAJEEV, K. G., TUSCHL, T., MANOHARAN, M. & STOFFEL, M. 2005. Silencing of microRNAs in vivo with 'antagomirs'. *Nature,* 438**,** 685-689.

KUKKO, H., BOHLING, T., KOLJONEN, V., TUKIAINEN, E., HAGLUND, C., POKHREL, A., SANKILA, R. & PUKKALA, E. 2012. Merkel cell carcinoma - a population-based epidemiological study in Finland with a clinical series of 181 cases. *European Journal of Cancer,* 48**,** 737-42.

KUMAR, S., XIE, H., SCICLUNA, P., LEE, L., BJORNHAGEN, V., HOOG, A., LARSSON, C. & LUI, W. O. 2018. miR-375 regulation of LDHB plays distinct roles in Polyomavirus-positive and -negative Merkel cell carcinoma. *Cancers (Basel),* 10**,** pii: E443.

KUMAR, S., XIE, H., SHI, H., GAO, J., JUHLIN, C. C., BJÖRNHAGEN, V., HÖÖG, A., LEE, L., LARSSON, C. & LUI, W. O. 2019. Merkel cell polyomavirus

oncoproteins induce microRNAs that suppress multiple autophagy genes. *International journal of cancer*.

KUSS-DUERKOP, S. K., WESTRICH, J. A. & PYEON, D. 2018. DNA tumor virus regulation of host DNA methylation and its implications for immune evasion and oncogenesis. *Viruses,* 10**,** pii: E82.

KWUN, H. J., GUASTAFIERRO, A., SHUDA, M., MEINKE, G., BOHM, A., MOORE, P. S. & CHANG, Y. 2009. The minimum replication origin of Merkel cell polyomavirus has a unique large T-antigen loading architecture and requires small T-antigen expression for optimal replication. *Journal of Virology,* 83**,** 12118-12128.

KWUN, H. J., SHUDA, M., FENG, H., CAMACHO, C. J., MOORE, P. S. & CHANG, Y. 2013. Merkel cell polyomavirus small T antigen controls viral replication and oncoprotein expression by targeting the cellular ubiquitin ligase SCFFbw7. *Cell Host & Microbe,* 14**,** 125-135.

LA MANNO, G., SOLDATOV, R., ZEISEL, A., BRAUN, E., HOCHGERNER, H., PETUKHOV, V., LIDSCHREIBER, K., KASTRITI, M. E., LONNERBERG, P., FURLAN, A., FAN, J., BORM, L. E., LIU, Z., VAN BRUGGEN, D., GUO, J., HE, X., BARKER, R., SUNDSTROM, E., CASTELO-BRANCO, G., CRAMER, P., ADAMEYKO, I., LINNARSSON, S. & KHARCHENKO, P. V. 2018. RNA velocity of single cells. *Nature,* 560**,** 494-498.

LAGOS-QUINTANA, M., RAUHUT, R., LENDECKEL, W. & TUSCHL, T. 2001. Identification of novel genes coding for small expressed RNAs. *Science,* 294**,** 853-858.

LAGOS-QUINTANA, M., RAUHUT, R., MEYER, J., BORKHARDT, A. & TUSCHL, T. 2003. New microRNAs from mouse and human. *Rna-a Publication of the Rna Society,* 9**,** 175-179.

LAKINS, M. A., GHORANI, E., MUNIR, H., MARTINS, C. P. & SHIELDS, J. D. 2018. Cancer-associated fibroblasts induce antigen-specific deletion of CD8(+) T Cells to protect tumour cells. *Nature Communications,* 9**,** 948.

LAUDE, H. C., JONCHERE, B., MAUBEC, E., CARLOTTI, A., MARINHO, E., COUTURAUD, B., PETER, M., SASTRE-GARAU, X., AVRIL, M. F., DUPIN, N. & ROZENBERG, F. 2010. Distinct merkel cell polyomavirus molecular features in tumour and non tumour specimens from patients with merkel cell carcinoma. *Plos Pathogens,* 6**,** e1001076.

LE, M. T. N., HAMAR, P., GUO, C. Y., BASAR, E., PERDIGAO-HENRIQUES, R., BALAJ, L. & LIEBERMAN, J. 2014. miR-200-containing extracellular vesicles promote breast cancer cell metastasis. *Journal of Clinical Investigation,* 124**,** 5109-5128.

LEE, S., PAULSON, K. G., MURCHISON, E. P., AFANASIEV, O. K., ALKAN, C., LEONARD, J. H., BYRD, D. R., HANNON, G. J. & NGHIEM, P. 2011. Identification and validation of a novel mature microRNA encoded by the Merkel cell polyomavirus in human Merkel cell carcinomas. *Journal of Clinical Virology,* 52**,** 272-5.

LEE, Y., AHN, C., HAN, J. J., CHOI, H., KIM, J., YIM, J., LEE, J., PROVOST, P., RADMARK, O., KIM, S. & KIM, V. N. 2003. The nuclear RNase III Drosha initiates microRNA processing. *Nature,* 425**,** 415-419.

LEE, Y. S., PRESSMAN, S., ANDRESS, A. P., KIM, K., WHITE, J. L., CASSIDY, J. J., LI, X., LUBELL, K., LIM, D. H., CHO, I. S., NAKAHARA, K., PREALL, J. B., BELLARE, P., SONTHEIMER, E. J. & CARTHEW, R. W. 2009. Silencing by small RNAs is linked to endosomal trafficking. *Nature Cell Biology,* 11**,** 1150-U243.

LEHMANN, U., HASEMEIER, B., CHRISTGEN, M., MULLER, M., ROMERMANN, D., LANGER, F. & KREIPE, H. 2008. Epigenetic inactivation of microRNA gene hsa-mir-9-1 in human breast cancer. *Journal of Pathology,* 214**,** 17-24.

LI, J., WANG, X., DIAZ, J., TSANG, S. H., BUCK, C. B. & YOU, J. X. 2013. Merkel cell polyomavirus large T antigen disrupts host genomic integrity and inhibits cellular proliferation. *Journal of Virology,* 87**,** 9173-9188.

LI, J. H., LIU, S., ZHOU, H., QU, L. H. & YANG, J. H. 2014. starBase v2.0: decoding miRNA-ceRNA, miRNA-ncRNA and protein-RNA interaction networks from large-scale CLIP-Seq data. *Nucleic Acids Res,* 42**,** D92-7.

LIANG, X., ZHANG, L., WANG, S., HAN, Q. & ZHAO, R. C. 2016. Exosomes secreted by mesenchymal stem cells promote endothelial cell angiogenesis by transferring miR-125a. *Journal of Cell Science,* 129**,** 2182-9.

LIBERZON, A., BIRGER, C., THORVALDSDOTTIR, H., GHANDI, M., MESIROV, J. P. & TAMAYO, P. 2015. The molecular signatures database (MSigDB) hallmark gene set collection. *Cell Systems,* 1**,** 417-425.

LIM, L. P., LAU, N. C., WEINSTEIN, E. G., ABDELHAKIM, A., YEKTA, S., RHOADES, M. W., BURGE, C. B. & BARTEL, D. P. 2003. The microRNAs of Caenorhabditis elegans. *Genes & Development,* 17**,** 991-1008.

LINDAHL, L. M., FREDHOLM, S., JOSEPH, C., NIELSEN, B. S., JONSON, L., WILLERSLEV-OLSEN, A., GLUUD, M., BLUMEL, E., PETERSEN, D. L., SIBBESEN, N., HU, T., NASTASI, C., KREJSGAARD, T., JAEHGER, D., PERSSON, J. L., MONGAN, N., WASIK, M. A., LITVINOV, I. V., SASSEVILLE, D., KORALOV, S. B., BONEFELD, C. M., GEISLER, C., WOETMANN, A., RALFKIAER, E., IVERSEN, L. & ODUM, N. 2016. STAT5 induces miR-21 expression in cutaneous T cell lymphoma. *Oncotarget,* 7**,** 45730-45744.

LIU, F., LOU, Y. L., WU, J., RUAN, Q. F., XIE, A., GUO, F., CUI, S. P., DENG, Z. F. & WANG, Y. 2012. Upregulation of microRNA-210 regulates renal angiogenesis mediated by activation of VEGF signaling pathway under ischemia/perfusion injury in vivo and in vitro. *Kidney and Blood Pressure Research,* 35**,** 182-91.

LIU, G., HUANG, K. M., JIE, Z. W., WU, Y. Z., CHEN, J. X., CHEN, Z. Z., FANG, X. Q. & SHEN, S. Y. 2018. CircFAT1 sponges miR-375 to promote the expression of Yes-associated protein 1 in osteosarcoma cells. *Molecular Cancer,* 17**,** 170.

LIU, Y., XING, R., ZHANG, X., DONG, W., ZHANG, J., YAN, Z., LI, W., CUI, J. & LU, Y. 2013. miR-375 targets the p53 gene to regulate cellular response to ionizing radiation and etoposide in gastric cancer cells. *DNA Repair,* 12**,** 741-50.

LOYO, M., GUERRERO-PRESTON, R., BRAIT, M., HOQUE, M. O., CHUANG, A., KIM, M. S., SHARMA, R., LIEGEOIS, N. J., KOCH, W. M., CALIFANO, J. A., WESTRA, W. H. & SIDRANSKY, D. 2010. Quantitative detection of Merkel cell virus in human tissues and possible mode of transmission. *International Journal of Cancer,* 126**,** 2991-2996.

LUJAMBIO, A. & ESTELLER, M. 2007. CpG island hypermethylation of tumor suppressor microRNAs in human cancer. *Cell Cycle,* 6**,** 1455-1459.

LYNGAA, R., PEDERSEN, N. W., SCHRAMA, D., THRUE, C. A., IBRANI, D., MET, O., STRATEN, P. T., NGHIEM, P., BECKER, J. C. & HADRUP, S. R. 2014. T-cell responses to oncogenic Merkel cell polyomavirus proteins distinguish patients with Merkel cell carcinoma from healthy donors. *Clinical Cancer Research,* 20**,** 1768-1778.

LYTLE, N. K., BARBER, A. G. & REYA, T. 2018. Stem cell fate in cancer growth, progression and therapy resistance. *Nature Reviews Cancer,* 18**,** 669-680.

MAACHA, S., BHAT, A. A., JIMENEZ, L., RAZA, A., HARIS, M., UDDIN, S. & GRIVEL, J. C. 2019. Extracellular vesicles-mediated intercellular communication: roles in the tumor microenvironment and anti-cancer drug resistance. *Molecular Cancer,* 18.

MAHN, R., HEUKAMP, L. C., ROGENHOFER, S., VON RUECKER, A., MULLER, S. C. & ELLINGER, J. 2011. Circulating microRNAs (miRNA) in serum of patients with prostate cancer. *Urology,* 77**,** 1265 e9-16.

MARICICH, S. M., WELLNITZ, S. A., NELSON, A. M., LESNIAK, D. R., GERLING, G. J., LUMPKIN, E. A. & ZOGHBI, H. Y. 2009. Merkel cells are essential for light-touch responses. *Science,* 324**,** 1580-1582.

MARTEL-JANTIN, C., FILIPPONE, C., CASSAR, O., PETER, M., TOMASIC, G., VIELH, P., BRIERE, J., PETRELLA, T., AUBRIOT-LORTON, M. H., MORTIER, L., JOUVION, G., SASTRE-GARAU, X., ROBERT, C. & GESSAIN, A. 2012. Genetic variability and integration of Merkel cell polyomavirus in Merkel cell carcinoma. *Virology,* 426**,** 134-42.

MARTENS, J. W. M., SIEUWERTS, A. M., BOLT-DE VRIES, J., BOSMA, P. T., SWIGGERS, S. J. J., KLIJN, J. G. M. & FOEKENS, J. A. 2003. Aging of stromal-derived human breast fibroblasts might contribute to breast cancer progression. *Thrombosis and Haemostasis,* 89**,** 393-404.

MATHIEU, M., MARTIN-JAULAR, L., LAVIEU, G. & THERY, C. 2019. Specificities of secretion and uptake of exosomes and other extracellular vesicles for cell-to-cell communication. *Nature Cell Biology,* 21**,** 9-17.

MEIJER, H. A., KONG, Y. W., LU, W. T., WILCZYNSKA, A., SPRIGGS, R. V., ROBINSON, S. W., GODFREY, J. D., WILLIS, A. E. & BUSHELL, M. 2013. Translational repression and eIF4A2 activity are critical for microRNA-mediated gene regulation. *Science,* 340**,** 82-85.

MICHAEL, M. Z., O'CONNOR, S. M., PELLEKAAN, N. G. V., YOUNG, G. P. & JAMES, R. J. 2003. Reduced accumulation of specific microRNAs in colorectal neoplasia. *Molecular Cancer Research,* 1**,** 882-891.

MITCHELL, A. J., GRAY, W. D., HAYEK, S. S., KO, Y. A., THOMAS, S., ROONEY, K., AWAD, M., ROBACK, J. D., QUYYUMI, A. & SEARLES, C. D. 2016.

Platelets confound the measurement of extracellular miRNA in archived plasma. *Scientific Reports,* 6**,** 32651.

MITCHELL, P. S., PARKIN, R. K., KROH, E. M., FRITZ, B. R., WYMAN, S. K., POGOSOVA-AGADJANYAN, E. L., PETERSON, A., NOTEBOOM, J., O'BRIANT, K. C., ALLEN, A., LIN, D. W., URBAN, N., DRESCHER, C. W., KNUDSEN, B. S., STIREWALT, D. L., GENTLEMAN, R., VESSELLA, R. L., NELSON, P. S., MARTIN, D. B. & TEWARI, M. 2008. Circulating microRNAs as stable blood-based markers for cancer detection. *Proceedings of the National Academy of Sciences of the United States of America,* 105**,** 10513-10518.

MITRA, A. K., ZILLHARDT, M., HUA, Y. J., TIWARI, P., MURMANN, A. E., PETER, M. E. & LENGYEL, E. 2012. MicroRNAs reprogram normal fibroblasts into cancer-associated fibroblasts in ovarian cancer. *Cancer Discovery,* 2**,** 1100-1108.

NACHMANI, D., LANKRY, D., WOLF, D. G. & MANDELBOIM, O. 2010. The human cytomegalovirus microRNA miR-UL112 acts synergistically with a cellular microRNA to escape immune elimination. *Nature Immunology,* 11**,** 806-U57.

NARDI, V., SONG, Y., SANTAMARIA-BARRIA, J. A., COSPER, A. K., LAM, Q., FABER, A. C., BOLAND, G. M., YEAP, B. Y., BERGETHON, K., SCIALABBA, V. L., TSAO, H., SETTLEMAN, J., RYAN, D. P., BORGER, D. R., BHAN, A. K., HOANG, M. P., IAFRATE, A. J., CUSACK, J. C., ENGELMAN, J. A. & DIAS-SANTAGATA, D. 2012. Activation of PI3K signaling in Merkel cell carcinoma. *Clinical Cancer Research,* 18**,** 1227-1236.

NEVIANI, P., WISE, P. M., MURTADHA, M., LIU, C. W., WU, C. H., JONG, A. Y., SEEGER, R. C. & FABBRI, M. 2019. Natural Killer-derived exosomal miR-186 inhibits neuroblastoma growth and immune escape mechanisms. *Cancer Research,* 79**,** 1151-1164.

NGHIEM, P. T., BHATIA, S., LIPSON, E. J., KUDCHADKAR, R. R., MILLER, N. J., ANNAMALAI, L., BERRY, S., CHARTASH, E. K., DAUD, A., FLING, S. P., FRIEDLANDER, P. A., KLUGER, H. M., KOHRT, H. E., LUNDGREN, L., MARGOLIN, K., MITCHELL, A., OLENCKI, T., PARDOLL, D. M., REDDY, S. A., SHANTHA, E. M., SHARFMAN, W. H., SHARON, E., SHEMANSKI, L. R., SHINOHARA, M. M., SUNSHINE, J. C., TAUBE, J. M., THOMPSON, J. A., TOWNSON, S. M., YEARLEY, J. H., TOPALIAN, S. L. & CHEEVER, M. A. 2016. PD-1 blockade with pembrolizumab in advanced Merkel-cell carcinoma. *The New England Journal of Medicine,* 374**,** 2542-52.

NING, M. S., KIM, A. S., PRASAD, N., LEVY, S. E., ZHANG, H. & ANDL, T. 2014. Characterization of the Merkel cell carcinoma miRNome. *Journal of Skin Cancer,* 2014**,** 289548.

NISHIKAWA, E., OSADA, H., OKAZAKI, Y., ARIMA, C., TOMIDA, S., TATEMATSU, Y., TAGUCHI, A., SHIMADA, Y., YANAGISAWA, K., YATABE, Y., TOYOKUNI, S., SEKIDO, Y. & TAKAHASHI, T. 2011. miR-375 is activated by ASH1 and inhibits YAP1 in a lineage-dependent manner in lung cancer. *Cancer Research,* 71**,** 6165-6173.

NORTHCOTT, P. A., FERNANDEZ-L, A., HAGAN, J. P., ELLISON, D. W., GRAJKOWSKA, W., GILLESPIE, Y., GRUNDY, R., VAN METER, T., RUTKA, J. T., CROCE, C. M., KENNEY, A. M. & TAYLOR, M. D. 2009. The miR-17/92 polycistron is up-regulated in Sonic Hedgehog-driven medulloblastomas and induced by N-myc in Sonic Hedgehog-treated cerebellar neural precursors. *Cancer Research,* 69**,** 3249-3255.

OGATA-KAWATA, H., IZUMIYA, M., KURIOKA, D., HONMA, Y., YAMADA, Y., FURUTA, K., GUNJI, T., OHTA, H., OKAMOTO, H., SONODA, H., WATANABE, M., NAKAGAMA, H., YOKOTA, J., KOHNO, T. & TSUCHIYA, N. 2014. Circulating Exosomal microRNAs as Biomarkers of Colon Cancer. *Plos One,* 9**,** e92921.

OHLUND, D., ELYADA, E. & TUVESON, D. 2014. Fibroblast heterogeneity in the cancer wound. *Journal of Experimental Medicine,* 211**,** 1503-1523.

OHLUND, D., HANDLY-SANTANA, A., BIFFI, G., ELYADA, E., ALMEIDA, A. S., PONZ-SARVISE, M., CORBO, V., ONI, T. E., HEARN, S. A., LEE, E. J., CHIO, II, HWANG, C. I., TIRIAC, H., BAKER, L. A., ENGLE, D. D., FEIG, C., KULTTI, A., EGEBLAD, M., FEARON, D. T., CRAWFORD, J. M., CLEVERS, H., PARK, Y. & TUVESON, D. A. 2017. Distinct populations of inflammatory fibroblasts and myofibroblasts in pancreatic cancer. *Journal of Experimental Medicine,* 214**,** 579-596.

OKADA, C., YAMASHITA, E., LEE, S. J., SHIBATA, S., KATAHIRA, J., NAKAGAWA, A., YONEDA, Y. & TSUKIHARA, T. 2009. A high-resolution structure of the pre-microRNA nuclear export machinery. *Science,* 326**,** 1275-1279.

OKAMURA, K., HAGEN, J. W., DUAN, H., TYLER, D. M. & LAI, E. C. 2007. The mirtron pathway generates microRNA-class regulatory RNAs in Drosophila. *Cell,* 130**,** 89-100.

OLUMI, A. F., GROSSFELD, G. D., HAYWARD, S. W., CARROLL, P. R., TISTY, T. D. & CUNHA, G. R. 1999. Carcinoma-associated fibroblasts direct tumor progression of initiated human prostatic epithelium. *Cancer Research,* 59**,** 5002-5011.

ONO, M., KOSAKA, N., TOMINAGA, N., YOSHIOKA, Y., TAKESHITA, F., TAKAHASHI, R. U., YOSHIDA, M., TSUDA, H., TAMURA, K. & OCHIYA, T. 2014. Exosomes from bone marrow mesenchymal stem cells contain a microRNA that promotes dormancy in metastatic breast cancer cells. *Science Signaling,* 7.

ORIMO, A., GUPTA, P. B., SGROI, D. C., ARENZANA-SEISDEDOS, F., DELAUNAY, T., NAEEM, R., CAREY, V. J., RICHARDSON, A. L. & WEINBERG, R. A. 2005. Stromal fibroblasts present in invasive human breast carcinomas promote tumor growth and angiogenesis through elevated SDF-1/CXCL12 secretion. *Cell,* 121**,** 335-48.

ÖSTERREICHER, C. H., PENZ-ÖSTERREICHER, M., GRIVENNIKOV, S. I., GUMA, M., KOLTSOVA, E. K., DATZ, C., SASIK, R., HARDIMAN, G., KARIN, M. & BRENNER, D. A. 2011. Fibroblast-specific protein 1 identifies an inflammatory subpopulation of macrophages in the liver. *Proceedings of the National Academy of Sciences of the United States of America,* 108**,** 308-313.

OSTROWSKI, S. M., WRIGHT, M. C., BOLOCK, A. M., GENG, X. & MARICICH, S. M. 2015. Ectopic Atoh1 expression drives Merkel cell production in embryonic, postnatal and adult mouse epidermis. *Development,* 142**,** 2533-44.

PAGGETTI, J., HADERK, F., SEIFFERT, M., JANJI, B., DISTLER, U., AMMERLAAN, W., KIM, Y. J., ADAM, J., LICHTER, P., SOLARY, E., BERCHEM, G. & MOUSSAY, E. 2015. Exosomes released by chronic lymphocytic leukemia cells induce the transition of stromal cells into cancer-associated fibroblasts. *Blood,* 126**,** 1106-1117.

PARK, E. T., OH, H. K., GUM, J. R., CRAWLEY, S. C., KAKAR, S., ENGEL, J., LEOW, C. C., GAO, W. Q. & KIM, Y. S. 2006. HATH1 expression in mucinous cancers of the colorectum and related lesions. *Clinical Cancer Research,* 12**,** 5403-5410.

PASTRANA, D. V., TOLSTOV, Y. L., BECKER, J. C., MOORE, P. S., CHANG, Y. & BUCK, C. B. 2009. Quantitation of human seroresponsiveness to Merkel cell polyomavirus. *Plos Pathogens,* 5**,** e1000578.

PAULSON, K. G., CARTER, J. J., JOHNSON, L. G., CAHILL, K. W., IYER, J. G., SCHRAMA, D., BECKER, J. C., MADELEINE, M. M., NGHIEM, P. & GALLOWAY, D. A. 2010. Antibodies to merkel cell polyomavirus T antigen oncoproteins reflect tumor burden in merkel cell carcinoma patients. *Cancer Research,* 70**,** 8388-97.

PAULSON, K. G., IYER, J. G., TEGEDER, A. R., THIBODEAU, R., SCHELTER, J., KOBA, S., SCHRAMA, D., SIMONSON, W. T., LEMOS, B. D., BYRD, D. R., KOELLE, D. M., GALLOWAY, D. A., LEONARD, J. H., MADELEINE, M. M., ARGENYI, Z. B., DISIS, M. L., BECKER, J. C., CLEARY, M. A. & NGHIEM, P. 2011. Transcriptome-wide studies of Merkel cell carcinoma and validation of intratumoral CD8+ lymphocyte invasion as an independent predictor of survival. *Journal of Clinical Oncology,* 29**,** 1539-1546.

PAULSON, K. G., LEMOS, B. D., FENG, B., JAIMES, N., PENAS, P. F., BI, X. H., MAHER, E., COHEN, L., LEONARD, J. H., GRANTER, S. R., CHIN, L. & NGHIEM, P. 2009. Array-CGH reveals recurrent genomic changes in Merkel cell carcinoma including amplification of L-Myc. *Journal of Investigative Dermatology,* 129**,** 1547-1555.

PAULSON, K. G., LEWIS, C. W., REDMAN, M. W., SIMONSON, W. T., LISBERG, A., RITTER, D., MORISHIMA, C., HUTCHINSON, K., MUDGISTRATOVA, L., BLOM, A., IYER, J., MOSHIRI, A. S., TARABADKAR, E. S., CARTER, J. J., BHATIA, S., KAWASUMI, M., GALLOWAY, D. A., WENER, M. H. & NGHIEM, P. 2017. Viral oncoprotein antibodies as a marker for recurrence of Merkel cell carcinoma: A prospective validation study. *Cancer,* 123**,** 1464-1474.

PENA, C., CESPEDES, M. V., LINDH, M. B., KIFLEMARIAM, S., MEZHEYEUSKI, A., EDQVIST, P. H., HAGGLOF, C., BIRGISSON, H., BOJMAR, L., JIRSTROM, K., SANDSTROM, P., OLSSON, E., VEERLA, S., GALLARDO, A., SJOBLOM, T., CHANG, A. C. M., REDDEL, R. R., MANGUES, R., AUGSTEN, M. & OSTMAN, A. 2013. STC1 expression by cancer-associated fibroblasts drives metastasis of colorectal cancer. *Cancer Research,* 73**,** 1287-1297.

PENG, Y. & CROCE, C. M. 2016. The role of MicroRNAs in human cancer. *Signal Transduction and Targeted Therapy,* 1.

PENG, Y., DAI, Y. T., HITCHCOCK, C., YANG, X. J., KASSIS, E. S., LIU, L. X., LUO, Z. H., SUN, H. L., CUI, R., WEI, H. J., KIM, T., LEE, T. J., JEON, Y. J., NUOVO, G. J., VOLINIA, S., HE, Q. C., YU, J. H., NANA-SINKAM, P. & CROCE, C. M.

2013. Insulin growth factor signaling is regulated by microRNA-486, an underexpressed microRNA in lung cancer. *Proceedings of the National Academy of Sciences of the United States of America,* 110**,** 15043-15048.

PETERSEN, C. P., BORDELEAU, M. E., PELLETIER, J. & SHARP, P. A. 2006. Short RNAs repress translation after initiation in mammalian cells. *Molecular Cell,* 21**,** 533-542.

PIETRAS, K., PAHLER, J., BERGERS, G. & HANAHAN, D. 2008. Functions of paracrine PDGF signaling in the proangiogenic tumor stroma revealed by pharmacological targeting. *Plos Medicine,* 5**,** 123-138.

PITT, J. M., ANDRE, F., AMIGORENA, S., SORIA, J. C., EGGERMONT, A., KROEMER, G. & ZITVOGEL, L. 2016. Dendritic cell-derived exosomes for cancer therapy. *Journal of Clinical Investigation,* 126**,** 1224-1232.

POLISENO, L., SALMENA, L., ZHANG, J. W., CARVER, B., HAVEMAN, W. J. & PANDOLFI, P. P. 2010. A coding-independent function of gene and pseudogene mRNAs regulates tumour biology. *Nature,* 465**,** 1033-U90.

POPP, S., WALTERING, S., HERBST, C., MOLL, I. & BOUKAMP, P. 2002. UV-B-type mutations and chromosomal imbalances indicate common pathways for the development of Merkel and skin squamous cell carcinomas. *International Journal of Cancer,* 99**,** 352-60.

POY, M. N., ELIASSON, L., KRUTZFELDT, J., KUWAJIMA, S., MA, X., MACDONALD, P. E., PFEFFER, S., TUSCHL, T., RAJEWSKY, N., RORSMAN, P. & STOFFEL, M. 2004. A pancreatic islet-specific microRNA regulates insulin secretion. *Nature,* 432**,** 226-30.

PRASAD, R. & KATIYAR, S. K. 2017. Crosstalk Among UV-Induced Inflammatory Mediators, DNA Damage and Epigenetic Regulators Facilitates Suppression of the Immune System. *Photochemistry and Photobiology,* 93**,** 930-936.

PRITCHARD, C. C., KROH, E., WOOD, B., ARROYO, J. D., DOUGHERTY, K. J., MIYAJI, M. M., TAIT, J. F. & TEWARI, M. 2012. Blood cell origin of circulating microRNAs: a cautionary note for cancer biomarker studies. *Cancer Prevention Research,* 5**,** 492-497.

PROCOPIO, M. G., LASZLO, C., AL LABBAN, D., KIM, D. E., BORDIGNON, P., JO, S. H., GORUPPI, S., MENIETTI, E., OSTANO, P., ALA, U., PROVERO, P., HOETZENECKER, W., NEEL, V., KILARSKI, W. W., SWARTZ, M. A., BRISKEN, C., LEFORT, K. & DOTTO, G. P. 2015. Combined CSL and p53

downregulation promotes cancer-associated fibroblast activation. *Nature cell biology,* 17**,** 1193-204.

QIAO, Y., ZHANG, C., LI, A., WANG, D., LUO, Z., PING, Y., ZHOU, B., LIU, S., LI, H., YUE, D., ZHANG, Z., CHEN, X., SHEN, Z., LIAN, J., LI, Y., WANG, S., LI, F., HUANG, L., WANG, L., ZHANG, B., YU, J., QIN, Z. & ZHANG, Y. 2018. IL6 derived from cancer-associated fibroblasts promotes chemoresistance via CXCR7 in esophageal squamous cell carcinoma. *Oncogene,* 37**,** 873-883.

QUAIL, D. F. & JOYCE, J. A. 2013. Microenvironmental regulation of tumor progression and metastasis. *Nature Medicine,* 19**,** 1423-1437.

QUANTE, M., TU, S. P., TOMITA, H., GONDA, T., WANG, S. S. W., TAKASHI, S., BAIK, G. H., SHIBATA, W., DIPRETE, B., BETZ, K. S., FRIEDMAN, R., VARRO, A., TYCKO, B. & WANG, T. C. 2011. Bone marrow-derived myofibroblasts contribute to the mesenchymal stem cell niche and promote tumor growth. *Cancer Cell,* 19**,** 257-272.

RAVER-SHAPIRA, N., MARCIANO, E., MEIRI, E., SPECTOR, Y., ROSENFELD, N., MOSKOVITS, N., BENTWICH, Z. & OREN, M. 2007. Transcriptional activation of miR-34a contributes to p53-mediated apoptosis. *Molecular Cell,* 26**,** 731-743.

RENWICK, N., CEKAN, P., MASRY, P. A., MCGEARY, S. E., MILLER, J. B., HAFNER, M., LI, Z., MIHAILOVIC, A., MOROZOV, P., BROWN, M., GOGAKOS, T., MOBIN, M. B., SNORRASON, E. L., FEILOTTER, H. E., ZHANG, X., PERLIS, C. S., WU, H., SUAREZ-FARINAS, M., FENG, H., SHUDA, M., MOORE, P. S., TRON, V. A., CHANG, Y. & TUSCHL, T. 2013. Multicolor microRNA FISH effectively differentiates tumor types. *Journal of Clinical Investigation,* 123**,** 2694-2702.

RITTER, C., FAN, K., PASCHEN, A., HARDRUP, S. R., FERRONE, S., NGHIEM, P., UGUREL, S., SCHRAMA, D. & BECKER, J. C. 2017. Epigenetic priming restores the HLA class-I antigen processing machinery expression in Merkel cell carcinoma. *Scientific Reports,* 7.

RODRIGUEZ, A., GRIFFITHS-JONES, S., ASHURST, J. L. & BRADLEY, A. 2004. Identification of mammalian microRNA host genes and transcription units. *Genome Research,* 14**,** 1902-1910.

RUBY, J. G., JAN, C. H. & BARTEL, D. P. 2007. Intronic microRNA precursors that bypass Drosha processing. *Nature,* 448**,** 83-86.

SAMANTA, S., RAJASINGH, S., DROSOS, N., ZHOU, Z. G., DAWN, B. & RAJASINGH, J. 2018. Exosomes: new molecular targets of diseases. *Acta Pharmacologica Sinica,* 39**,** 501-513.

SANTANGELO, L., GIURATO, G., CICCHINI, C., MONTALDO, C., MANCONE, C., TARALLO, R., BATTISTELLI, C., ALONZI, T., WEISZ, A. & TRIPODI, M. 2016. The RNA-binding protein SYNCRIP is a component of the hepatocyte exosomal machinery controlling microRNA sorting. *Cell Reports,* 17**,** 799-808.

SCHERZ-SHOUVAL, R., SANTAGATA, S., MENDILLO, M. L., SHOLL, L. M., BEN-AHARON, I., BECK, A. H., DIAS-SANTAGATA, D., KOEVA, M., STEMMER, S. M., WHITESELL, L. & LINDQUIST, S. 2014. The reprogramming of tumor stroma by HSF1 is a potent enabler of malignancy. *Cell,* 158**,** 564-578.

SCHOWALTER, R. M. & BUCK, C. B. 2013. The Merkel cell polyomavirus minor capsid protein. *Plos Pathogens,* 9**,** e1003558.

SCHRAMA, D., PEITSCH, W. K., ZAPATKA, M., KNEITZ, H., HOUBEN, R., EIB, S., HAFERKAMP, S., MOORE, P. S., SHUDA, M. & THOMPSON, J. F. 2011. Merkel cell polyomavirus status is not associated with clinical course of Merkel cell carcinoma. *Journal of Investigative Dermatology,* 131**,** 1631-1638.

SCHRAMA, D., SAROSI, E. M., ADAM, C., RITTER, C., KAEMMERER, U., KLOPOCKI, E., KONIG, E. M., UTIKAL, J., BECKER, J. C. & HOUBEN, R. 2019. Characterization of six Merkel cell polyomavirus-positive Merkel cell carcinoma cell lines: Integration pattern suggest that large T antigen truncating events occur before or during integration. *International Journal of Cancer,* 145**,** 1020-1032.

SETO, A. G., BEATTY, X., LYNCH, J. M., HERMRECK, M., TETZLAFF, M., DUVIC, M. & JACKSON, A. L. 2018. Cobomarsen, an oligonucleotide inhibitor of miR-155, co-ordinately regulates multiple survival pathways to reduce cellular proliferation and survival in cutaneous T-cell lymphoma. *British Journal of Haematology,* 183**,** 428-444.

SHAFFIEY, F., CROSS, E. & SATHYANARAYANA, P. 2013. Mir-590 is a novel STAT5 regulated oncogenic miRNA and targets FasL in acute myeloid leukemia. Am Soc Hematology.

SHAMAY, M., KRITHIVAS, A., ZHANG, J. & HAYWARD, S. D. 2006. Recruitment of the de novo DNA methyltransferase Dnmt3a by Kaposi's sarcoma-associated

herpesvirus LANA. *Proceedings of the National Academy of Sciences of the United States of America,* 103**,** 14554-9.

SHINTANI, Y., FUJIWARA, A., KIMURA, T., KAWAMURA, T., FUNAKI, S., MINAMI, M. & OKUMURA, M. 2016. IL-6 secreted from cancer-associated fibroblasts mediates chemoresistance in NSCLC by increasing epithelial-mesenchymal transition signaling. *Journal of Thoracic Oncology,* 11**,** 1482-1492.

SHUDA, M., CHANG, Y. & MOORE, P. S. 2014. Merkel cell polyomavirus-positive Merkel cell carcinoma requires viral small T-antigen for cell proliferation. *Journal of Investigative Dermatology,* 134**,** 1479-1481.

SHUDA, M., FENG, H., KWUN, H. J., ROSEN, S. T., GJOERUP, O., MOORE, P. S. & CHANG, Y. 2008. T antigen mutations are a human tumor-specific signature for Merkel cell polyomavirus. *Proceedings of the National Academy of Sciences of the United States of America,* 105**,** 16272-16277.

SHUDA, M., KWUN, H. J., FENG, H. C., CHANG, Y. & MOORE, P. S. 2011. Human Merkel cell polyomavirus small T antigen is an oncoprotein targeting the 4E-BP1 translation regulator. *Journal of Clinical Investigation,* 121**,** 3623-3634.

SHUDA, M., VELASQUEZ, C., CHENG, E. D., CORDEK, D. G., KWUN, H. J., CHANG, Y. & MOORE, P. S. 2015. CDK1 substitutes for mTOR kinase to activate mitotic cap-dependent protein translation. *Proceedings of the National Academy of Sciences of the United States of America,* 112**,** 5875-5882.

SHUKLA, N., YAN, I. K. & PATEL, T. 2018. Multiplexed detection and quantitation of extracellular vesicle RNA expression using nanoString. *Extracellular RNA.* Springer.

SOHEL, M. H. 2016. Extracellular/circulating microRNAs: release mechanisms, functions and challenges. *Achievements in the Life Sciences,* 10**,** 175-186.

SOLTANI, A. M., ALLAN, B. J., BEST, M. J., PANTHAKI, Z. J. & THALLER, S. R. 2014. Merkel cell carcinoma of the hand and upper extremity: current trends and outcomes. *Journal of Plastic, Reconstructive & Aesthetic Surgery,* 67**,** e71-7.

SPURGEON, M. E., CHENG, J. W., BRONSON, R. T., LAMBERT, P. F. & DECAPRIO, J. A. 2015. Tumorigenic activity of Merkel Cell Polyomavirus T antigens expressed in the stratified epithelium of mice. *Cancer Research,* 75**,** 1068-1079.

SQUADRITO, M. L., BAER, C., BURDET, F., MADERNA, C., GILFILLAN, G. D., LYLE, R., IBBERSON, M. & DE PALMA, M. 2014. Endogenous RNAs modulate

microRNA sorting to exosomes and transfer to acceptor cells. *Cell Reports,* 8**,** 1432-1446.

STANG, A., BECKER, J. C., NGHIEM, P. & FERLAY, J. 2018. The association between geographic location and incidence of Merkel cell carcinoma in comparison to melanoma: An international assessment. *European Journal of Cancer,* 94**,** 47-60.

STRAUSSMAN, R., MORIKAWA, T., SHEE, K., BARZILY-ROKNI, M., QIAN, Z. R., DU, J. Y., DAVIS, A., MONGARE, M. M., GOULD, J., FREDERICK, D. T., COOPER, Z. A., CHAPMAN, P. B., SOLIT, D. B., RIBAS, A., LO, R. S., FLAHERTY, K. T., OGINO, S., WARGO, J. A. & GOLUB, T. R. 2012. Tumour micro-environment elicits innate resistance to RAF inhibitors through HGF secretion. *Nature,* 487**,** 500-U118.

SU, S. C., CHEN, J. N., YAO, H. R., LIU, J., YU, S. B., LAO, L. Y., WANG, M. H., LUO, M. L., XING, Y., CHEN, F., HUANG, D., ZHAO, J. H., YANG, L. B., LIAO, D., SU, F. X., LI, M. F., LIU, Q. & SONG, E. W. 2018. CD10(+) GPR77(+) Cancer-associated fibroblasts promote cancer formation and chemoresistance by sustaining cancer stemness. *Cell,* 172**,** 841-856.

SU, Y. Y., SUN, L., GUO, Z. R., LI, J. C., BAI, T. T., CAI, X. X., LI, W. H. & ZHU, Y. F. 2019. Upregulated expression of serum exosomal miR-375 and miR-1307 enhance the diagnostic power of CA125 for ovarian cancer. *J Ovarian Res,* 12**,** 6.

SUBRAMANIAN, A., TAMAYO, P., MOOTHA, V. K., MUKHERJEE, S., EBERT, B. L., GILLETTE, M. A., PAULOVICH, A., POMEROY, S. L., GOLUB, T. R., LANDER, E. S. & MESIROV, J. P. 2005. Gene set enrichment analysis: a knowledge-based approach for interpreting genome-wide expression profiles. *Proceedings of the National Academy of Sciences of the United States of America,* 102**,** 15545-50.

SULLIVAN, C. S., GRUNDHOFF, A. T., TEVETHIA, S., PIPAS, J. M. & GANEM, D. 2005. SV40-encoded microRNAs regulate viral gene expression and reduce susceptibility to cytotoxic T cells. *Nature,* 435**,** 682-686.

SUNSHINE, J. C., JAHCHAN, N. S., SAGE, J. & CHOI, J. 2018. Are there multiple cells of origin of Merkel cell carcinoma? *Oncogene,* 37**,** 1409-1416.

SVENSSON, K. J., CHRISTIANSON, H. C., WITTRUP, A., BOURSEAU-GUILMAIN, E., LINDQVIST, E., SVENSSON, L. M., MORGELIN, M. & BELTING, M. 2013. Exosome uptake depends on ERK1/2-heat shock protein 27 signaling and lipid raft-

mediated endocytosis negatively regulated by Caveolin-1. *Journal of Biological Chemistry,* 288**,** 17713-17724.

SZCZYRBA, J., NOLTE, E., WACH, S., KREMMER, E., STOHR, R., HARTMANN, A., WIELAND, W., WULLICH, B. & GRASSER, F. A. 2011. Downregulation of Sec23A protein by miRNA-375 in prostate carcinoma. *Molecular Cancer Research,* 9**,** 791-800.

TANG, R., LI, L. M., ZHU, D. H., HOU, D. X., CAO, T., GU, H. W., ZHANG, J., CHEN, J. Y., ZHANG, C. Y. & ZEN, K. 2012. Mouse miRNA-709 directly regulates miRNA-15a/16-1 biogenesis at the posttranscriptional level in the nucleus: evidence for a microRNA hierarchy system. *Cell Research,* 22**,** 504-515.

TCHOU, J., ZHANG, P. J., BI, Y. T., SATIJA, C., MARJUMDAR, R., STEPHEN, T. L., LO, A., CHEN, H. Y., MIES, C., JUNE, C. H., CONEJO-GARCIA, J. & PURE, E. 2013. Fibroblast activation protein expression by stromal cells and tumor-associated macrophages in human breast cancer. *Human Pathology,* 44**,** 2549-2557.

TERHEYDEN, P. & BECKER, J. C. 2017. New developments in the biology and the treatment of metastatic Merkel cell carcinoma. *Current Opinion in Oncology*.

THAYANITHY, V., DICKSON, E. L., STEER, C., SUBRAMANIAN, S. & LOU, E. 2014. Tumor-stromal cross talk: direct cell-to-cell transfer of oncogenic microRNAs via tunneling nanotubes. *Translational Research,* 164**,** 359-65.

TILLING, T., WLADYKOWSKI, E., FAILLA, A. V., HOUDEK, P., BRANDNER, J. M. & MOLL, I. 2014. Immunohistochemical analyses point to epidermal origin of human Merkel cells. *Histochem Cell Biol,* 141**,** 407-21.

TOKER, C. 1972. Trabecular carcinoma of the skin. *Archives of Dermatology,* 105**,** 107-10.

TOLSTOV, Y. L., KNAUER, A., CHEN, J. G., KENSLER, T. W., KINGSLEY, L. A., MOORE, P. S. & CHANG, Y. 2011. Asymptomatic primary Merkel cell polyomavirus infection among adults. *Emerging Infectious Diseases,* 17**,** 1371-1380.

TOMASEK, J. J., GABBIANI, G., HINZ, B., CHAPONNIER, C. & BROWN, R. A. 2002. Myofibroblasts and mechano-regulation of connective tissue remodelling. *Nature Reviews Molecular Cell Biology,* 3**,** 349-363.

TOULLEC, A., GERALD, D., DESPOUY, G., BOURACHOT, B., CARDON, M., LEFORT, S., RICHARDSON, M., RIGAILL, G., PARRINI, M. C., LUCCHESI, C., BELLANGER, D., STERN, M. H., DUBOIS, T., SASTRE-GARAU, X.,

DELATTRE, O., VINCENT-SALOMON, A. & MECHTA-GRIGORIOU, F. 2010. Oxidative stress promotes myofibroblast differentiation and tumour spreading. *Embo Molecular Medicine,* 2**,** 211-230.

TOUZÉ, A., LE BIDRE, E., LAUDE, H., FLEURY, M. J., CAZAL, R., ARNOLD, F., CARLOTTI, A., MAUBEC, E., AUBIN, F. & AVRIL, M.-F. 2011. High levels of antibodies against merkel cell polyomavirus identify a subset of patients with merkel cell carcinoma with better clinical outcome. *Journal of Clinical Oncology,* 29**,** 1612-1619.

TSUKAMOTO, Y., NAKADA, C., NOGUCHI, T., TANIGAWA, M., LAM, T. N., UCHIDA, T., HIJIYA, N., MATSUURA, K., FUJIOKA, T., SETO, M. & MORIYAMA, M. 2010. MicroRNA-375 is downregulated in gastric carcinomas and regulates cell survival by targeting PDK1 and 14-3-3 zeta. *Cancer Res,* 70**,** 2339-2349.

TURCHINOVICH, A., SAMATOV, T. R., TONEVITSKY, A. G. & BURWINKEL, B. 2013. Circulating miRNAs: cell–cell communication function? *Frontiers in genetics,* 4**,** 119.

TURCHINOVICH, A., WEIZ, L., LANGHEINZ, A. & BURWINKEL, B. 2011. Characterization of extracellular circulating microRNA. *Nucleic Acids Research,* 39**,** 7223-7233.

VASUDEVAN, S. & STEITZ, J. A. 2007. AU-rich-element-mediated upregulation of translation by FXR1 and argonaute 2. *Cell,* 128**,** 1105-1118.

VASUDEVAN, S., TONG, Y. C. & STEITZ, J. A. 2007. Switching from repression to activation: MicroRNAs can up-regulate translation. *Science,* 318**,** 1931-1934.

VEIJA, T., SAHI, H., KOLJONEN, V., BOHLING, T., KNUUTILA, S. & MOSAKHANI, N. 2015. miRNA-34a underexpressed in Merkel cell polyomavirus-negative Merkel cell carcinoma. *Virchows Archiv,* 466**,** 289-295.

VERHAEGEN, M. E., MANGELBERGER, D., HARMS, P. W., EBERL, M., WILBERT, D. M., MEIRELES, J., BICHAKJIAN, C. K., SAUNDERS, T. L., WONG, S. Y. & DLUGOSZ, A. A. 2017. Merkel Cell Polyomavirus small T antigen initiates Merkel Cell Carcinoma-like tumor development in mice. *Cancer Research,* 77**,** 3151-3157.

VERHAEGEN, M. E., MANGELBERGER, D., HARMS, P. W., VOZHEIKO, T. D., WEICK, J. W., WILBERT, D. M., SAUNDERS, T. L., ERMILOV, A. N., BICHAKJIAN, C. K., JOHNSON, T. M., IMPERIALE, M. J. & DLUGOSZ, A. A.

2015. Merkel cell polyomavirus small T antigen is oncogenic in transgenic mice. *Journal of Investigative Dermatology,* 135**,** 1415-1424.

VICKERS, K. C., PALMISANO, B. T., SHOUCRI, B. M., SHAMBUREK, R. D. & REMALEY, A. T. 2015. MicroRNAs are transported in plasma and delivered to recipient cells by high-density lipoproteins (vol 13, pg 423, 2011). *Nature Cell Biology,* 17**,** 104-104.

VILLARROYA-BELTRI, C., GUTIERREZ-VAZQUEZ, C., SANCHEZ-CABO, F., PEREZ-HERNANDEZ, D., VAZQUEZ, J., MARTIN-COFRECES, N., MARTINEZ-HERRERA, D. J., PASCUAL-MONTANO, A., MITTELBRUNN, M. & SANCHEZ-MADRID, F. 2013. Sumoylated hnRNPA2B1 controls the sorting of miRNAs into exosomes through binding to specific motifs. *Nature Communications,* 4**,** 2980.

VOJTECHOVA, Z. & TACHEZY, R. 2018. The role of miRNAs in virus-mediated oncogenesis. *International Journal of Molecular Sciences,* 19.

WALSH, N. M., FLEMING, K. E., HANLY, J. G., HACHE, K. D., DOUCETTE, S., FERRARA, G. & CERRONI, L. 2016. A morphological and immunophenotypic map of the immune response in Merkel cell carcinoma. *Human Pathology,* 52**,** 190-196.

WALZ, A. L., OOMS, A., GADD, S., GERHARD, D. S., SMITH, M. A., AUVIL, J. M. G., MEERZAMAN, D., CHEN, Q. R., HSU, C. H., YAN, C. H., NGUYEN, C., HU, Y., BOWLBY, R., BROOKS, D., MA, Y., MUNGALL, A. J., MOORE, R. A., SCHEIN, J., MARRA, M. A., HUFF, V., DOME, J. S., CHI, Y. Y., MULLIGHAN, C. G., MA, J., WHEELER, D. A., HAMPTON, O. A., JAFARI, N., ROSS, N., GASTIER-FOSTER, J. M. & PERLMAN, E. J. 2015. Recurrent DGCR8, DROSHA, and SIX homeodomain mutations in favorable Histology Wilms Tumors (vol 27, pg 286, 2015). *Cancer Cell,* 27**,** 426-426.

WANG, H., PENG, R., WANG, J. J., QIN, Z. L. & XUE, L. X. 2018. Circulating microRNAs as potential cancer biomarkers: the advantage and disadvantage. *Clinical Epigenetics,* 10.

WANG, K., YUAN, Y., CHO, J.-H., MCCLARTY, S., BAXTER, D. & GALAS, D. J. 2012a. Comparing the MicroRNA spectrum between serum and plasma. *PloS One,* 7**,** e41561.

WANG, S., QIU, L., YAN, X., JIN, W., WANG, Y., CHEN, L., WU, E., YE, X., GAO, G. F., WANG, F., CHEN, Y., DUAN, Z. & MENG, S. 2012b. Loss of microRNA 122

expression in patients with hepatitis B enhances hepatitis B virus replication through cyclin G(1) -modulated P53 activity. *Hepatology,* 55**,** 730-41.

WANG, Y. 2016. Upregulated lncRNA-HNGA1, a target of miR-375, contributes to aerobic glycolysis of head and neck squamous cell carcinoma through increasing levels of the glucose transporter protein SCL2A1. *European Journal of Cancer,* 61**,** S14-S15.

WEBBER, J., STEADMAN, R., MASON, M. D., TABI, Z. & CLAYTON, A. 2010. Cancer exosomes trigger fibroblast to myofibroblast differentiation. *Cancer Research,* 70**,** 9621-9630.

WEBER, J. A., BAXTER, D. H., ZHANG, S. L., HUANG, D. Y., HUANG, K. H., LEE, M. J., GALAS, D. J. & WANG, K. 2010. The MicroRNA spectrum in 12 body fluids. *Clinical Chemistry,* 56**,** 1733-1741.

WEI, L. S., YE, H. L., LI, G. L., LU, Y. T., ZHOU, Q. B., ZHENG, S. Y., LIN, Q., LIU, Y. M., LI, Z. H. & CHEN, R. F. 2018. Cancer-associated fibroblasts promote progression and gemcitabine resistance via the SDF-1/SATB-1 pathway in pancreatic cancer. *Cell Death & Disease,* 9**,** 1065.

WONG, S. Q., TOTHILL, R. W., DAWSON, S.-J. & HICKS, R. J. 2017. Wet or dry? Do liquid biopsy techniques compete with or complement PET for disease monitoring in oncology? *The Journal of Nuclear Medicine,* 58**,** 869-870.

WONG, S. Q., WALDECK, K., VERGARA, I. A., SCHRODER, J., MADORE, J., WILMOTT, J. S., COLEBATCH, A. J., DE PAOLI-ISEPPI, R., LI, J., LUPAT, R., SEMPLE, T., ARNAU, G. M., FELLOWES, A., LEONARD, J. H., HRUBY, G., MANN, G. J., THOMPSON, J. F., CULLINANE, C., JOHNSTON, M., SHACKLETON, M., SANDHU, S., BOWTELL, D. D. L., JOHNSTONE, R. W., FOX, S. B., MCARTHUR, G. A., PAPENFUSS, A. T., SCOLYER, R. A., GILL, A. J., HICKS, R. J. & TOTHILL, R. W. 2015. UV-associated mutations underlie the etiology of MCV-negative Merkel Cell Carcinomas. *Cancer Research,* 75**,** 5228-5234.

WORTZEL, I., DROR, S., KENIFIC, C. M. & LYDEN, D. 2019. Exosome-Mediated Metastasis: Communication from a Distance. *Developmental Cell,* 49**,** 347-360.

XIE, H., LEE, L., CARAMUTA, S., HOOG, A., BROWALDH, N., BJORNHAGEN, V., LARSSON, C. & LUI, W. O. 2014. MicroRNA expression patterns related to Merkel cell polyomavirus infection in human Merkel cell carcinoma. *Journal of Investigative Dermatology,* 134**,** 507-517.

XU, L., YANG, B. F. & AI, J. 2013. MicroRNA transport: a new way in cell communication. *Journal of Cellular Physiology,* 228**,** 1713-9.

YAN, W., WU, X. W., ZHOU, W. Y., FONG, M. Y., CAO, M. H., LIU, J., LIU, X. J., CHEN, C. H., FADARE, O., PIZZO, D. P., WU, J. W., LIU, L., LIU, X. X., CHIN, A. R., REN, X. B., CHEN, Y., LOCASALE, J. W. & WANG, S. E. 2018a. Cancer-cell-secreted exosomal miR-105 promotes tumour growth through the MYC-dependent metabolic reprogramming of stromal cells. *Nature cell biology,* 20**,** 597-609.

YAN, Y. Y., KUMAR, A. B., FINNES, H., MARKOVIC, S. N., PARK, S., DRONCA, R. S. & DONG, H. D. 2018b. Combining immune checkpoint inhibitors with conventional cancer therapy. *Frontiers in Immunology,* 9.

YEKTA, S., SHIH, I. H. & BARTEL, D. P. 2004. MicroRNA-directed cleavage of HOXB8 mRNA. *Science,* 304**,** 594-6.

YOU, X. Y., ZHANG, Z. P., FAN, J. Y., CUI, Z. Q. & ZHANG, X. E. 2012. Functionally orthologous viral and cellular microRNAs studied by a novel dual-fluorescent reporter system. *Plos One,* 7**,** e36157.

YOULDEN, D. R., SOYER, H. P., YOUL, P. H., FRITSCHI, L. & BAADE, P. D. 2014. Incidence and survival for Merkel cell carcinoma in Queensland, Australia, 1993-2010. *JAMA Dermatology,* 150**,** 864-72.

ZAAR, O., GILLSTEDT, M., LINDELOF, B., WENNBERG-LARKO, A. M. & PAOLI, J. 2016. Merkel cell carcinoma incidence is increasing in Sweden. *Journal of the European Academy of Dermatology and Venereology,* 30**,** 1708-1713.

ZENG, Y. & CULLEN, B. R. 2004. Structural requirements for pre-microRNA binding and nuclear export by Exportin 5. *Nucleic Acids Research,* 32**,** 4776-4785.

ZENG, Z. C., LI, Y. L., PAN, Y. J., LAN, X. L., SONG, F. Y., SUN, J. B., ZHOU, K., LIU, X. L., REN, X. L., WANG, F. F., HU, J. L., ZHU, X. H., YANG, W., LIAO, W. T., LI, G. X., DING, Y. Q. & LIANG, L. 2018. Cancer-derived exosomal miR-25-3p promotes pre-metastatic niche formation by inducing vascular permeability and angiogenesis. *Nature Communications,* 9**,** 5395.

ZHANG, L., ZHAN, S. Y., YAO, J., LOWERY, F. J., ZHANG, Q. L., HUANG, W. C., LI, P., LI, M., WANG, X., ZHANG, C. Y., WANG, H., ELLIS, K., CHEERATHODI, M., MCCARTY, J. H., PALMIERI, D., SAUNUS, J., LAKHANI, S., HUANG, S. Y., SAHIN, A. A., ALDAPE, K. D., STEEG, P. S. &

YU, D. H. 2015a. Microenvironment-induced PTEN loss by exosomal microRNA primes brain metastasis outgrowth. *Nature,* 527**,** 100-104.

ZHANG, X., YANG, Y. T., ZHU, R., BAI, J. Y., TIAN, Y., LI, X. H., PENG, Z. H., HE, Y. H., CHEN, L., FANG, D. C., CHEN, W. S., ZOU, Q. M., MAO, X. H. & WANG, R. Q. 2012. H. pylori induces the expression of Hath1 in gastric epithelial cells via interleukin-8/STAT3 phosphorylation while suppressing Hes1. *Journal of Cellular Biochemistry,* 113**,** 3740-3751.

ZHANG, X., YUAN, X., SHI, H., WU, L. J., QIAN, H. & XU, W. R. 2015b. Exosomes in cancer: small particle, big player. *Journal of Hematology & Oncology,* 8.

ZHANG, X. H. F., JIN, X., MALLADI, S., ZOU, Y. L., WEN, Y. H., BROGI, E., SMID, M., FOEKENS, J. A. & MASSAGUE, J. 2013. Selection of bone metastasis seeds by mesenchymal signals in the primary tumor stroma. *Cell,* 154**,** 1060-1073.

ZHENG, G. X., TERRY, J. M., BELGRADER, P., RYVKIN, P., BENT, Z. W., WILSON, R., ZIRALDO, S. B., WHEELER, T. D., MCDERMOTT, G. P., ZHU, J., GREGORY, M. T., SHUGA, J., MONTESCLAROS, L., UNDERWOOD, J. G., MASQUELIER, D. A., NISHIMURA, S. Y., SCHNALL-LEVIN, M., WYATT, P. W., HINDSON, C. M., BHARADWAJ, R., WONG, A., NESS, K. D., BEPPU, L. W., DEEG, H. J., MCFARLAND, C., LOEB, K. R., VALENTE, W. J., ERICSON, N. G., STEVENS, E. A., RADICH, J. P., MIKKELSEN, T. S., HINDSON, B. J. & BIELAS, J. H. 2017. Massively parallel digital transcriptional profiling of single cells. *Nature Communications,* 8**,** 14049.

ZHOU, J., SONG, S. D., CEN, J. N., ZHU, D. M., LI, D. C. & ZHANG, Z. X. 2012. MicroRNA-375 is downregulated in pancreatic cancer and inhibits cell proliferation in vitro. *Oncology Research,* 20**,** 197-203.

ZHU, H. T., HASAN, A. M. E., LIU, R. B., ZHANG, Z. C., ZHANG, X., WANG, J., WANG, H. Y., WANG, F. & SHAO, J. Y. 2016. Serum microRNA profiles as prognostic biomarkers for HBV-positive hepatocellular carcinoma. *Oncotarget,* 7**,** 45622-45633.

ZHU, L., KALIMUTHU, S., GANGADARAN, P., OH, J. M., LEE, H. W., BAEK, S. H., JEONG, S. Y., LEE, S. W., LEE, J. & AHN, B. C. 2017. Exosomes derived from natural killer cells exert therapeutic effect in melanoma. *Theranostics,* 7**,** 2732-2745.

ZITVOGEL, L., REGNAULT, A., LOZIER, A., WOLFERS, J., FLAMENT, C., TENZA, D., RICCIARDI-CASTAGNOLI, P., RAPOSO, G. & AMIGORENA, S. 1998.

Eradication of established murine tumors using a novel cell-free vaccine: dendritic cell-derived exosomes. *Nature Medicine,* 4**,** 594-600.

ZUR HAUSEN, A., RENNSPIESS, D., WINNEPENNINCKX, V., SPEEL, E. J. & KURZ, A. K. 2013. Early B-cell differentiation in Merkel cell carcinomas: clues to cellular ancestry. *Cancer Research,* 73**,** 4982-7.

6. Appendix

Table 1: MCC cell lines used in this thesis.

Type of cell lines	Name	Growth pattern	MCPyV status	Culture medium	Use in Paper
Variant MCC cell lines	MCC-13	Adherent	neg	RPMI 1640, 10% FBS	I, II
	MCC-26	Adherent	neg		I, II
	UISO	Adherent	neg		I, II
Classical MCC cell lines	AlDo	Suspension, aggregates	pos	RPMI 1640, 10% FBS	I, II
	BroLi	Suspension, aggregates	pos		I, II
	LoKe	Suspension, aggregates	pos		I, II
	MKL-1	Suspension, aggregates	pos		I, II, IV
	MKL-2	Suspension, aggregates	pos		I, II
	MS-1	Suspension, aggregates	pos		I, II
	PeTa	Suspension, aggregates	pos		I- IV
	WaGa	Suspension, single cells	pos		I- IV
	WoWe-2	Suspension, aggregates	pos		I, II
	UKE-MCC1a	Suspension, aggregates	pos		I, II
	UM-MCC9	Suspension, aggregates	neg	Modified neural crest stem cell self-renewal medium, 15% chick embryo extract	I, II
	UM-MCC13	Suspension, aggregates	pos		I, II, IV
	UM-MCC29	Suspension, aggregates	pos		I, II
	UM-MCC31	Suspension, aggregates	neg		I, II
	UM-MCC32	Suspension, aggregates	neg		I, II
	UM-MCC34	Suspension, aggregates	neg		I, II
	UM-MCC39	Suspension, aggregates	neg		I, II
	UM-MCC52	Suspension, aggregates	pos		I, II
	UM-MCC565	Suspension, aggregates	pos		I, II
	UM-MCC623	Suspension, aggregates	neg		I, II
	UM-MCC624	Suspension, aggregates	neg		I, II

Table 2: non-MCC cell lines used in this thesis.

Type of cell lines	Name	Growth pattern	Culture medium	Used in Paper
Melanoma	BLM	Adherent	RPMI 1640, 10% FBS	I, II
	MV3	Adherent		I, II
	Ma-Mel-02	Adherent		I, II
	Ma-Mel-12	Adherent		I, II
	Ma-Mel-13	Adherent		I, II
	Ma-Mel-47	Adherent		I, II
	Ma-Mel-61a	Adherent		I, II
	Ma-Mel-61f	Adherent		I, II
	Ma-Mel-66a	Adherent		I, II
	Ma-Mel-68	Adherent		I, II
	Ma-Mel-86a	Adherent		I, II
	Ma-Mel-86c	Adherent		I, II
	SK-Mel-28	Adherent		I, II
	WM-9	Adherent		I, II
Cutaneous squamous cell carcinoma	HSC-1	Adherent	RPMI 1640, 10% FBS	I, II
	MET-1	Adherent		I, II
	MET-4	Adherent		I, II
	SCL-1	Adherent		I, II
	SCL-2	Adherent		I, II, IV
Lung carcinoma	A549	Adherent	RPMI 1640, 10% FBS	I, II
Fibroblasts	MRC-5	Adherent	MEM Eagle, 10% FBS	I, II, IV
	Fibro 1.2	Adherent	DMEM, 15% FBS	I, II
	Fibro 1.4	Adherent	DMEM, 15% FBS	I, II, IV
	Fibro 1.7	Adherent	DMEM, 15% FBS	II
	Fibro 1.12	Adherent	DMEM, 15% FBS	IV
Epithelial cells	293T	Adherent	DMEM, 10% FBS	I, II, IV

Table 3: Sequence of primers used in the thesis

Gene	Forward primer	Reverse primer
ACTA2	CAGCCAAGCACTGTCAGG	CCAGAGCCATTGTCACACAC
CXCL2	GGGCAGAAAGCTTGTCTCAA	GCTTCCTTCCTTCTGGT
IL1B	GAGCTGATGGCCCTAAACA	AAGCCCTTGCTGTAGTGGTG
TGFB1	CGCCAGAGTGGTTATCT	TAGTGAACCCGTTGATGTC
CXCR4	GTTAATGCTTGCTGAATTGGAA	CTCGGTGTAGTTATCTGAAGTG
HPRT	GTCGTGATTAGTGATGATG	GTTCAGTCCTGTCCATAA
Pri-miR-375	CCTCACCTGAACGCATCTG	TGGGGACGAAGCCAAGCTA
RBPJ	CGGCCTCCACCTAAACGAC	TCCATCCACTGCCCATAAGAT
TP53	CAGCACATGACGGAGGTTGT	TCATCCAAATACTCCACACGC
ASCL1	CCCAAGCAAGTCAAGCGACA	AAGCCGCTGAAGTTGAGCC
ATOH1	TGAAGGAGTTGGGAGACCAC	GTAGACGGGATGCTCTCTCG
MCPyV-LTA	CTCGTCAACCTCATCAAAC	GGAGCAAATTCCAGCAAA
RPLP0	CCATCAGCACCACAGCCTTA	GGCGACCTGGAAGTCCAACT
RPLP0 probe	YY-ATCTGCTGCATCTGCTTGGAGCCCA-BHQ1	

Table 4: Primary antibodies used for Multicolor IF (Paper IV)

	Antigen retrieval	Antibody	Clone /product number	Clonality	Supplier	Dilution	Fluoro-phore
1	AR9	TE-7	CBL271	monoclonal	Millipore	1:600	Opal 520
2	AR9	Caveolin 1	PA5-17447	polyclonal	Thermo Fischer	1:500	Opal 570
3	AR9	alpha-SMA	1A4	monoclonal	Dako	1:600	Opal 540
4	AR9	S100A4	EPR2761(2)	monoclonal	Abcam	1:1200	Opal 620
5	AR6	FAP	HPA059739	polyclonal	Atlas antibody	1:500	Opal 650
6	AR6	CK20	D9Z1Z	monoclonal	Cell signaling	1:800	Opal 690